Morphological and genomic profiling of circulating tumor cells in metastatic colorectal cancer

Ph.D. Thesis of

Dipl.-Biol. Jana-Aletta Thiele

Charles University

Faculty of Medicine in Pilsen

2018

Mentor: Dr. Pavel Pitule

Advisors: Dr. Peter Kuhn and Dr. Pavel Ostašov

In collaboration with the Kuhn-Hicks Laboratory at the

University of Southern California

Abstract

Colorectal cancer (CRC) is the third most common cancer worldwide; it is responsible for nearly 10% of all newly diagnosed cancers and is the second most cause of cancer related death in Europe. Biomarkers for therapy guidance, targeted therapy and survival prognosis are still limited. As CRC is a heterogeneous disease, different parts of the tumor might have varying molecular characteristics which may change during therapy or disease progression. Through solid biopsies and screenings, these local or temporal differences are impossible to monitor. To facilitate detection of these possible temporal changes, a regularly and non-invasively accessible biomarker is required for disease monitoring. Circulating tumor cells (CTCs) might represent such a biomarker as they have been shown to be fluid surrogates of the solid tumor. EpCAM positive CTCs have shown to be prognostic in CRC for survival, but their full potential has not yet been evaluated further. By using the High Definition Single Cell Analysis (HD-SCA) workflow, we were able to analyze the entire spectrum of CTCs and categorize them as the regular CTCs (HD-CTC), CTCs with a smaller nuclear area (CTC-Small), CTCs with low expression of epithelial marker cytokeratin (CTC-LowCK) and CTCs undergoing apoptosis and therefore releasing cell free DNA (CTC-cfDNA producing). In addition we observed and analyzed CTC clusters (CTCCs). The analysis included not only morphology and enumeration of CTCs, but also copy number variation (CNV) profiles on single-cell level.

In the first part of this study we focused on enumeration of all sub-categories of CTCs and CTCCs detected in the blood of stage IV CRC patients before surgery and in a follow-up draw. The goal was to characterize and define a subset of CTCs associated with metastases or reduced survival. Unlike previous publications we have not observed an association of the regular CTC (HD-CTCs) category with survival, but we observed that the CTC-Small category in the follow-up draw was associated to overall survival (OS, p=0.040). These findings are not concordant with common literature. This might be caused by the non-EpCAM based detection method or it could be specific for the Czech patient cohort.

However, the number of CTCCs per ml blood in the pre-resection draw was associated with shorter OS (p=0.021). We also detected an association of metastatic status at the time of CRC diagnosis (M1 vs. M0) with higher average amount of cells per cluster (p=0.035) which indicates, that larger CTCCs may be drivers for metastases.

In the second part of this study we extracted and analyzed single HD-CTCs from the pre-resection draws and also single cells from tumor tissue touch preparations. We amplified the whole genome and used next-generation sequencing to compare CNV profiles. The goal was to study clonality within CTCs and distinguish cancer promoting CTCs from less invasive and non-proliferating CTCs. Also, we wanted to compare CNV profiles and clones of tissue samples with those of CTCs to gain knowledge

about tumor evolution in CRC. After analysis of 136 single HD-CTCs from 11 CRC patients we could not detect any clonality (two or more single cells showing similar CNV changes). Compared to that, analysis of single cells from CRC touch preparations revealed clonality in 83.3% of tested patients. Comparison between tissue cells from the primary tumor and the metastasis showed similar clonal profiles with minor adaptions in the hepatic metastasis.

Overall, we were able to detect and characterize four morphologically different groups of CTCs showing the high heterogeneity of CTCs in CRC patients. The missing association of HD-CTC counts with survival may be caused by the limitation of the cohort, but also due to possible mischaracterization of endothelial cells as HD-CTCs. This study serves as a preliminary study for future projects focused on both, CTC detection in earlier stage CRC in a prospective observational study, and characterization of CTCs and cells within CTCCs through multiplex protein detection.

Preface and statement

This Ph.D. thesis is a result of my work at the Biomedical Center, Faculty of Medicine in Pilsen as part of the Charles University under supervision of Dr. Pavel Pitule and Dr. Milena Králíčková. Part of this work was performed in the laboratories of Dr. Peter Kuhn and Dr. James Hicks as part of a colaboration with the University of Southern California. The motivation for this project arose from my former position in Research and Development for cancer detection products based on circulating tumor cells and my believe that further analysis of single cells and subsets of these cells may offer valuable information for oncologists. This work has been supported by the Charles University Research Fund (Progres Q39) and the National Sustainability Program I (NPU I) Nr. LO1503 provided by the Ministry of Education Youth and Sports of the Czech Republic and travelling cost has been mainly covered by the Fund of Mobility of the Charles University and Fund of Mobility of the Faculty of Medicine in Plzeň.

I thank Dr. Pavel Pitule and Dr. Pavel Ostašov for their assistance and willingness for scientific discussions, constructive advice and inviting work atmosphere. Their office was always open to discuss challenges, experiments and theories and this thesis would have not been possible without them.

Also I thank Dr. Peter Kuhn, Dr. James Hicks and Dr. Anna Sandström Gerdtsson for their supervision in Los Angeles. As well as the entire staff of the Kuhn-Hicks laboratory for teaching me the HD-SCA workflow, introducing me to scientific writing and being helpful in all areas of my life in the US.

Dr. Petr Hošek I have to thank for everything he taught me about statistics and thanks to him the statistical analysis finally reached the here presented form. Besides that, he made the office a place I enjoyed coming each day and I will always remember all his input regarding bicycles.

Dr. Milena Králíčková I thank for creating this collaboration with the laboratories of Dr. Hicks and Dr. Kuhn and compile sufficient financial support to secure my time here at the Faculty of Medicine in Plzeň.

My special thanks go to my parents Elke and Dieter Thiele and my fiancé Olaf Grunenberg for their loving and moral support, understanding and patience that enabled me to participate in this international project and supported me in the execution of this work.

I declare that this thesis has been composed by myself and that this work has not been submitted for any other professional qualification or degree.

I affirm that the submitted work is my own, except where work has been included that has been partly formed by jointly authored publications.

My own contribution and those of other authors has been explicitly indicated and I affirm that appropriate acknowledgement has been given within this thesis where reference has been made to the work of others.

Pilsen, …… ……

Table of Contents

1 Abbreviations

5-FU	5-Fluorouracil
AJJCC	American Joint Committee on Cancer
APC	Adenomatous-polyposis-coli
AR	Androgen receptor
BF	Bright field
BRAF	V-Raf murine sarcoma viral oncogene homolog B
CA125	Cancer antigen 125
CDB	Cell deposition buffer
CDX2	Homeobox protein CDX-2
CEA	Carcinoembryonic antigen
CEC	Circulating endothelial cell
cfDNA	Cell-free DNA
CIMP	CpG island methylation phenotype
CIN	Chromosomal Instability
CK	Cytokeratin
CKpan	Cytokeratin pan mix
CNV	Copy number variation
COI	Cell of interest
CRC	Colorectal Cancer
CT	Chemotherapy
CTC	Circulating Tumor Cell
CTCC	Circulating tumor cell clusters (two or more HD-CTCs)
CTC-cfDNA prod.	Probably apoptotic HD-CTC
CTC-LowCK	CTC with low or none CK signal
CTC-Small	CTC with a smaller nucleus
ctDNA	Circulating tumor DNA
DAPI	4',6-Diamidine-2'-phenylindole dihydrochloride
ddH_2O	Double deionized water
DNA	Deoxyribonucleic acid
DTT	Dithiothreitol
ECM	Extracellular matrix
EGFR	Epidermal growth factor receptor
EpCAM	Epithelial cell adhesion molecule
ERK	Extracellular signal–regulated kinase
EtOH	Ethanol
EU	European Union
FAP	Familial adenomatous polyposis

FDA	US Food and Drug Administration
FGFR1	Fibroblast growth factor receptor 1
FISH	Fluorescence in situ hybridization
FOBT	Fecal occult blood test
FOXC2	Forkhead transcription factor 2
FS	Flexible sigmoidoscopy
HD-CTC	Circulating tumor cell detected by the HD-SCA workflow
HD-SCA	High definition single cell analysis
HIFs	Hypoxia inducible factors
JAK	Janus tyrosine kinase
KOH	Potassium hydroxide
lncRNA	Long non-coding RNA
LOH	Loss of heterozygosity
LS	Lynch Syndrome
mAB	Monoclonal antibody
mCRPC	Metastatic castration-resistant prostate cancer
MEK	Mitogen-activated protein kinase kinase
miRNA	Micro RNA
MMR	Mismatch repair
mRNA	Messenger RNA
MSI	Microsatellite Instability
MTsDNA	Multi-target stool DNA
N/C ratio	Nucleus/cytoplasm ratio
NCCN	The National Comprehensive Cancer Network
NGS	Next generation sequencing
OS	Overall survival
PFS	Progression free survival
PSA	Prostate-specific antigen
RBC	Red blood cell
RNA	Ribonucleic acid
RT	Radiotherapy
SDOM	Standard deviation over mean
STAT	Signal transducer and activator of transcription
TE	Tris-EDTA
TGF- β	Transforming growth factor beta
TKI	Tyrosine kinase inhibitor
TNM	Tumor, nodes and metastasis (classification system)
TTF1	Thyroid transcription factor 1
Twist	Twist Basic Helix-Loop-Helix Transcription Factor 1
UCSC	University of California Santa Cruz

USC	University of Southern California
VEGF	Vascular endothelial growth factor
WBC	White blood cell
WGA	Whole genomes amplification
WHO	World Health Organization
ZEB1	Zinc finger E-box-binding homeobox 1

2 Introduction

Within the European Union (EU) there were 1.373.500 new cancer related deaths expected for the year 2017 [1]. And even though cancer mortality rates are predicted to decline, cancer is still the second most common cause of death after cardiovascular disease with colorectal cancer (CRC) being the second most common cause of cancer death in Europe [2]. Compared to other solid cancers like breast cancer and prostate cancer, CRC has limited biomarkers for treatment decisions or targeted therapy. Besides, CRC is highly driven by epigenetic and genetic alterations and in about 75% of cases it occurs sporadically [3]. Even though the three major pathways for the development of an adenocarcinoma from normal colon mucosa have been studied extensively [4–6] and their major drivers have been identified, therapy targets and biomarkers for regular disease development monitoring for prevention or detection of possible relapse are still missing. This is where a liquid biopsy could close the gap for improvement of personalized cancer care. Circulating tumor cells (CTCs) as easy accessible markers from a peripheral blood draw have already proven to be predictive for survival of CRC patients, but are presumably holding further potential, once single-cell molecular analysis follows their detection [7].

2.1 Introduction to Colorectal Cancer

2.1.1 CRC Epidemiology

Worldwide, CRC is the third most common cancer, responsible for nearly 10% of newly diagnosed cancers with 1.360.602 new cases worldwide (in the year of 2012) from which 447.136 new cases were diagnosed in Europe [8]. In the Czech Republic incidences of and mortality from CRC have been highest amongst Central and Western European countries ranking 4th worldwide for men and 16th for women [8]. The distribution of CRC mortality within Europe for both sexes combined is displayed in **Figure 1**. One cause for the high mortality rate may be the lack of easy accessible biomarkers for detection of early stage CRC. In the US, less than 40% of patients are diagnosed with localized disease. This has severe impact to 5-year survival, which drops from 90% for localized disease down to 12% for patients with distant metastasis [9–11].

After colonoscopy as the main early detection method has been introduced in Germany in 2002 a reduction of CRC incidence was expected by 2010 due to early detection and removal of pre-cancerous polyps [12]. In 2014 Brenner et al. confirmed the expectations, showing that colonoscopy can reduce incidence and mortality of CRC by 40-60% [13]. The changes of CRC mortality rates within Europe are unevenly distributed between women and men. Whereas the mortality from CRC increased by 6% for men, it decreased by 14.7% for women within Europe [2]. In some countries like

Germany, Switzerland and the Czech Republic, mortality was even decreased in men by 25% and 30% in women [2]. These regional differences could be explained by differing lifestyle (alcohol intake, diet and exercise), availability of treatment, regular screenings (like in Germany, Austria and the Czech Republic) and improvements in public awareness. In 2017 the World Cancer Research Fund and the American Institute for Cancer Research released a report about lifestyle risk factors, that increase the risk of CRC which included obesity, smoking, alcoholic intake (>1-2 drinks/day), processed meat (and red meat in general), low intake of fruits and vegetables and the lack of physical activity [14]. Additionally, the report stated that CRC is one of the cancers, which incidence is expected to increase worldwide to more than 2 million new cases per year. Other reports and research results during the last years confirm the recommendations to reduce meat and alcohol intake, stay active and within a healthy weight to prevent cancer in general or reduce the risk of relapse after cancer therapy [15–17].

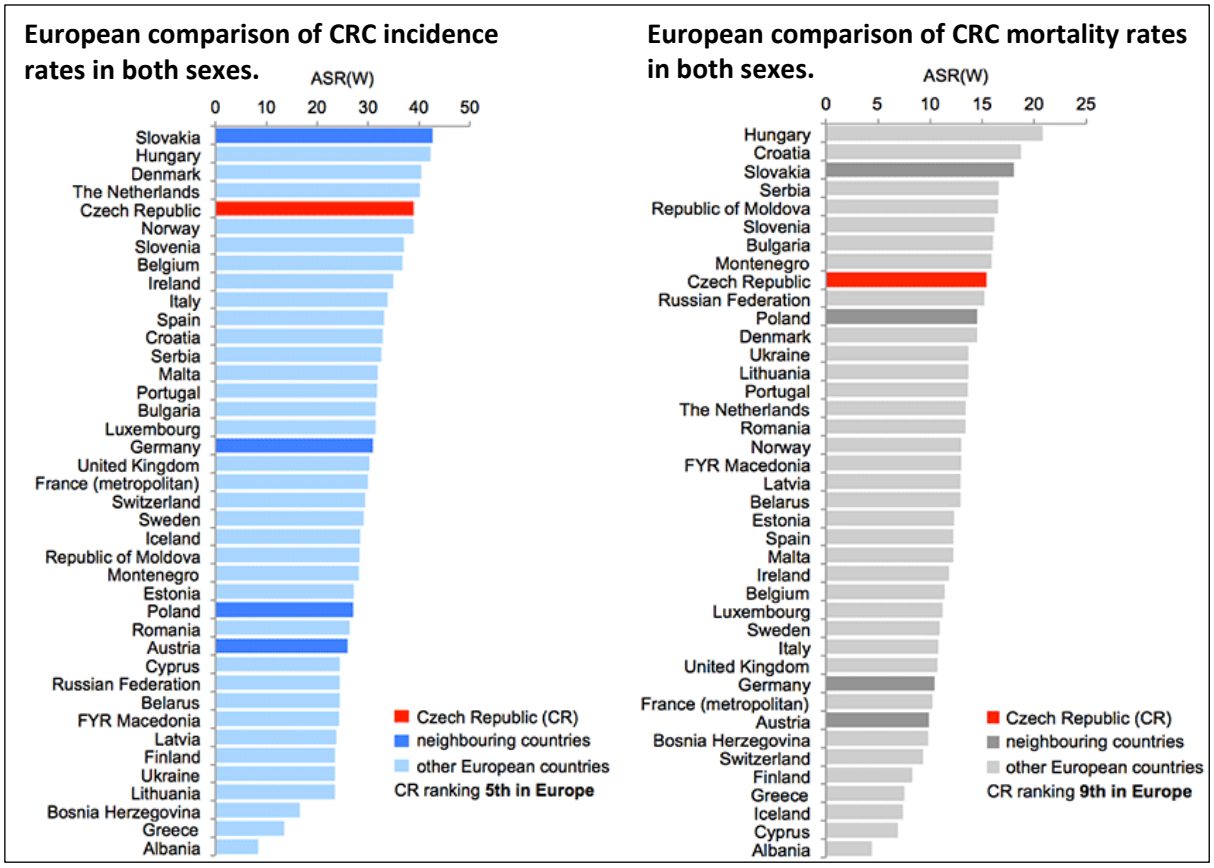

Figure 1: Incidence and mortality of CRC in both sexes within Europe (2013). Shown are incidences (left side) and mortality (right side) of CRC in both sexes combined within Europe. Source: http://www.crcprevention.eu/index.php?pg=colorectal-cancer-epidemiology, accessed June 14th, 2018.

2.1.2 CRC Development

The basis for the development of CRC in healthy colon epithelium is the acquisition of multiple alterations in the genome that drive progression of tumorigenesis from healthy mucosa to adenocarcinoma. About 25% of CRC patients have a familial background of CRC, but in only 5-10% of all CRC cases the cancer can be traced back to one of two hereditary forms of CRC with well described mutations in CRC related genes [3]. In case of the 75% sporadic CRC the path of development could be divided in three different phenotypes of genomic and epigenetic alterations: chromosomal instability (CIN), microsatellite instability (MSI) and CpG island methylation phenotype (CIMP). How these alterations lead to malignant neoplasm is explained in this chapter.

2.1.2.1 Molecular development of CRC

In the human genome, multiple protective strategies to assure genome integrity are in place. However, mutations may add up, especially in highly mitotic tissues, and the colonic epithelium is one of those with a weekly cell replacement rate [18]. Progenitors of these new epithelial cells are intestinal stem cells (ISCs), of which between 5 and 16 are situated at the bottom of each crypt (intestinal glands formed by colonic mucosa) [19]. One of the protective strategies at the cellular level is the 'neutral drift' within the intestinal crypts that continuously replaces individual ISCs by the descendants of their neighbors. Therefore, even if a mutation occurs in these ISCs (due to errors in DNA replication and/or exposure to carcinogens), the chance of whole crypt repopulation by the mutated ISC is very low [20]. Research has shown that the probability of a mutant's success to populate the entire crypt depends on the type of mutation. A *KRAS* mutation is more likely than an *APC* mutation to survive as a fixed mutation and populate the crypt [21].

In addition to ISCs, also differentiated cells in the colon epithelium have the potential to initiate CRC.

No matter which cell initiated CRC, additional alterations are acquired over time, separating CRC into three phenotypes:

<u>The Chromosomal Instability Phenotype</u>

This pathway of CRC development is also named the adenoma-carcinoma sequence [22]. It is based on subsequent genomic changes with its respective morphologic and histologic transformations. The result of genomic instability in CRC is alteration of entire arms or even whole chromosomes that leads to aneu- or polyploidy. These changes are presumed to be a result of abnormal regulation of the mitotic spindle apparatus and repair mechanisms for double-strand DNA breaks [6]. One of the first steps of the CIN pathway is the loss or inactivation of tumor suppressor genes. The most common alterations are mutations of the adenomatous-polyposis-coli (*APC*, 5q21), *TP53* gene

(17p13) and the loss of heterozygosity (LOH) of 18q21 [23]. Also, activating mutations of oncogenes like KRAS and PIK3CA are crucial later steps for the cells of colon mucosa to change cell adhesion, signaling and cell growth [5].

Microsatellite Instability Phenotype

When cells replicate, the DNA polymerase protein, using the original strand as a template, synthesizes new DNA. In case that error occurs and DNA polymerase fails to correct it by its proofreading function, sections of DNA can be removed and repaired later by a system composed of mismatch repair (MMR) proteins. This protective mechanism is a crucial way to protect genome integrity [24]. Sometimes so-called DNA polymerase stutter causes errors in areas of the genome with short tandem repetitions (microsatellites). If these mismatches are not repaired due to the reduced activity or loss of MMR function, these regions might change their length resulting in MSI [5]. Inactivation of MMR genes is caused either by somatic mutations or by abnormal DNA methylation [25]. The main MMR genes are MSH2, MSH6, PMS2 and MLH1. To identify MSI in CRC, a biopsy tissue sample is tested in 5-10 loci and separated in categories defined by the National Cancer Institute in 1998, so that tumors with ≥30% instability are named MSI high (MSI-H), if 10-29% of the markers are instable the tumor is categorized MSI-low (MSI-L) and instability <10% is defined as microsatellite stable (MSS) [26]. MSI is also one of the main criteria to diagnose a hereditary form of CRC – the hereditary non-polyposis colorectal cancer (HNPCC), or short: Lynch Syndrome (LS, as discussed in detail below).

CpG island methylation phenotype

Epigenetic silencing through aberrant methylation of the promoter regions of a tumor suppressor gene is as effective as a mutation of the DNA [5]. DNA methylation can occur at the adenine and cytosine bases. A high frequency of cytosine can be found in the promoter region of genes within repetitive sequences of the CG-dinucleotide (cytosine connected to guanosine through a phosphodiester bond, CpG). These repetitive areas of CpG sequences are called CpG-islands and are (depending on the cell type and promoter) mostly not methylated in regular cells, so that the gene is expressed normally. If the CpG-island within the promoter region is methylated, the gene expression will be reduced or, with increasing methylation, eventually even be silenced. Responsible mechanisms for methylation of CpG islands have been investigated and presumably there are multiple factors involved, like elevated expression of DNA methyltransferase DNMT1, inactivation of methylation barriers, the epigenetic drift of aging, lifestyle (e.g. smoking) or mutations of chromosome remodeling gene CHD8 [4, 6, 27, 28]. The CIMP phenotype is still studied to characterize different subsets of CRC CIMP states [29]. One of the typical genes silenced by excessive

promotor CpG island methylation are members of the MMR system, resulting in similar changes as in case of MSI-H tumors, linking these two phenotypes together.

2.1.2.2 Hereditary predispositions for CRC

Lynch Syndrome

This form of predisposition for CRC, also called HNPCC is characterized by a MSI-H phenotype, which is observed in 95% of these cases [30]. In LS the MSI occurs as a result of germline mutations in a gene of the MMR family, in contrast to silencing of MMR genes through aberrant methylation or somatic mutation during the development of sporadic CRC [31]. Most common for LS are mutations of MLH1 and MSH2. Additionally, the deletion of the epithelial cell adhesion molecule (EpCAM) could lead to silencing of MSH2 and therefore lead to LS [32]. A common marker for LS is also a family history of CRC and a marker to distinguish sporadic CRC from LS is a mutation in BRAF, which is rare in LS, but common in sporadic, MSI-H tumors [33]. Of all CRC cases, LS only accounts for 3% [34], and is presented at the early age of 45 years [32]. A person with LS has a 50% chance of developing CRC within their lifetime [35].

Familial adenomatous polyposis

This form of hereditary CRC is associated with a heterozygous mutation of the tumor suppressor gene APC, which is known as the 'gatekeeper' of CRC [36]. It only accounts for 1% of all CRC and is typically clinically manifested by up to thousands of small adenomatous polyps that develop at an early age (15 to 35 years) [32].

2.1.3 Diagnostics of CRC

As over 400.000 people in the EU are diagnosed every year with CRC and over 200.000 CRC patients per year die from it [37], regular screening for early diagnosis is essential as 5 year CRC survival chances drop from 90% for localized disease down to 12% for patients with distant metastasis [10]. Due to varying health care systems and clinical standards through the EU even in the year 2007 there were still eight countries without any CRC screening, six with two screening methods and twelve countries with at least one screening method [37].

2.1.3.1 Molecular screening and diagnostic methods

The most frequently practiced screening method for CRC is the analysis of stool for occult blood (fecal occult blood test, FOBT), which has been implemented as regular screening in 17 countries of

the EU. Gastrointestinal bleeding can have many sources like adenomas, polyps, cancer, but also hemorrhoids or inflammation [38]. Because of its non-invasive character, FOBT is widely accepted by the populations worldwide and has been recommended in 1999 as standard screening for CRC by the EU Committee on Cancer Prevention [39]. After implementation of FOBT in Europe a marked decrease in CRC mortality (15-33%, depending on the country) was observed [40].

Colonoscopy was first performed in 1969, but not yet as clinical routine, as research was still ongoing assessing the risk for patients undergoing this procedure [41]. Soon studies proofed that colonoscopy is reducing CRC mortality and incidence through early detection and possibility to remove adenomas and polyps [42]. As one of the first European countries, Germany made colonoscopy available for CRC screening of the population over 55 years of age in the year 2002 [12]. A less invasive and preparation-requiring, but still endoscopic procedure is the flexible sigmoidoscopy (FS), which inspects the distal part of the colon and identifies patients of a risk group, that require a total colonoscopy. FS has been stated to also reduce CRC mortality up to 26% [43]. Minimally invasive but reported to be as successful as a detection method for CRC and polyps is computed tomographic colonography. This is a radiological test that produces multiple images of the colon. The computed tomographic colonoscopy has not yet proven in clinical trials to be as effective as colonoscopy in reducing CRC mortality [44].

Molecular screening methods also underwent a huge development in the past decade – focusing especially on non-invasive, accurate tests for early detection of CRC. Various possible markers have been evaluated including: DNA, proteins, CTCs, cell-free DNA (cfDNA), messenger RNA (mRNA), micro RNA (miRNA) and long non-coding RNA (lncRNA) [45]. The only successful method adapted by the clinic (approved by the US Food and Drug Administration (FDA)) is a multi-target stool DNA (MTsDNA) test targeting various point-mutations (e.g. of *KRAS* and *CTNNB1*) and methylation status of genes like *Vim* [45]. The MTsDNA has shown a higher sensitivity for detecting CRC compared to FOBT, but a reduced specificity [46]. Besides the analysis of stool, blood markers accessible from a peripheral blood draw (liquid biopsy) have been studied as well to be able to monitor tumors. Detection of circulating tumor DNA (ctDNA) within the cfDNA from plasma has been demonstrated by multiple groups (using either quantitative PCR or sequencing techniques) to have a high concordance with tissue biopsy analysis for important CRC mutations like KRAS and BRAF or methylation status of certain genes and has therefore been concluded to be a promising biomarker in CRC care [47]. The potential of lncRNAs for early diagnosis of CRC has been evaluated as promising as well: CRC adenocarcinoma hypermethylated (CAHM), CRNDE or CCAT1 (a lncRNA from the gene desert region 8q24.21 near *MYC* gene) - all of these lncRNAs have been detected in blood and/or stool and shown a higher frequency in CRC (40-90%) compared to healthy volunteers [48]. Other

markers obtainable from a blood sample are miRNAs which also have shown diagnostic potential in CRC detection in a comparative study of eight miRNAs in plasma and matching tissue of 75 CRC patients and blood of 32 healthy controls [49]. If miRNAs are useful for early diagnosis is still not answered, but studies showed their elevation may only occur around the time point of possible clinical diagnosis of CRC with conventional methods [50]. Another blood-based marker that has been evaluated for CRC are CTCs. They were enriched from the blood of CRC patients in multiple studies using platforms like CellSearch® or CanPatrol® and their evaluation resulted in predictive value of CTCs for poor progression free survival (PFS) and overall survival (OS). Analysis of epithelial and mesenchymal markers allowed to classify patients into higher and lower metastatic potential, but CTCs have not yet proven to be helpful in early CRC diagnosis [51].

2.1.3.2 Classification of CRC

To be able to classify CRC worldwide in a standardized manner, there are a few classification systems using the size of the tumor, how it penetrated different layers of the colon wall, the spread to lymph nodes and the spread to distant sites, to give clinicians a base to determine appropriate treatment choices and probable survival time. The most commonly used staging method is the TNM system by the American Joint Committee on Cancer (AJCC) in which the letters are describing the primary tumor (T), spreading to lymph nodes (N) and probable spread to distant organs (metastasis, (M)). The official classification with description of all possible values for T, N and M are described in **Table 1.**

Table 1: TNM staging in colorectal cancer

Source: https://www.cancer.net/cancer-types/colorectal-cancer/stages; accessed June 14th, 2018

T0	There is no evidence of cancer in the colon or rectum.	**N0**	No spread to regional lymph nodes
Tis	Carcinoma in situ (Cancer cells are found only in the epithelium or lamina propria)	**N1a**	Tumor cells found in 1 regional lymph node
T1	The tumor has grown into the submucosa	**N1b**	There are tumor cells found in 2 to 3 regional lymph nodes
T2	The tumor has grown into the muscularis propria	**N2a**	There are tumor cells found in 4 to 6 regional lymph nodes
T3	The tumor has grown through the muscularis propria and into the subserosa	**N2b**	There are tumor cells found in 7 or more regional lymph nodes
T4a	The tumor has grown into the surface of the visceral peritoneum	**M0**	The cancer has not spread to a distant part of the body
T4b	The tumor has grown into or has attached to other organs or structures	**M1a**	The cancer has spread to 1 other part of the body beyond the colon or rectum
		M1b	The cancer has spread to more than 1 part of the body other than the colon or rectum.
		M1c	The cancer has spread to the peritoneal surface

Tumor staging usually happens at time of diagnosis using imaging techniques (e.g. x-ray, CT scans and others) for M and by pathologists after surgery for N and T. Doctors determine how far the tumor has grown from the colon or rectum epithelium through submucosa, muscle, serosa or even spread to surrounding lymph nodes or distant organs (layers of the colon wall are illustrated in **Figure 2**).

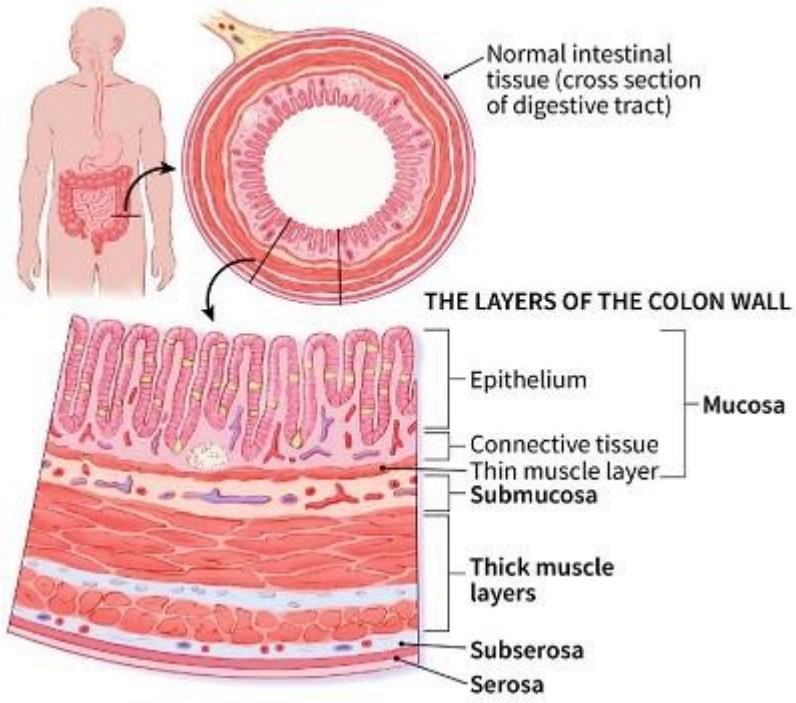

Figure 2: Layers of the colon wall. For TNM staging it is important for pathologists to determine how far through the colon tissue the tumor has grown to determine the T stage. Here the layers of the colon are shown in cross sections from the inner epithelium that forms together with the connective tissue and a thin muscle layer the mucosa, then the submucosa, thick muscle layers to the outer subserosa and serosa. Source: https://www.cancer.org/cancer/colon-rectal-cancer/detection-diagnosis-staging/staged.html, accessed July 5th, 2018.

After all three factors have been evaluated; an overall clinical stage is appointed taking the TNM classifications into consideration. Stages reach from 0 to IV, with higher numbers being associated with further advanced cancer. How the overall stage is composed of the varying TNM stages is shown in **Table 2**.

Table 2: AJCC staging with according TNM stages in CRC

(8th edition, manually adjusted, source: https://www.cancer.org/cancer/colon-rectal-cancer/detection-diagnosis-staging/staged.html, accessed July 5th, 2018)

AJCC Stage	T	N	M
0	Tis	N0	M0
I	T1 or T2	N0	M0
IIA	T3	N0	M0
IIB	T4a	N0	M0
IIC	T4b	N0	M0
IIIA	T1 or T2	N1 or N1c	M0
	T1	N2a	M0
IIIB	T3 or T4a	N1 or N1c	M0
	T2 or T3	N2a	M0
	T1 or T2	N2b	M0
IIIC	T4a	N2a	M0
	T3 or T4a	N2b	M0
	T4b	N1 or N2	M0
IVA	Any T	Any N	M1a
	Any T	Any N	M1b
	Any T	Any N	M1c

Additionally to the TNM staging, other factors are taken into consideration for clinical classification of colorectal tumors. The grade (G) is determining the degree of differentiation of tumor cells. The lower the grade (most commonly in the range G1-G3) the more similar are the cells to healthy intestine mucosa. CRC with a high grade can grow faster and might need more intense treatment than the staging may advise. In addition to tumor morphology, it has been proven within the past five years that primary tumor location is relevant for survival prognosis and treatment choice [52]. The cecum and ascending colon are right-side CRC, the descending and sigmoid colon as well as the rectum are considered left-side CRC (see **Figure 3**). The transverse colon is considered right-sided from the proximal point to the splenic flexure, as this part arose from the hindgut and the rest from the midgut [53]. Loupakis et al. showed that patients with left-side tumors have longer OS and PFS and suggested this might result from observed differing molecular alterations in right-sided CRC like higher *BRAF* mutations and higher expression of ERCC1 (which was associated to chemoresistance) [54, 55].

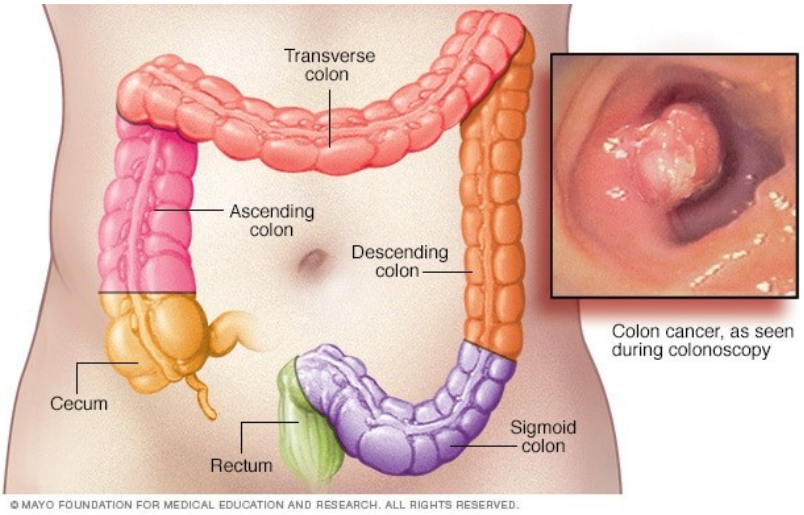

Figure 3: Locations of colorectal cancer. The cecum and ascending colon are considered right sided CRC, the descending and sigmoid colon and the rectum left sided CRC. The transverse colon is mostly considered right-sided CRC, but might make up a third category of CRC locations. Source: https://www.mayoclinic.org/diseases-conditions/colon-cancer/symptoms-causes/syc-20353669, accessed July 5th, 2018.

2.1.3.3 Molecular markers for therapy decision

Molecular markers are also used for therapy decision making in CRC. For example levels of CRC markers like cancer antigen 125 (CA125) and carcinoembryonic antigen (CEA) are evaluated in blood serum [56, 57]. From solid biopsies of CRC tumors, the mutation status of the proto-oncogenes *KRAS (*a regulator of cell signaling controlling proliferation) and *BRAF* (involved in cell growth) in tissue are essential for treatment decision making. These two genes (and lately also other genes like *NRAS*) have been proven to be markers of resistance to anti-EGFR therapy [58].

In addition to pathologic and radiologic classification, molecular features of CRC have to be taken into account. Therefore, a classification in two groups has been proposed for CRC: 1) hypermutated CRC with MSI (defect in MMR) and 2) non-hypermutated CRC that shows the frequent mutations of genes involved in CRC development (like *KRAS*, *TP53*, *APC*, *PIK3CA*), but is microsatellite stable [59]. Further molecular classification systems that are separating CRC in four groups were proposed, with a split of the MSS CRC into three groups [60]. These molecular features have also shown to be different depending on the location of the tumor as for example right-sided CRC has been observed to have a higher prevalence of MSI-high tumors, BRAF mutation and high CIMP [61].

An international consortium of data sharing has developed the consensus molecular subtypes (CMS) for consistency in CRC classification by using six classification systems to form 4 molecular subtypes of CRC: CMS1, which is MSI immune and makes 14% of all CRC; CMS2, the canonical CRC making 37%

of CRC, epithelial type with WNT and MYC signal activation. CMS3, the metabolic subtype representing 13% of CRC with dysregulation of metabolic pathways and finally CMS4, the mesenchymal subtype with transforming growth factor-ß (TGF-ß) activation and angiogenesis, which covers about 23% of CRC cases [62].

Together with information of familiar predisposition these various classifications allow the clinician a precise choice of cancer care.

2.1.4 Therapies for CRC

The therapy options for CRC have improved immensely through the past two decades as new targets have been discovered and drugs have been developed and approved as in detail explained in this chapter. Treatment can be classified in: local treatment (surgery, ablation and radiation) and systemic treatment (chemotherapy, targeted therapy and immunotherapy). If the cancer has not spread to distant organs (M0), CRC is mainly treated with surgery in a curative intent [63]. In case of lymph node involvement (AJCC stage III) adjuvant (applied post resection) chemotherapy has proven to prolong overall survival (OS) [64]. For patients with stage IV CRC, surgery is still the only chance for a cure as other therapies may prolong survival but have no curative impact. Surgery techniques and approaches have been improved, allowing simultaneous resection (liver metastasis and bowel tumor). It is also possible, in selected cases of younger patients with enough liver volume, that liver metastasis is resected before the bowel tumor resection [65]. For resection of liver metastases, the limitation is always the remnant liver volume, number of lesions, involvement of vasculature and the location of the lesions within the liver [64]. In case of bowel obstruction, the primary tumor must always be resected first. The safety and longest possible survival of the patient are always the priority when choosing the best possible treatment plan.

2.1.4.1 Radiotherapy

Radiotherapy (RT) can be given preoperative (neoadjuvant) or adjuvant. Before resection, it will contribute to shrinkage of the tumor and therefore support or facilitate complete tumor removal. Additionally, tissue is more sensitive to radiation before surgery but complications might occur due to higher fragility of the tissue caused by the radiation [66]. Before surgery, RT is usually given in combination with chemotherapy to enhance the mentioned benefits. After surgery, RT may be applied in case of impossible complete resection of the tumor or to prevent recurrence. Also, intraoperative RT may be applied for the same reason. Last, RT can be used as palliative therapy to

improve life quality by easing symptoms if the patient is not stable enough for surgery or advanced tumors are causing pain or the cancer has spread to multiple distant organs [67].

2.1.4.2 Chemotherapy

Much like RT, chemotherapy (CT) can be given neoadjuvant (to shrink tumor mass) or adjuvant (to eliminate residual disease) or palliative (in advanced cases). CT can be taken systemically (influencing the entire body) or regionally, e.g. through hepatic artery infusion to reach liver metastasis and therefore reduce side effects by using a lower dosage [68]. The National Comprehensive Cancer Network (NCCN) released CRC treatment guidelines containing a comprehensive list and description of treatment possibilities and explanation of decision making in particular cases [69].

The most common and successful CT for CRC is 5-Fluorouracil (5-FU) which has been developed by Dr. Charles Heidelberger in 1957 [70]. This antimetabolism drug is a pyrimidine analog and it's activation inhibits synthesis of thymidine [71]. After activation of 5-FU, 5-F-dUTP is incorporated into RNA and DNA and those lesions are then recognized by excision repair enzymes, leading to cell cycle arrest and finally cell death [71]. Its efficacy can be potentiated by higher folinic acid levels [72]. Studies of biomodulation of 5-FU by the 5-formyl derivative of tetrahydrofolic acid (leukovorin) confirmed its anti-tumor impact in supporting 5-FU function and it is now always applied together with 5-FU [73]. Other substances are also using the same mechanisms as 5-FU, like Capecitabine (a precursor of 5-FU). Antimetabolites like 5-FU are however limited by low selectivity and therefore they cause toxicity in other areas of the patient's body like the nervous system [74].

Another cell toxin used in CT against CRC is Irinotecan which is a campothecin analog and causes inhibition of DNA synthesis resulting in cell death [75].

A major branch of CT in CRC is platinum-based therapy. The three major platinum complex drugs used in CRC are cisplatin, carboplatin and oxaliplatin [76]. CRC cells tend to overexpress organic cation transporters providing entry into the cell for platinum complexes which make CRC especially sensitive for these drugs [77]. Once within the cell, the platinum complexes are activated by water (exchange of chloride for water molecules) and react with purine bases of DNA. This leads to cross-linking of neighboring guanine bases or even inter-strand cross-linking [78]. The generated DNA lesions may be repaired or bypassed, but cell division is stopped and often apoptosis is induced. It was proven to prolong survival even in stage III patients, but the side effects of platinum therapy (70% of patients experience peripheral neuropathy) are common reasons for therapy discontinuance, even more common than tumor progression [76]. Standard treatment for metastatic CRC is oxaliplatin in combination with 5-FU and leucovorin (FOLFOX). Other combination CTs in CRC

standard of care are FOLFIRI (5-FU, leucovorin and irinotecan), CAPEOX (capecitabine and oxaliplatin) and FOLFOXIRI (5-FU, leucovorin, oxaliplatin and irinotecan) [69].

2.1.4.3 Biologic targeted Therapy

As the pathways of the heterogeneous CRC development got uncovered, researchers developed targeted therapies to attack tumor specific molecular features. The two available targeted therapies against CRC are containing antibodies that recognize the vascular endothelial growth factor (VEGF) or the epidermal growth factor receptor (EGFR). The VEGF protein plays a major role in vasculogenesis and angiogenesis, both processes are necessary for growth and to supply the tumor with oxygen and nutrients. Tumor cells use VEGF signaling to communicate with endothelial cells to activate blood vessel growth. There are multiple members in the VEGF family (VEGF-A, -B, -C, -D), but VEGF-A has been identified as the major player. In 2004 bevacizumab (Avastin®, Genentech), a monoclonal antibody (mAb) that neutralizes human VEGF-A was approved by the FDA for treating metastatic CRC [79]. Until this year, the European Medicines Agency (EMA) has approved in total four anti-angiogenesis agents (bevacizumab, aflibercept, ramucirumab and regorafenib) who are targeting various VEGF family members and the VEGF receptors for the treatment of metastatic CRC (mCRC). Nevertheless, biomarkers to predict anti-VEGF treatment efficacy to prevent needless side effects and overtreatment are still missing [80].

Cellular growth is essential for cancer development. When the epidermal growth factor (EGF) binds to the surface receptor for EGF (EGFR) on cancer cells, a signaling cascade resulting in cell proliferation is triggered. This cascade includes RAS/RAF families, MEK and ERK. To block this signaling pathway, two mechanisms have been developed for application in the clinic: 1) tyrosine kinase inhibitors (TKIs) that bind to the catalytic domain of EGFR and block downstream signaling or 2) monoclonal antibodies that bind with high affinity to the extracellular EGFR domain, blocking the protein for ligands and inhibiting cell growth, metastases and even initiating cell death [81, 82]. Available drugs that act as TKIs currently on the market are erlotinib and gefitinib and mAbs against EGFR are amongst others cetuximab and panitumumab. Unlike for the anti-VEGF therapy, there are biomarkers for anti-EGFR therapy. If a patient carries an activating mutation in a gene downstream of EGFR, anti-EGFR therapy will not be successful. This prediction was confirmed for mutations in *KRAS*, *PIK3CA* and *BRAF* [83, 84]. Even if there is no mutation in KRAS, only about 35% of patients respond to anti-EGFR therapy, which makes a comprehensive molecular profile of the tumor for personalized therapy even more desirable [85]. Besides the already named mutations, there are other resistance mechanisms influencing anti-EGFR therapy efficacy. In case of PTEN loss, downstream EGFR cascade is activated independent of EGFR signaling. Also, activation of JAK (Janus tyrosine kinase) and STAT

(signal transducer and activator of transcription) families as well as amplification of MET and Her-2 contribute to anti-EGFR therapy resistance [86].

2.1.4.4 Other perspectives

Discoveries in immunotherapy revealed that it is possible to activate or block immune system checkpoints acting as an on/off-switch of immune response. The protein programmed death 1 (PD-1) on the surface of T-cells prevents an immune attack of a cell if it binds to PD-L1. A PD-1 inhibitor (pembrolizumab) has shown prolonged OS and PFS for patients with high MSI tumors or mismatch repair gene deficiency in a phase II trial [87].

Just last year the FDA approved two PD-1 inhibitors (nivolumab and pembrolizumab) for patients with unresectable or metastatic CRC that is also MSI-high or has mismatch repair deficiencies [88, 89]. Different checkpoint inhibitors have been developed against PD-L1 (avelumab) and cytotoxic T-lymphocyte-associated protein 4 (CTLA-4, ipilimumab) [90].

Discovering new targets in the four subtypes of CRC (CMS1 – 4) in combination with immunotherapy has been discussed as a next goal with tumor infiltrating lymphocytes as possible targets as the presence of immune cell infiltration within the tumor tissue has recently been proven to be an even stronger prognostic marker than TNM classification [91].

Another category of novel approaches are epigenetic therapies in CRC. Epigenetic regulation of gene expression functions through DNA methylation, alteration of histone or non-coding RNAs regulation, have an important function in CRC. It has been suggested that a combination therapy of epigenetic agents like histone deacetylase together with conventional chemotherapy as 5-FU, oxaliplatin or irinotecan may be effective and prevent drug resistance. These epigenetic agents are still being evaluated in clinical trials [92].

2.1.5 Biomarkers in CRC

In chapter 2.1.3 and 2.1.4 many biomarkers have already been mentioned. The following chapter will give a compact overview of all relevant biomarkers currently used or investigated in the clinic for CRC detection, therapy guidance and survival prediction.

2.1.5.1 Markers for CRC detection and classification

Besides colonoscopy, FOBT is still the most commonly used test for CRC detection, though with low sensitivity and specificity, therefore analysis of fecal DNA is tested to improve FOBT results in the future [93].

The most commonly accessed molecular markers through detection of tumor DNA in stool are mutations in *KRAS*, *APC*, *TP53* and markers to detect MSI [94], all of them allow further classification of CRC tumors as described earlier.

Evolving blood-based markers are represented by the non-coding microRNAs (miRNA). They are detectable in peripheral blood, originate e.g. from exosomes or are secreted by tumor cells [61], and they possess a high stability in blood. Their sequence may cause silencing of target genes, which could influence progression of tumors. Multiple studies validating miRNAs with q-PCR have successfully shown differential expression of various miRNAs in CRC and advanced adenoma compared to healthy individuals [95, 96]. These studies show that miRNAs are potential biomarkers for early detection of CRC.

2.1.5.2 Predictive markers for possible targeted-treatment

For targeted treatment against EGFR, the regularly assessed biomarkers in the clinic predicting therapy inefficacy are mutations of the *RAS* family genes and *BRAF*. All these genes act downstream from the EGFR receptor and a mutation in either of them predicts failure of anti-EGFR treatment. As resistance against anti-EGFR therapy arises usually a few months after first administration, additional targets in *KRAS* wildtype (*KRAS*-wt) patients have been tested. In *KRAS*-wt CRC, HER2 (human epidermal growth factor receptor 2) positive tumors have shown a response rate of 30% when treated additionally with trastuzumab and lapatinib (both anti-HER2 therapies) [97]. This result makes HER*2* a promising biomarker for *KRAS*-wt CRC in the future.

Another marker for targeted therapy is already the CRC location. Boeckx et al. have shown that patients with left-sided and *RAS* wt CRC benefit more from panitumumab (anti-EGFR) treatment than right-sided *RAS* wt patients [98]. Also has left-sided CRC been proven to be associated with longer PFS in *KRAS*-wt patients treated with cetuximab, while there was no benefit for right-sided CRC patients [99].

2.1.5.3 Predictive markers for Chemotherapy

The CRC location together with mutation status of genes like *KRAS*/*BRAF* can already be predictive for CT success [100], as described earlier.

Studies for predictive biomarkers of 5-FU CT are hard to execute as it is unethical to have a non-treated control group. The expression of thymidylate synthase (enzyme that is inhibited by 5-FU) has been tested in CRC as a probable marker for 5-FU sensitivity prognosis [101], but as control groups are missing the results are no proof for predictive value of thymidylate synthase, even though low levels were associated with improved OS. Another biomarker associated with 5-FU is MMR status as MMR-deficient tumors do not benefit from adjuvant 5-FU therapy [61] and so according to the latest guidelines for CRC, new diagnosed patients with AJCC stage II CRC will have their tumor tested for MMR status.

Studies for predictive biomarkers for response to irinotecan have been performed, but only few and with controversial results [102], therefore none of the tested markers is ready for clinical use. But the most promising one was TOP1 (topoisomerase 1), the target of irinotecan. In a study from Braun et al. an increased expression of TOP1 was associated with benefit from irinotecan and interestingly also with benefit from oxaliplatin [103]. Other promising predictive markers for oxaliplatin benefit have been expression of members of the pathway of DNA nucleotide excision repair (NER) proteins. ERCC1 has shown potential to be predictive for benefit from oxaliplatin, but ERCC3 and ERCC4 have been also considered for future analysis [102].

2.1.5.4 Prognostic markers in CRC for survival

One of the first prognostic markers in CRC was CEA. When this blood serum marker is elevated (>5ng/ml) the patients have a poorer prognosis than those without elevated levels of CEA [104]. CEA has been widely used in the clinic for patient monitoring. Additionally the Carbohydrate-Antigen 19-9 (CA19-9) has been tested in serum and a cut-off of 37U/ml is associated with shorter OS [104].

As already mentioned, patients with left-sided CRC have also a better survival prognosis which is caused by differing molecular features of left- and right-sided CRC [61]. Right-sided CRC has a higher prevalence of CIMP, MSI and *BRAF* mutation and therefore causes shorter survival. BRAF mutation alone has been associated to shorter OS in a study of 56 patients with mutated *BRAF* in advanced CRC [105].

Expression of ERCC1 has been tested as a predictive marker for benefit from oxaliplatin treatment, but has shown a stronger association with survival [106]. Patients with ERCC1-negative tumors had significant longer OS.

Presence of CTCs detected in peripheral blood has also proven association with reduced survival in CRC patients [7]. More detailed information about origin, properties and clinical implications of CTCs will be discussed in the following chapter.

2.2 Introduction to circulating tumor cells

Studies have shown that cancer is a heterogeneous disease with specific subtypes of malignant cells within one tumor [107, 108]. Each subtype may express different growth factors or have varying gene mutation status and therefore be responsive to varying chemotherapy [109]. Especially the discordance between the primary tumor and the metastatic lesion is a strong indicator that the expression of important oncogenes is not static, but rather a dynamic process [110–112]. Evolution of cancer in the patient causes a challenge for oncologists. With a changing expression pattern and mutation status of oncogenes, therapy should be adjusted. To be able to detect newly occurring therapy targets, the tumor would have to be sampled regularly, which is clinically unfeasible to do with an invasive solid biopsy and might constitute a risk for the patient. Therefore, the concept of regularly and easy accessible sampling of the changing tumor by utilizing CTCs as fluid surrogates of dynamic tumor evolution in the blood (detectable through a 'liquid biopsy') is getting more and more important in the clinic. Liquid biopsy could contain cells from the tumor and multiple metastatic sites and therefore might provide an even more informative sample of the tumor burden of the patient than a solid biopsy sample from a single site or when solid biopsy is impossible. Also it can detect minimal residual disease after chemotherapy or radiation.

Most localized solid tumors can be cured by surgery [9], but with the occurrence of metastasis, surgical resection of the tumor is often insufficient. In CRC, spread of the disease to metastatic sites is shortening patient survival [113]. Expansion of the tumor to distant sites can occur either by lymphatic spread of tumor cells, direct intracavitary spread or by cells, that have dissociated from the solid tumor then intravasated the vasculature and travel in the blood either as single cells or as cell clusters (two or more cells attached) [114]. These circulating tumor cells (CTCs) have the potential to establish distant metastasis, even though not every CTC will contribute to metastatic seeding. In CRC, even early diagnosed patients that have undergone tumor surgery may experience recurrent or metastatic disease within five years. An explanation may be a latent metastatic disease process or shedding of tumor cells i.e. CTCs with metastatic potential into the blood stream [115, 116]. Thus, it should be possible to detect metastatic potential in CRC patients early through the detection of CTCs. So far, studies showed that CTC enumeration is a prognostic biomarker in advanced CRC, but in the non-metastatic setting results are controversial [117].

The physician Thomas Ashworth first described CTCs in 1869 after observing cells in the blood of a cancer patient with a morphology identical to the cells in the patient's tumor [118]. These rare cells are challenging to detect and are not necessarily present at all time points a blood draw is taken from a cancer patient. They are hidden amongst the large variety of hematopoietic cells in the vasculature and account only for approximately 1-10 cells/ml blood [119]. Today there have been many

properties detected that distinguish CTCs from WBCs and are useable for the detection of CTCs. Many methods are on the market, but the development of more effective and sensitive methods for CTC detection is still ongoing. What these methods are, what markers and CTC specific properties they use and how CTCs are influencing clinical practice at present is described in the following paragraphs.

2.2.1 Biological and physical properties of CTCs

CTCs from solid tumors are cells with epithelial origin and therefore possess biological and physical properties that enable their differentiation from surrounding blood cells.

2.2.1.1 Biological properties of CTCs

Epithelium specific protein markers

The most commonly used marker to detect CTCs in the blood is the epithelium specific cell adhesion molecule EpCAM. This transmembrane glycoprotein is mediating cell-cell adhesion in healthy epithelium and because it is exclusively expressed by epithelial cells, it clearly distinguishes CTCs from blood cells. Other epithelium specific markers are cytokeratins. These keratin proteins are part of intermediate filaments in the cytoskeleton of an epithelial cell. Under certain conditions CTCs of epithelial origin may undergo changes and loose the expression of epithelial markers like EpCAM (further explanation in chapters 2.2.2.1 and 2.2.2.3).

Tumor origin specific markers

The proteomic profile of a CTC does not only reflect its epithelial origin, but also the protein profile of the tissue from which it originated, and is therefore organ-specific. The established immunohistochemistry stains used on tissue biopsy samples in pathology can be used on CTCs as well for either enrichment of CTCs in a blood sample or for determining their origin. Markers used are e.g. the prostate-specific antigen (PSA), thyroid transcription factor 1 (TTF-1) or the homeobox protein CDX2 (for gastrointestinal differentiation) [120].

Clinically actionable markers

Several particular protein markers assessed from tissue biopsies are used for therapy guidance and clinical practice. Those markers can also be detected in CTCs and numerous studies are comparing the presence of those markers in CTCs and corresponding primary tumors and metastatic lesions [121]. Markers valuable for treatment decisions are for example the epidermal growth factor receptor (EGFR) in CRC [122] or the receptor tyrosine-protein kinase HER2 in metastatic breast

cancer [123]. Patients are evaluated by the presence of therapy targets to determine if targeted chemotherapy (like cetuximab or lapatinib) can be applied and might be beneficial. During disease development, the protein expression profile might change quickly, so that the distant metastasis or CTCs may vary in gene expression and mutation status of possible therapy targets from the primary lesions. Therefore CTCs are investigated for their potential advantage over solid biopsies in therapy decision making and monitoring of disease evolution [124].

2.2.1.2 Physical properties of CTCs

Cells derived from a tumor can possess structural changes within the cytoskeleton, variable size and shape or chromosomal alterations which lead to varying nucleus/cytoplasm (N/C) ratio. This leads to various physical properties that allow differentiation of CTCs from blood cells.

Diameter of CTCs

Depending on the tissue type a CTC derives from, their size can vary, but usually exceeds the size of most of the surrounding blood cells. Whereas small cell lung cancer CTCs may only reach a diameter of 10 µm (around the same size as a the most abundant WBC, a neutrophil), a breast cancer derived CTC might reach a diameter as big as 70 µm and some CTCs from prostate cancer have been shown to reach a diameter of up to 100 µm [125]. The blood cells surrounding CTCs have varying diameters depending of the cell type (overall though smaller than most CTCs): erythrocytes are the smallest blood cell (pseudo cell, as they do not have a nucleus) group with about 8 µm, followed by lymphocytes with up to 15 µm and monocytes being the largest blood cell group in peripheral blood with up to 20 µm [126].

Deformability of CTCs

The varying ability of a cell to change shape under the application of stress is called deformability. Experiments have shown that CTCs have a higher deformability the higher their metastatic potential but are in general less deformable than WBCs [127]. The stiffness of CTCs results from a larger nucleus and protein expression causing changes in the cytoskeleton differing from those in a WBC. It was shown that CTCs with a high metastatic potential activate expression of proteins linked to shape change and increased motility, which modifies the cell to be more flexible, but still stiffer than a WBC [128].

Electrical charge of CTCs

Due to the different protein expression profile and changes in the DNA content due to polyploidy, CTCs possess a higher amount of polarizable molecules suspended in the cytoplasm and nucleus. This

differing ratio between the solvent and the polarized particles results in a useable dielectric property to distinguish CTCs from WBCs [129].

Density of CTCs

The weight per volume of a cell is measured as its density. In whole blood the densest cell type are erythrocytes, because they contain the protein hemoglobin, which binds iron [130]. A study proved that leukocytes have the lowest density from all nucleated blood cells and therefore CTCs reside in the buffy coat, the layer between red blood cells (RBCs) and plasma [131].

2.2.2 Dynamics of CTCs

CTCs are considered as originally being part of a sessile epithelial cell collective attached to a basal membrane and connected through various junctions. A huge part of CTC research was and still is uncovering the mechanisms how and why exactly tumor cells are leaving their sedentary state to enter the vasculature, which causes hemodynamic stress and immune response [132]. Some of the processes involved have been already discovered and are described in the following paragraphs.

2.2.2.1 Active CTC migration

The active migration of epithelial tumor cells away from their sedentary state has been extensively studied. The main and mostly accepted theory is that the tumor cells undergo epithelial-to-mesenchymal transition (EMT). Various intracellular pathways are taking part in this process, where epithelial cells lose their junctions, adhesion to basal membrane, apical-basal polarity and change into an elongated cell with increased motility and invasive potential [133].

The signaling cascade triggering EMT is partly activated by the tumor microenvironment [134]. Main factors for higher invasiveness are the transforming growth factor β (TGF-β), which is secreted by WBCs, macrophages and platelets [135], secretion of pro-inflammatory cytokines by fibroblasts [136] and interactions between macrophages that also secrete the epidermal growth factor (EGF) and the cancer cells carrying the EGF-receptor. The attracted tumor cells are then moving along collagen fibers towards the vasculature driven by this paracrine-loop induced chemotaxis [137].

When a tumors oxygen supply is low (<40 mmHg), hypoxia inducible factors (HIFs) are activated and trigger EMT through binding to the promoter regions of transcription factors responsible for EMT [138, 139]. These triggers and the activation of various transcription factors including Zinc finger E-box-binding homeobox 1 (ZEB1), forkhead transcription factor 2 (FOXC2), twist family bHLH transcription factor 1 (TWIST) and the snail family transcription repressors SNAIL and SLUG [133]. The

induced signaling networks result amongst others in the down regulation of E-cadherin (a cell adhesion molecule) and the upregulation of N-cadherin (which is called the cadherin-switch) and eventually leads to motility and invasive characteristics [140]. Other regulatory factors increased during EMT are Twist, Zeb1, integrins (e.g. ß1 and αVß5), Akt2 and others. Some proteins are dissociated from epithelial complexes and moved towards the nucleus (β-catenin) and protein expression for epithelial characteristics might be down regulated (cytokeratins) [141–144]. The former anchor-dependent epithelial cell is rebuilt: the cytoskeleton now mainly contains vimentin-rich intermediate filaments instead of cytokeratins [145], migration is enabled by lamellipodia or filopodia formation and cell adhesion and polarity are lost. This allows movement through stroma and intravasation into the vasculature and survival in the blood stream [142, 145]. It has even been observed by pathologists that small aggregates of cells detach from an adenocarcinoma and migrate over short distances; this observation has been called tumor budding and was related to EMT and considered a parameter of tumor progression [146, 147].

2.2.2.2 Passive CTC shedding

In contrast to active migration of tumor cells into blood stream, the passive shedding of cells into the vasculature through parts of the tumor breaking off is supported by pathologists observations of tumors growing inside blood vessels [148, 149]. Single cells or even clusters of cells could be torn off by the hemodynamic suction and then circulate in the vasculature. It is even suspected that circulating tumor cell clusters (CTCCs), that have broken off a tumor may get stuck in small capillaries, which could eventually support metastasation [150]. Other studies show that the luminal surface of tumor blood vessels are often composed of a mix of tumor cells and endothelial cells (mosaic vessels). In colorectal cancer biopsies the group of Chang et al. has observed that 13.4% of the blood vessels in the tumor were mosaic. The group suggests that after endothelial cells are shed, tumor cells get exposed to the blood vessel lumen and may participate in vessel wall composition [151].

2.2.2.3 Survival of CTCs in Circulation and possible seeding

Survival in the bloodstream

In a healthy epithelial tissue, a cell that has lost its interactions to the surrounding cells and to the extracellular matrix will undergo anoikis [152]. This cell death is a protection from cells that detach from their surrounding extracellular matrix (ECM) during uncontrolled growth. CTCs that have just lost their connections to neighboring cells and intravasated into the blood stream are additionally

facing the sheer force in the vasculature and elimination by the immune system. In order to survive, they instantly associate with platelets through cell surface tissue factors. This association offers physical protection (platelets shielding the CTCs), but platelets also secrete growth factors like transforming growth factor beta (TGF-ß) and platelet derived growth factor (PDGF) which are able to inhibit natural killer cell activity and sustain already induced pathways of EMT [153]

Studies measuring the survival rate and time of CTCs in a mouse model of kidney cancer report 89% non-viable cells immediately after shedding and an approximate survival time of maximal 24 hours in breast cancer patients [154, 155]. However, one option to prolong survival is activation of a dormant state. During dormancy, proteins for cell proliferation are down regulated (cell proliferation protein Ki-67) and cells remain in a temporarily stopped cell state in the blood or bone marrow. Researchers suggest that cells might apply this mechanism to acclimate to new microenvironments [156].

Establishment of metastasis

To establish a distant metastasis, a CTC has to extravasate the vasculature and start to proliferate at a distant site. In 1889 Dr. Stephen Paget proposed the 'seed-and-soil' theory, which proposed the need of a favorable microenvironment in order for a tumor cell to be able to establish metastasis [118]. This 'soil' has to be composed of stromal cells and proteins of the ECM to support proliferation and survival of the 'seed' [157]. The travelling cells have to undergo a redesign to regain cell-cell and cell-matrix interactions. This reverse process of EMT was proposed as mesenchymal-to-epithelial transition (MET) [133]. Key proteins in MET include cell adhesion molecules (CAMs) and all proteins supporting epithelial state (like E-cadherin and β-catenin) [158].

2.2.3 Methods to detect and capture CTCs

As already explained in chapter 2.2.1 (page 21), CTCs can be distinguished from surrounding blood cells by their physical and biological properties. Many methods have been developed over the last 70 years since the surgeon Dr. Engell in 1955 first used saponin to lyse red blood cells and thus enriched the WBCs and CTCs [159]. But to detect such rare cells with necessary sensitivity is a 'needle in the haystack' challenge.

2.2.3.1 Positive selection of CTCs

Despite all efforts over the last decades, up till today, there is only one CTC detection system approved by the EU and the FDA, the CELLSEARCH® system (Veridex, Warren, USA). This system is performing positive selection of CTCs utilizing ferrofluid nanoparticles coated with antibodies against EpCAM. EpCAM expressing cells are magnetically separated from leukocytes and then stained with

anti CK antibodies (CK8, CK18, CK19), anti CD45 (a specific leukocyte antibody) and the nucleic acid stain DAPI (4',6-Diamidin-2-phenylindol). CTCs are defined as EpCAM expressing cells that have a nucleus ($DAPI^{pos}$), are CK^{pos} and $CD45^{neg}$ [160].

Other CTC detection techniques have been developed, but the majority is utilizing EpCAM for detection and enrichment of CTCs [161]. There are microchips like the CTC-chip where CTCs are captured on EpCAM-coated microposts [162], the MagSweeper®, where the sample is mixed with EpCAM labeled antibodies and then a magnetic shaft is 'sweeping' CTCs out of the sample, or the *in vivo* CellCollector® (GILUPI GmbH, Potsdam, Germany) that utilizes an EpCAM-coated nanoguidewire, which is inserted in a patients vein for 30 min to capture CTCs [163, 164]. Instead of using only EpCAM for positive CTC enrichment the AdnaTest® (QIAGEN, Hilden, Germany) uses a combination of antibodies against other markers of CTCs (EpCAM, Her2, MUC1), but is still limited to enrichment of CTCs expressing at least one of the targets [165].

Sensitivity for these methods can be evaluated using cancer cell line spiking experiments. A known number of cells are spiked into a blood sample of a healthy donor and the recovery rate is determined.

Sensitivities and specificities vary excessively depending on the method applied. For the CELLSEARCH® system a sensitivity of at least 85% and specificity of 99.7% has been stated in a study with 964 metastatic breast cancer patients and 199 women diagnosed with benign breast disease and 145 healthy women [166]. For the AdnaTest® 80% sensitivity and 97% specificity were reported in metastatic breast cancer [165].

2.2.3.2 Negative selection by WBC depletion

Another method to enrich CTCs is the depletion of leukocytes after RBC lysis. The EasySep® (STEMCELL Technologies, Vancouver, Canada) utilizes magnetic beads, that are labeled with anti CD45 antibodies [167]. An advantage of this method is the viability of the CTCs, which is not always assured after positive selection methods that use EpCAM detection [168]. But due to a portion of leukocytes being left behind, the purity of CTCs enriched by WBC depletion is lower compared to positive selection of CTCs [169].

2.2.3.3 Other methods

<u>Enrichment of CTCs by physical properties</u>

Using the differing density of CTCs (as mentioned in chapter 2.2.1.2), the OncoQuick® system (Greiner Bio-One GmbH, Frickenhausen, Germany) separates CTCs from other blood cell types by

density gradient centrifugation [170]. Other systems make use of the differing size of CTCs and WBCs. The best-known filtration device for CTC isolation is ISET® (RARECELLS US Inc., Austin, USA) using a polycarbonate filter with a pore size of 8 µm [171].

Combined methods of CTC detection

The approaches mentioned above can also be combined to achieve a higher specificity in CTC detection. An example is the epithelial immunospot technology EPISPOT, that first utilizes CD45 depletion and then detects viable CTCs by observation of protein secretion using culture plates pre-coated with antibodies for the proteins of interest [172]. Furthermore, techniques have been developed combining RBC lysis and density centrifugation with CTC detection through anti-EpCAM labeled antibodies (maintrac®, Simfo GmbH, Bayreuth, Germany) [173] or the combination of filtration by size and RNA in situ hybridization (CanPatrol®, SurExam Biotech Ltd., Guangzhou, China) [174].

Nonenrichment strategy: Direct Analysis of CTCs

One strategy that avoids any pre-selection of a cell population carrying a specific marker is the high definition single cell analysis (HD-SCA) platform (Epic Sciences, San Diego, USA), that has been developed by Dr. Kuhn and colleagues [175]. Only RBC lysis is performed before all other blood components (leukocytes, platelets, exosomes and CTCs) are plated on a microscopy slide and then stained with fluorescence tagged antibodies against CD45 (leukocyte marker), CKpan (epithelial specific cytokeratin pan mix) and a nucleic acid stain (DAPI). Whole slides are then scanned and customized software detects cells of interest using fluorescent signal positivity and absence of it, but also taking nuclear size and cell size into consideration. Thus cells of interest and therefore probable CTCs are detected depending on their epithelial or cancer specific marker and depending on their morphology, as availability of a picture for each cell on the slide allows analysis of CTCs on the background of surrounding WBCs. The potential of the HD-SCA workflow to reflect the entire population of CTCs and the possibility to continue after CTC detection with single cell analysis by isolating single CTCs from a slide with a micro-manipulator was exploited by our laboratory thanks to the collaboration with the group of Dr. Kuhn. Specifics about this method are in detail explained in chapter 4.

2.2.4 Downstream characterization of CTCs

Most of the techniques for CTC detection and capturing mentioned in 2.2.3 have the goal of CTC enumeration. This strategy has been proven effective for some solid tumors like breast, prostate and lung, but has not been sufficient for treatment decisions, early detection or disease monitoring [176].

Therefore, during the last years the focus of CTC research became more and more targeted on the methods that reach further than enumeration itself. As CTCs are the interstage between a primary tumor and the distant metastasis, it could be very valuable for clinical research to characterize single-CTCs or establish CTC cell cultures and xenograft models.

2.2.4.1 Cell cultures and xenograft models established from viable CTCs

CTCs are very rare in a blood sample of a cancer patient as explained in chapter 2.2. and there are only a few methods being able to enrich viable CTCs (see chapter 2.2.3), hence establishing a cell culture of CTCs is a challenge. It is reported that at least 100 CTCs are necessary to successfully culture CTCs [177], but only few patients possess that high quantity of CTCs in their blood draw.

Successful CTC cultures can be utilized for drug sensitivity tests or for creation of xenograft models in immunodeficient mice, where broader drug testing and analysis of genetic profile of the tumor development is possible [178–180].

2.2.4.2 Molecular Characterization of CTCs

For clinical applications CTCs are analyzed for sub-groups that may mostly be responsible for metastasation and chemo-resistance. In most solid cancers, metastasis is still the prevalent cause of death. If it would be possible to detect a sub-group of CTCs, which causes metastasis and develop targeted therapy to detect and destroy this sub-group while it is still in circulation it would be a major breakthrough for cancer research. Additionally, through mutation analysis of CTCs, patients may be chosen for a therapy switch independently of the mutational profile of their primary tumor to better reflect the tumor evolution.

The simplest downstream approach is the investigation of CTCs on the protein level through fluorescence labeled antibodies against proteins of interest. Most CTC detection methods already use EpCAM for CTC identification and are often able to add detection of additional proteins [181]. In case of breast cancer, therapy decision can be based on the hormone receptor status of a patient ($ER^{pos/neg}$, $PR^{pos/neg}$, $HER2^{pos/neg}$) and researchers still investigate if the changing hormone status of CTCs might predict a valuable early therapy switch [182].

Next generation sequencing (NGS) techniques have evolved through the last decade and broaden the knowledge about cancer genotypes, driver mutations and tumor heterogeneity [183, 184]. To execute NGS, the DNA content of a single CTC has to be amplified by whole genome amplification (WGA). Consecutively the cell genome can either be analyzed for mutations or for changes in copy numbers and may be useful for detection of new therapy targets for drug development [185–188].

Like the hormone status in breast cancer, the *KRAS* mutation status in CRC is an important predictor of anti-EGFR therapy success, therefore a changing mutation status in CTCs compared to the mutation status in the primary tumor could also enable a switch to more appropriate treatment and save time for the patient [187, 189].

Other techniques for downstream analysis can be profiling of CTCs on the RNA level by fluorescence in situ hybridization (FISH) [122], quantitative PCR after reverse transcription PCR [185] or mRNA sequencing [190].

2.2.5 Clinical implications of CTC detection today

Methods for CTC detection have been developed in numerous ways (see. 2.2.3), as well as methods that go further than enumeration (as described in 2.2.4). CTCs are promising biomarkers, as they represent the liquid phase of the evolving tumor and its interphase to metastasis, and even though much has been discovered in laboratories, research now focuses more on the transfer of knowledge about CTCs to personalized medicine.

2.2.5.1 Therapeutic target discovery

There are two scenarios in which CTCs might be useful biomarkers regarding therapeutic targets. First is the detection of already known therapeutic targets in CTCs which could be helpful in different situations. Tissue biopsies come often with a high risk for the patient or may not be sufficient for pathological tests. In NSCLC for example, researchers evaluate if CTCs could serve as the indicating biomarker if the treatment with the ALK and ROS1 inhibitor Crizotinib can be efficient [191]. Another example of CTC utility is the change in a hormone receptor profile of a tumor. In prostate cancer, mutation of the androgen receptor (AR) gene can result in hormone therapy resistance. Emerging modifications in AR cannot be measured by repeated tissue biopsy, but CTCs have been tested for their predictive value and have shown a promising potential [192].

Secondly CTCs might help discovering new therapeutic targets through recognizing and investigating heterogeneity of tumor tissue within CTCs. They also might be therapeutic targets themselves. Once a sub-population of CTCs is discovered with a higher metastatic potential, targeted therapy could be developed against the cells themselves. Current research already aims to characterize the metastatic genotype and phenotype of CTCs in NSCLC using markers common in EMT like vimentin or N-cadherin to characterize a subset of CTCs responsible for metastasis. They also showed that these CTCs may have lost cytokeratin and may be harder to detect with general methods [193].

2.2.5.2 Disease and treatment monitoring

Through regular application of CTC detection and characterization, disease evolution could be monitored by using a blood draw of a cancer patient. Changes in hormone receptor or mutation status of CTCs may provide information about treatment response, efficacy or resistance [194, 195]. As a large trial with metastatic breast cancer patients (SWOGS0500) could not confirm that a therapy switch based only on CTC enumeration can improve survival [196], it supported the approaches of many research groups that are convinced that only further characterization of CTCs can improve cancer care. A successful example is a recent study of AR-V7 analysis on CTCs in prostate cancer patients showing reliable prediction of abiraterone and enzalutamide resistance. This proved that regular CTC analysis can alert clinicians early and reliably for a therapy switch [197].

2.2.5.3 Relapse prediction

To confine the emergence of metastasis, early knowledge about the risk of relapse can be live saving. Studies have shown that CTC enumeration has potential to predict metastatic relapse in bladder cancer, prostate cancer and breast cancer [198–200].

This is where downstream analysis steps in and focuses on the identification of metastasis-initiating markers on CTCs which could guide therapy decision making in early stage patients or before predicted relapse.

3 Goals and hypotheses

In this study we utilized the HD-SCA workflow to analyze CTCs without prior enrichment in stage IV CRC patients. We aimed for in-depth analysis and categorization of the CTC subpopulations that may be responsible for relapse or are associated to metastatic disease. This may broaden previously published studies that have shown the predictive and prognostic value of CTC enumeration (association with OS, PFS and tumor stages) [117, 201].

We chose a patient cohort of stage IV CRC patients with distant metastases in the liver. Our goal was to classify subsets of detected CTCs and analyze CTC clusters for their potential value as biomarkers to further stratify patients risk status. Also we characterized single CTCs on the molecular level and utilized CNV profiles to uncover their origin by comparison of CTC profiles with cells of the primary tumor and/or the liver metastasis. We also chose a cohort of patients that underwent different surgery strategies to be able to track CTC counts after resection of primary tumors or metastases.

3.1 Enumeration of CTCs in CRC

Our goal was to enumerate all CTCs using the HD-SCA workflow to determine a subcategory of CTCs based on morphologic heterogeneity associated with survival and/or metastasis. The approach extends previously existing studies using mostly the CellSearch® system that was criticized before as insufficient for their limitation by detection of only $EpCAM^{pos}$ cells [202]. Also, we planned to analyze clusters of detected epithelial cells to evaluate their potential as unique indicators of disease progression. CTCCs have been analyzed before and have shown potential to be unique indicators of cancer [203, 204]. For CTCCs the HD-SCA is an optimal method due to its high-definition images.

Hypothesis 1: It will be possible to distinguish different subsets of CTCs by morphological characteristics.

Hypothesis 2: One or more of the classified CTC categories will be associated to survival.

3.2 Copy number variation profiles of CTCs in CRC

The molecular analysis of CTCs has been demonstrated to provide more information and a novel source of predictive potential. For example, in lung cancer the CNV profiles of CTCs have shown the ability of predicting chemo-sensitivity [205]. Using the HD-SCA workflow it has already been shown that multiple clones can exist within the CTCs of one prostate cancer patient [206]. So far CNV

profiles of single CTCs of CRC patients have not been analyzed, but may offer differentiation between cancer promoting CTCs and those less relevant for survival prognosis.

Our goal was to observe clonality within the CTCs of our CRC cohort and to compare the detected profiles with those of the individual cells extracted from corresponding tissue samples. We wanted to find out if it is possible to monitor a clonal evolution of the cancer in the blood of a CRC patient.

Hypothesis 3: We will observe CNV clonality within CTCs of CRC patients and at least one clone will be associated to survival.

Hypothesis 4: A detected clone within CTCs will also be discovered in the individual cells of corresponding tumor tissue of the primary tumor or cells of the liver metastasis of the same patient and therefore be proof of tumor evolution and descent of CTCs in CRC.

4 Materials and methods

As discussed in chapter 2.2.3, a CTC detection method was used that allows single-cell analysis after capture including imaging and CNV profiling. Collaboration with Dr. Peter Kuhn at 'The Bridge' institute of the University of Southern California (USC) allowed implementation of major parts of the High-Definition Single-Cell Analysis (HD-SCA) workflow in the Laboratory of Tumor Biology at the Biomedical Center at the Faculty of Medicine in Pilsen. The method with basic information about the cell detection steps has been already described by Marrinucci et al. in 2012 [175] and the process is illustrated in **Figure 4**.

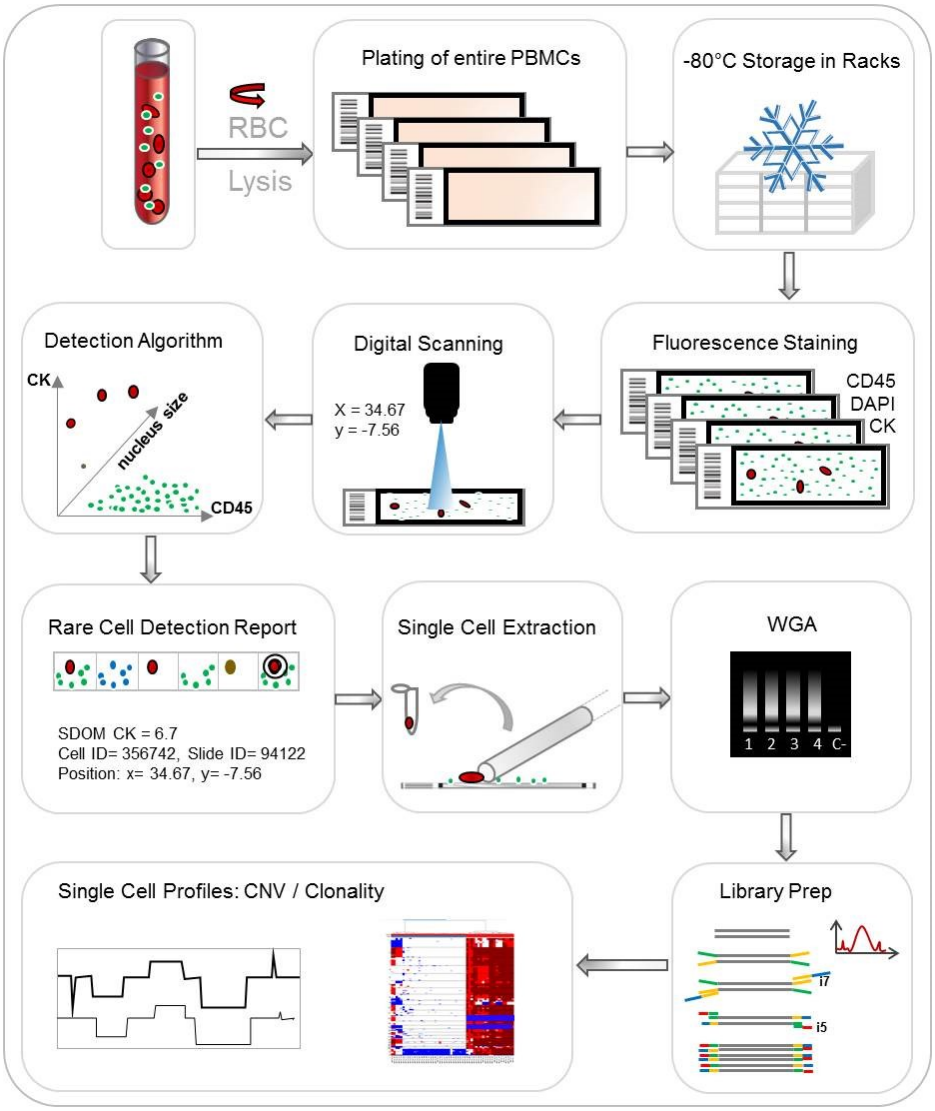

Figure 4: The High Definition Single Cell Analysis workflow. A blood sample undergoes red blood cell (RBC) lysis, all other blood components are plated on adhesive microscopy slides and these are stored at -80°C until further use. Fluorescent staining using CK, DAPI and CD45 is performed; slides are then scanned on an automated microscope and reports being generated by custom software using signal intensity and nuclear size for rare cell detection. Single cells are manually extracted, whole genome amplification is performed and libraries for Illumina sequencing are prepared. Sequencing data are used to generate CNV profiles and from those clonality is determined. Figure published in Thiele et al. (Molecular Meth Biol., accepted March 2018).

4.1 Blood sample collection and processing

4.1.1 Patient cohort

In this prospective study 47 patients from the Czech Republic with clinically confirmed CRC in AJCC stage IV were analyzed. Additionally, the blood from ten healthy donors has been drawn and analyzed. Details can be found in chapter 5.2 (page 47). Most of our patients have received neoadjuvant treatment, but given the size of the cohort and variability of the treatment used (both regarding the type and duration of treatment), it was not possible to reliably analyze correlation between the chemotherapy and CTC enumeration.

All patients and donors enrolled in the study agreed to the processing of their blood samples by signing informed consent. The study protocol was approved by the ethics committee of the Faculty of Medicine and University Hospital in Pilsen and complies with the International Ethical Guidelines for Biomedical research Involving Human Subjects. All blood samples were collected by clinical personnel of the University Hospital in Pilsen and patient data has been anonymized. An overview of cohort characteristics is presented in **Table 3**.

Table 3: Patient cohort characteristics

Category	Groups	No.	%
Gender	male	25	53.2
	female	22	46.8
Age	30-50	5	10.6
	50-70	30	63.8
	>70	12	25.5
CRC Location	Left	29	61.7
	Right	10	21.3
	Transvers	7	14.9
	Left & Right	1	2.1
Synchronous Disease	Yes	30	63.8
	No	16	34.0
	N.A.	1	2.1

4.1.2 Sample collection

4.1.2.1 Blood samples

Blood samples were collected before surgery and a follow up blood draw within two weeks up to 5 months after surgery through a peripheral blood draw. Blood was collected in 10 ml Cell-Free DNA

blood collection tubes from Streck© (STRECK Inc., USA). Blood was kept at room temperature (RT, 15-30°C) and processed within 16-36 hours. For healthy controls, blood has been obtained from healthy volunteers (without diagnosis of cancer or other life threatening or in blood detectable diseases) at the USC in Streck© tubes and these blood samples have been handled in the same way as blood samples of CRC patients up to analysis of enumeration data.

4.1.2.2 Tumor tissue touch preparations

During each patient's surgery, the operating surgeon also used a piece of resected tissue (metastasis or primary tumor and a piece of macroscopically tumor free tissue) to slightly touch it on a standard microscopy slide (touch prep). This slight contact with the slide left an imprint of a single cell layer of the tissue on the slide. The slide was then air dried, treated with 0.75 ml 7% bovine serum albumin (BSA), BSA was decanted and slide was dried; a cover glass was added, and the slide stored at -80°C. For each patient with sufficient tissue (89.4% of the cohort), five slides were produced from tumor tissue and five slides from non-malignant tissue. From here on, the touch prep slides were treated like blood preparation slides regarding the fluorescent staining (chapter 4.2), but imaged manually as distribution of cell patches is not homogenous on the slide. Fluorescent images were taken in all channels manually and coordinates noted in a database to allow single cell isolation as described in chapter 4.5 (page 39).

4.1.3 Blood processing

The blood samples were rocked for 5 min to be well mixed. 10X red blood cell lysis buffer was prepared by using 41.6 g ammonium chloride (NH_4Cl), 5.01 g potassium bicarbonate ($KHCO_3$), 0.186 g EDTA in 500 ml double deionized water (ddH_2O). A 1X working solution was prepared by adding 10 ml of 10X lysis buffer in 90 ml ddH_2O. 8 ml of blood were added to 40 ml of 1X lysis buffer (5 ml of 1X lysis buffer/1 ml blood) and the falcon tube was rocked for 5 min. 10 µl lysed blood was analyzed in a Buerker chamber to determine WBC concentration in million cells per ml. The HD-SCA method is using an amount of 3 million cells per slide and the number of slides to prepare was determined by the following formula:

$$y\ slides = \frac{x\ ml\ blood * WBC\ count\ (\frac{million}{ml})}{3\ (\frac{million\ WBC}{slide})}$$

The falcon tube with lysed blood was then centrifuged at 800 g for 5 min. The lysed red blood cells in the supernatant were taken off without touching the pellet. For correct concentration of WBCs per

slide the volume of 1X phosphate buffer saline (PBS) with a pH 7.4 (+/- 0.02) was calculated for final addition of 3 million cells in 0.75 ml cell suspension per slide:

$$amount\ of\ PBS = \left(No.of\ slides\ (y) * \frac{0.75ml}{slide}\right)$$

Custom made Marienfeld adhesive slides (Marienfeld, Germany) were washed until protective film (blue) comes completely off and stored at RT in a coplin jar (ThermoFisher Scientific, USA) in 1X PBS. Per slide 0.75 ml of the cell suspension was added. Slides were incubated for 40 min at 37°C to let cells attach. 7% bovine serum albumin (BSA) was prepared with a pH 7.4 (+/- 0.02). Cell suspension was decanted off the slides and 0.75 ml of 7% BSA added to the slides and incubated for 5 min at RT. BSA was decanted off, slides dried on a slide heater at 37°C and then a coverslip was added and attached with adhesive tape. Slides were wrapped in aluminum foil and stored at -80°C.

4.2 Fluorescent staining

Microscopy slides were thawed for 30 min at RT, cover slip taken off and 1 ml fresh prepared 2% PFA (paraformaldehyde) was added to each slide for 20 min at RT for fixation. PFA was tapped off; slides washed in 1X PBS for 3 min, then 0.75 ml ice cold methanol (MetOH, Fisher Scientific) was added and slides incubated for 5 min at RT. MetOH was tapped off, slides washed in 1X PBS for 3 min and 0.75 ml of 10% goat serum (Millipore, diluted in 1X PBS and sterile filtered) in 1X PBS was added and incubated for 20 min at 37°C to block unspecific bindings. Slides were then stained with anti-pan-cytokeratin in dilution 1:100 in 10% goat serum (1. Anti-cytokeratin mix IgG1 (CK1, 4, 5, 6, 8, 10, 13, 18, 19), Sigma, Cat. No.: C2562; 2. Anti-cytokeratin 19 IgG1, Dako, Cat. No.: M0888) and Alexa 647 conjugated antibody against CD45 in dilution 1:125 (mouse, monoclonal IgG2a, AbD Serotec, Cat. No. MCA87A647X). Primary antibodies were tapped off, slides washed in 1X PBS twice for 3 min in coplin jars. Secondary antibody mix was applied (0.75 ml per slide) containing goat anti-mouse Alexa Fluor® 555 IgG1 in 1:500 dilution in 10% goat serum and nucleic acid stain 4',6-diaminido-2-phenylindole (DAPI, Thermo Fisher Scientific, 5 mg/ml in 1:50000 dilution). Secondary antibody was tapped off, slides washed in 1X PBS twice for 3 min and then dipped only shortly in ddH_2O. 110 µl live cell mounting medium (0.05 g n-propyl gallate, 0.26 g Tris-HCl and 8 ml of ddH_2O were mixed; 4 ml of that solution were added to 36 ml glycerol) was distributed evenly over the active area of the slide and coverslip mounted without making bubbles. Slides were placed in a slide holder and settle overnight, the next day clear nail polish was used to seal coverslip on the slide. Slides were scanned immediately and then kept dry, dark and cool.

4.3 Whole slide imaging

A custom configured, fully automated epifluorescent microscopy system was used containing a broad spectrum illuminator, multiband filter (DAPI, FITC, TRITC, Cy5), a 20MHz 14-bit CCD camera with IEEE 1394 interface, 10X objective lens, a calibrated and automated x-y-z-stage with an insert fitting 4 slides and a control board integrating all components. All equipment for slide scanning was kept in a dark and air-conditioned room. The slides were cleaned carefully (only the bottom, not the coverslip) with 70% ethanol (EtOH). Compressed air was used to remove dust and EtOH residue. Slides were secured on the scanner insert with coverslip facing the objective. A custom imaging software was designed using Vollath's autocorrelation function and auto exposure function for ideal range. The software was using DAPI images with a 10X objective lens to set focus, then 6912 digital images were taken for one slide in 2304 frames totaling in images of approximately 3 million cells. All images were merged to create a representation of the entire slide using the SilverLight add-on for WindowsExplorer. Single-cell segmentation was implemented, allowing measurement of cellular characteristics like circularity, cell area, fluorescent signal intensity in each channel or DAPI nuclear size. Cells were annotated with a cell ID and Cartesian coordinates. Cells of interest (COIs) were categorized based on CK and CD45 signal intensities and extracted into a web-based report for pathological review.

4.4 Technical analysis of COIs

4.4.1 Image analysis

The custom imaging analysis software uses algorithms for the detection of COIs considering the signal of cytokeratin (CK), lymphocyte common antigen CD45 and DAPI. COIs were detected having either a high CK signal standard deviation over mean (SDOM), a large nuclear area and no CD45 signal or cells with a low CK signal or cells with a high CK SDOM, but a small nuclear size. All probable COIs detected by the software were presented to hematopathology trained personnel as images of the cell and its surrounding cells from all fluorescent channels to enable contextual comparison.

4.4.2 Hematopathological classification

COIs were then categorized through a defined decision making process as explained and visualized in **Figure 5**.

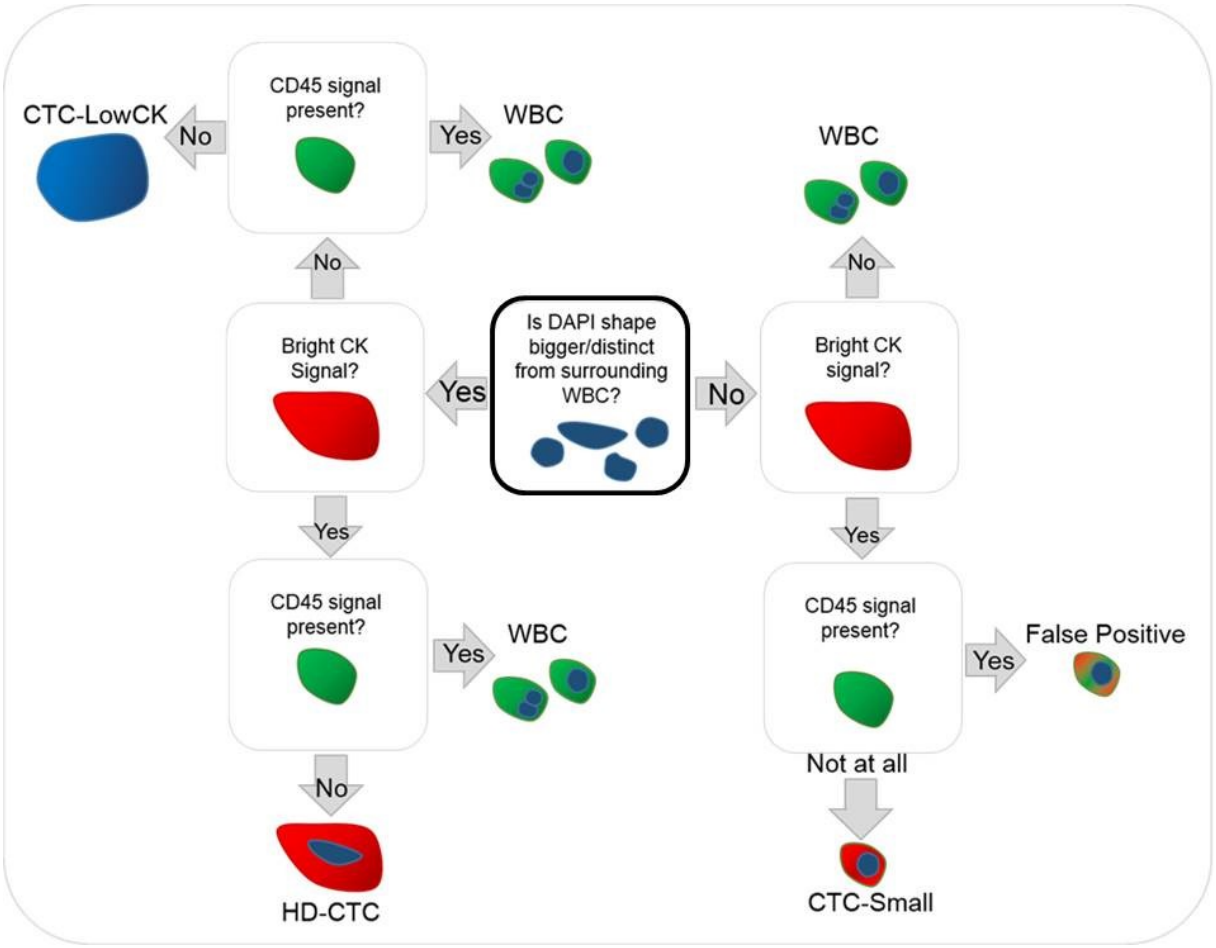

Figure 5: Decision chart for categorization of cells of interest (COIs). After automated scanning of the entire slide, the reported COIs must be categorized based on their nuclear shape and fluorescence signals. Decision making starts with the nuclear shape (middle), the next step is the CK signal intensity and eventually the CD45 signal is being evaluated.

COI subcategories were defined by the following characteristics:

- HD-CTC: CK^{pos}, $CD45^{neg}$, and distinct nucleus (larger than WBC, elongated, elliptical)
- CTC-LowCK: $CK^{low/neg}$, $CD45^{neg}$, and distinct nucleus
- CTC-Small: CK^{pos}, $CD45^{neg}$, with small and round nucleus
- CTC-cfDNA producing: CK^{pos}, $CD45^{neg}$, and shredded or minimized nucleus. CK signal might be shredded due to blebbing and visible as single dots.
- CTCCs: clusters of two or more HD-CTCs

If the presented COI does not fit in any of these criteria it can be one of the three categories for falsely detected COIs:

- False positive: CK^{pos}, $CD45^{pos}$ and small size nucleus
- WBC: CK^{neg}, $CD45^{pos}$
- Junk (staining residue, bubbles, etc.)

The final report provided a dataset of all categorized cells of interest with corresponding coordinates, allowing for relocation of each cell for downstream analysis. Additionally, it contained SDOMs of all markers, nuclear circularity, and many more. Using the enumeration data, the amount/ml blood was calculated for all CTC categories by dividing the detected number of cells with the amount of blood used for one slide.

4.5 Single cell isolation

Before single cell isolation, the COI may be reimaged at 400X magnification to obtain a high quality image. After reimaging, the nail polish sealing was carefully taken off using a scalpel, without moving of the coverslip. For isolation of single-cells from a microscopy slide, a fluorescence microscope was used (Olympus IX81) in combination with a micromanipulator (TransferMan® 4r, Eppendorf) and the imaging software ImagePro. Glass capillaries used for cell isolation were piezo drill tips (diameter of 15 µm, angle of 25°, lengths of 6.000 µm) from Eppendorf. All areas around the microscope and micromanipulator were cleaned with 70% EtOH and DNA AWAY®. The analyzed slide was placed in a tilted position within a ddH_2O filled coplin jar for at least 10 min to remove cover slip.

After cover slip was removed, the slide was placed on the microscope stage and 1 ml 1X PBS containing 0.1% Tween20 is added to the slide against dehydration. The stored coordinates were used to navigate the COI in field of vision using the 10X objective lens. In brightfield (BF) the focus was set on the capillary tip which was then moved down and in front of the cell. The cell was then slowly dislodged from the slide and the capillary moved up and out of the PBS buffer. A UV light sterilized 0.5 ml LoBind PCR tube (Eppendorf AG, Germany) was positioned on a cover slip next to the slide and 1 µl of cell deposition buffer (CDB, 10 mM Tris-HCl, 1 mM disodium EDTA, pH 8.0) was placed in the tube. The cell was then deposited in the CDB drop by moving the capillary down and releasing the cell. The tubes containing single cells were labeled and stored at -80°C immediately.

4.6 Whole genome amplification

4.6.1 Whole genome amplification using the WGA4 kit

To reach sufficient DNA amount from a single-cell, whole genome amplification (WGA) was performed. For WGA the GenomePlex® Single Cell Whole Genome Amplification Kit (WGA4, Sigma-Aldrich) was used. All surfaces were cleaned with DNA AWAY® and 70% EtOH. The tubes containing the single cells in 1 µl CDB were thawed and for each batch of tubes, one negative control (only Tris-EDTA buffer) and one positive control (1.5 µl of gDNA, 5 ng/ml) were added. To each tube 1.5 µl of lysis buffer (1:1 dithiothreitol (DTT, 100 mM) + potassium hydroxide (KOH, 400 mM)) was added and gently span down. Tubes were placed in a PCR cycler (Mastercycler™ pro PCR System, Eppendorf) and incubated at 95°C for 2 min. Immediately PCR tubes were placed on a PCR cooler (iceless cold storage system, Eppendorf). To each tube, 6.5 µl of 10 mM TE buffer (10 mM Tris-HCl, 1 mM disodium EDTA, pH 8.0) and 1 µl of the 10X Single-Cell Lysis and Fragmentation Buffer (contained in the WGA4 kit) were added. Tubes were then placed in the thermal cycler and incubated for 4 min at 99°C. Tubes were again immediately removed and placed on the PCR cooler. Per reaction, 2 µl of 1X Single Cell Library Preparation Buffer and 1 µl of Library Stabilization Solution (both part of the WGA4 kit) were added and tubes mixed thoroughly and placed in a thermal cycler for 2 min at 95°C followed by cooling them on the PCR cooler. 1 µl of Library Preparation Enzyme was added to each reaction and tubes placed in thermal cycler using the following program: 16°C for 20 min, 24°C for 20 min, 37°C for 20 min, 75°C for 5 min, 4°C hold. Then 7.5 µl 10X Amplification Master Mix, 48.5 µl of molecular grade water and 5 µl of WGA DNA Polymerase (all three part of the WGA4 kit) were added per reaction. Tubes were mixed thoroughly and incubated in a thermal cycler as follows: 95°C for 3 min, 24 cycles of: 94°C for 30 sec, 65°C for 5 min; then hold at 4°C.

4.6.2 Control of WGA products in agarose gel

A 1.5% agarose (GelPilot® agarose, Qiagen) gel was prepared including 10X SYBR®Safe DNA Gel Stain (Life Technologies). Samples were loaded using 8 µl of sample combined with 2 µl of the 5X Gel Pilot Loading Dye (Qiagen). In one well 8 µl of Quick-Load® 100 bp DNA ladder (New England BioLabs Ltd., USA) was loaded. Gel was run for approximately 35 min at 90 V for a 100 ml gel. WGA product was considered as successfully amplified when a continuous smear between 150 and 1000 bp was observed.

4.6.3 PCR product purification

The QIAquick PCR Purification kit (Qiagen, Germany) was used according to manufacturer‘s instructions. DNA samples were quantified using the Qubit™ dsDNA HS Assay Kit (ThermoFisher Scientific, Germany) according to manufacturer‘s instructions. DNA concentrations were saved in a database and all samples were diluted with 10 mM TE buffer to the same initial amount of 185 ng DNA in 55.5 µl total volume.

4.7 Library construction

4.7.1 DNA Fragmentation

All samples were transferred to sonication tubes (Snap Cap microTUBE, COVARIS) and the sonication device COVARIS S2 (COVARIS) was used according to manufacturer’s protocol to achieve a fragment size of 200 -250 bp. After fragmentation, DNA was transferred to strips of 0.2 ml PCR tubes.

4.7.2 Library preparation

The NebNext®Ultra DNA Library Prep kit for Illumina® (New England BioLabs Inc.) was used in combination with Agencourt® AMPure® XP Beads (Beckman Coulter) for size selection and cleanup according to manufacturer’s protocol. For PCR, the Mastercycler™ proPCR (Eppendorf) was used. After second bead selection for PCR product cleanup, 32 µl supernatant containing DNA was collected and DNA quantity measured using Qubit (ThermoFisher Scientific) in combination with the dsDNA HS Assay Kit (ThermoFisher Scientific) while following the manufacturer’s protocol. Quality of the library (correct size of 300-400 bp) was analyzed using the 2100 Bioanalyzer (Agilent Technologies) in combination with the High Sensitivity DNA Analysis Kit (Agilent Technologies) according to manufacturer’s protocol. Only libraries with a normal curve of distribution with a peak around 350 bp and with a low concentration of primer dimers (~80 bps) and adaptor dimers (~130 bp) were used for sequencing. Molarity of each library was calculated as follows:

$$library\ nM\ = \frac{\left[Qubit\ value\ (\frac{ng}{ul})\right] * 1000}{1} * \frac{1}{649\ \left(\frac{M}{bp}\right)} * \frac{1000}{size\ of\ library\ peak\ (bp)}$$

All libraries were pooled at a final concentration of 10 mM using a volume of 5 µl/sample; 10 mM TE buffer was used for dilution. The pooled library underwent a final cleanup using the Agencourt®

AMPure® XP Beads (Beckman Coulter) with a total volume of: $Total\ Vol. = Nr. of\ libraries * 5\mu l$. The beads were air dried and DNA is eluted in $Total\ Vol$ of 10 mM TE buffer.

4.8 Sequencing and Single-Cell CNV analysis

4.8.1 Sequencing

Protocols for next generation-sequencing are in detail described in Baslan et al. [207]. The DNA libraries were sequenced on the HiSeq2500 (Illumina, USA) platform using a single end read 50 base pair protocol (SR50).

4.8.2 Single Cell CNV analysis

Processing of sequencing data was performed and software and scripts were used according to Baslan et al. [207] to allow CNV profiling of single CTCs. In summary, sequencing results were transferred as a fastq-file to the Bowtie software (Bow Tie Pro Limited) and aligned to the reference genome hg19, which was acquired from the University of California Santa Cruz (UCSC) Genome browser (https://genome.ucsc.edu/). Before mapping the sequence, a set with an arbitrary number of bins was created across the genome. Each bin contained the same number of mappable positions. The appropriate number of bins was determined for each sample and has to balance between resolution (high number of bins) and noise (less bins). The process has been originally developed by Navin et al. [208] as optimized sparse sequencing. For simplification of binned data mathematical segementation was used [209], which quantifies amplitude and location of copy number gains and losses across the genome and creates a numerical copy number variation (CNV) profile for each cell. To visualize similarities among groups of individual cells, a custom software tool was used and heatmaps were generated using cluster method ‚ward.D' and distance method ‚manhattan'. A data resolution of 5k bins and a threshold of at least 50.000 bin counts was applied for inclusion of data.

4.9 Statistical analysis of CTC data

Standard frequency tables and descriptive statistics were used to characterize the patient cohort. For analysis of survival, progression-free survival (PFS) was determined from the date of surgery to the date of disease progression or death. The date of recurrence was set to the average date between the last negative and the first positive examination if the interval between the examinations was 180 days or less. In cases of longer examination interval, the recurrence date was set 90 days before the

first positive examination. Overall survival (OS) was determined from the date of surgery to the date of death.

For analysis of the association of CTC enumeration with OS and PFS, univariable Cox proportional hazards model was used for continuous variables including hazard rate calculations. In order to visualize these associations with Kaplan-Meier survival estimation plots, a threshold value needed to be determined for each prognostic variable and the patients had to be stratified in two groups according to it. This threshold was found through an automated optimization process implemented in Matlab (2014a, MathWorks Inc., Natick, USA), in which the threshold value producing the smallest Log-rank p-value was determined and selected.

For binary variables and their relation to survival indicators, Kaplan-Meier survival estimates in combination with significance tests (Gehan Wilcox, log-rank) were calculated.

Associations between two categorical variables have been tested through contingency tables with either Chi-square test or Fisher's exact test. For the associations between categorical and ordinal or quantitative variables, Mann Whitney U test or Kruskal-Wallis ANOVA (depending on the number of categories) was utilized. Spearman's correlation has been applied to test associations between two ordinal or quantitative variables.

All reported p-values are two-tailed and the level of statistical significance was set at $\alpha = 0.05$. Statistical analysis was performed in Statistica (ver. 12 Cz, TIBCO Software Inc., Palo Alto, CA, USA).

5 Results

The result section will start with analysis of the morphological and phenotypical heterogeneity of the detected COIs and continue with results from the evaluation of healthy donor samples.

For the analysis of enumeration data of the detected COIs, these will be separated into subchapters for HD-CTCs, followed by the detected subcategories (CTC-LowCK, CTC-Small and CTC-cfDNA producing) and then CTCCs.

The analysis of CNV profiles and probable clones will focus first on the single-cell analysis of HD-CTCs, then profiles of isolated cells from CRC touch preps and hepatic metastases and finally on the comparison of detected clonality of HD-CTCs and associated touch preps.

5.1 Phenotypic and morphological heterogeneity within CTCs of CRC patients

In total we analyzed 86 blood samples of 47 CRC patients and 10 blood samples of 10 healthy volunteers. Demographics for patients and volunteers are shown in **Table 3** and **Table 4,** respectively.

Morphological heterogeneity was observed within the detected cells and analyzed based on a basic study on CRC HD-CTCs morphology by Marrinucci et al. [210]. HD-CTCs were often elongated or elliptical but also round (as seen in **Figure 6a**) with many HD-CTCs having appendix-like cytoplasmic projections. The size of HD-CTCs varied with some being just a few µm larger than surrounding WBCs, but others being more than double the size of surrounding WBCs. The nucleus can nearly fill the entire cell and amount of cytoplasm is low, but other cells have an eccentric nucleus location on one end of the HD-CTC with a large amount of cytoplasm on the other side. The shape of the nuclei in HD-CTCs is often, but not always elongated or egg-shaped.

The CTC-Small category fulfill the same fluorescent signal characteristics as the HD-CTCs (CK^{pos}, $CD45^{neg}$), but the size of their nucleus is comparable to nuclei of surrounding WBCs (**Figure 6c**).

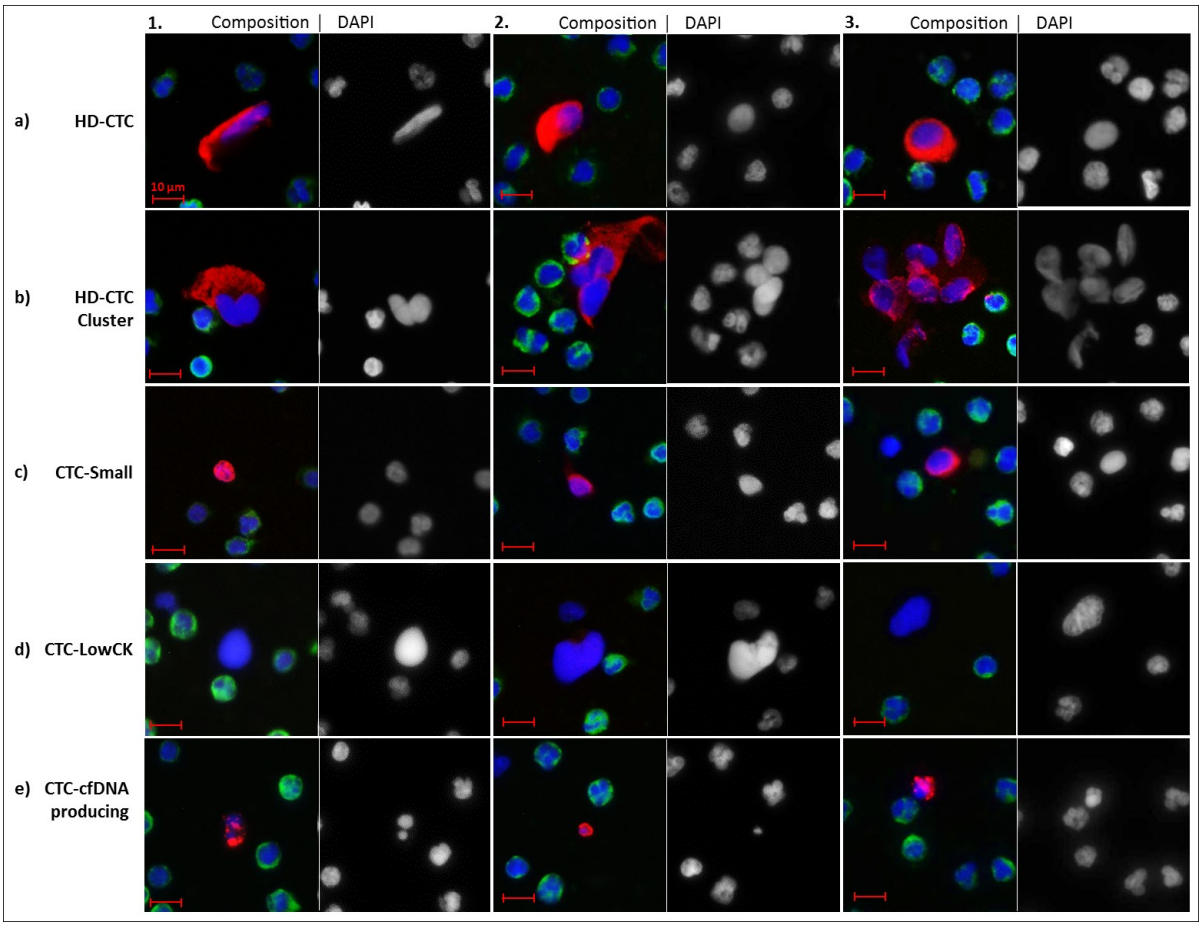

Figure 6: Heterogeneity within CTCs in CRC patients of the Czech Republic Each row contains three examples of the cell category stated on the left. Columns 1, 2 and 3 each consist of a channel composite (CK in red, CD45 in green and DAPI in blue) followed by the DAPI image. Row **a)** shows a variation within the HD-CTC category of cells with an enlarged nucleus compared to WBCs and a CK^{pos} and $CD45^{neg}$ signal. Row **b)** displays the variation of clusters from two CTCs up to over 6 cells. In row **c)** are the cells which are like HD-CTCs, but with a nucleus as small as the WBCs. Row **d)** displays COIs with low to no CK signal, $CD45^{neg}$ signal and enlarged nucleus. In row **e)** are the CTCs undergoing apoptosis and releasing cell free DNA. These cells show irregular CK signal and disrupted DAPI signal. The red scale bars equal 10 µm. Parts of this figure have been published in Thiele et al. [161].

Also the nuclei of CTC-Small cells are mostly not elongated or oddly shaped as the ones of HD-CTCs, but as round as the nuclei of WBCs, which is reflected by a higher detected nuclear roundness (**Figure 7a**) . The group of CTC-LowCKs shows enlarged nuclei at least twice the size of a WBC. Their shape is highly variable from rather round shapes (**Figure 6d**, 1.) to a wide elongated shape (**Figure 6d**, 3.), but overall with a larger nuclear area than all other CTC cell types (**Figure 7b**). The COIs undergoing apoptosis (CTC-cfDNA producing) have a disrupted nucleus and often cytoplasmic condensation (**Figure 6e** 1. and 3.). Sometimes apoptosis has progressed so far that the nucleus has already been reduced to a minimum (**Figure 6e** 2.).

Analysis of the stored values for nuclear roundness and nuclear area for the detected COIs represent the heterogeneity between the detected CTC subcategories and within the groups. For HD-CTCs the nuclear roundness resulted in a mean of 0.7, CTC-Small cells in contrast are more round with a median of 0.8. CTC-LowCK cells have a nucleus similar shaped as HD-CTC's nucleus with a median roundness of 0.72, but the nuclear area is more than double the size with a mean of 356.5 compared to 158 in case of HD-CTCs. Measurements for all COIs are shown in **Figure 7**.

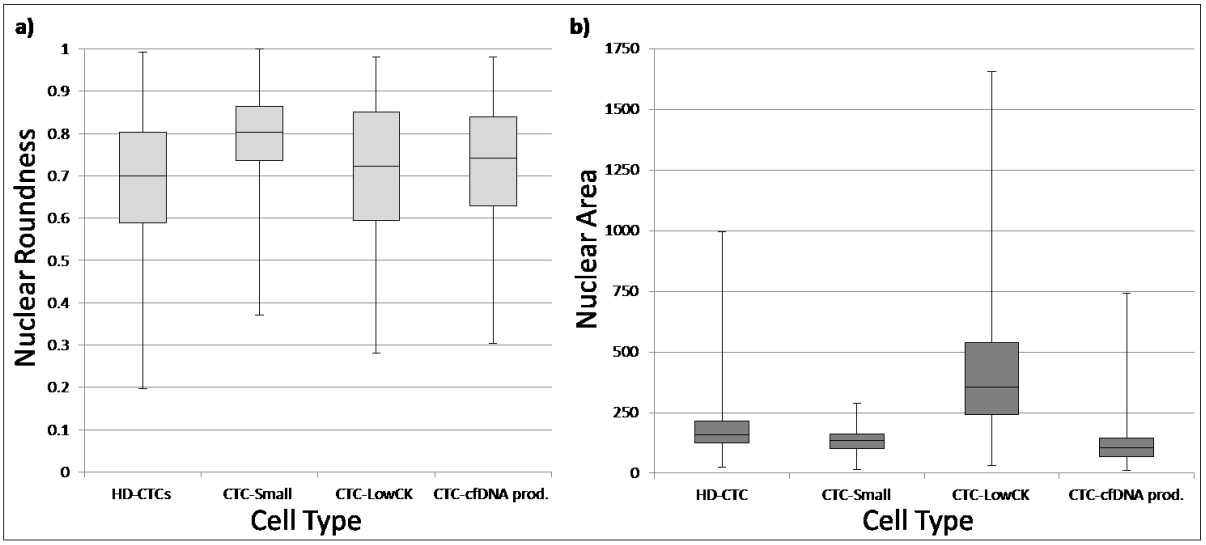

Figure 7: Nuclear Roundness and nuclear area of detected COIs. A total of 3001 HD-CTCs, 842 CTC-Small, 623 CTC-LowCK and 327 CTC-cfDNA producing cells have been analyzed for **a)** nuclear roundness. Nuclear roundness has been calculated as: 4x [signal area]/π x [major axis]^2. For CTC-cfDNA producing cells, the calculation for roundness is biased by the inability of the calculation to consider nuclear blebbing. **b)** Nuclear area is measured for all cell types in μm^2.

Besides single HD-CTCs and COIs we observed many CTCCs. These clusters were composed of at least two and up to 21 HD-CTCs in the largest observed cluster. The large heterogeneity of clusters is illustrated in **Figure 6b** and in **Figure 8**. Clusters can be composed of similar cell sizes, but also of HD-CTCs with varying cell sizes as in shown in **Figure 8a** and **b**. The signal intensity of the CK-signal can vary strongly between clusters but is mostly similar for cells within one cluster (**Figure 8**). Determination of cell counts within one cluster was carried out by applying cell masks on the DAPI image of the respective cluster as demonstrated in **Figure 8c**.

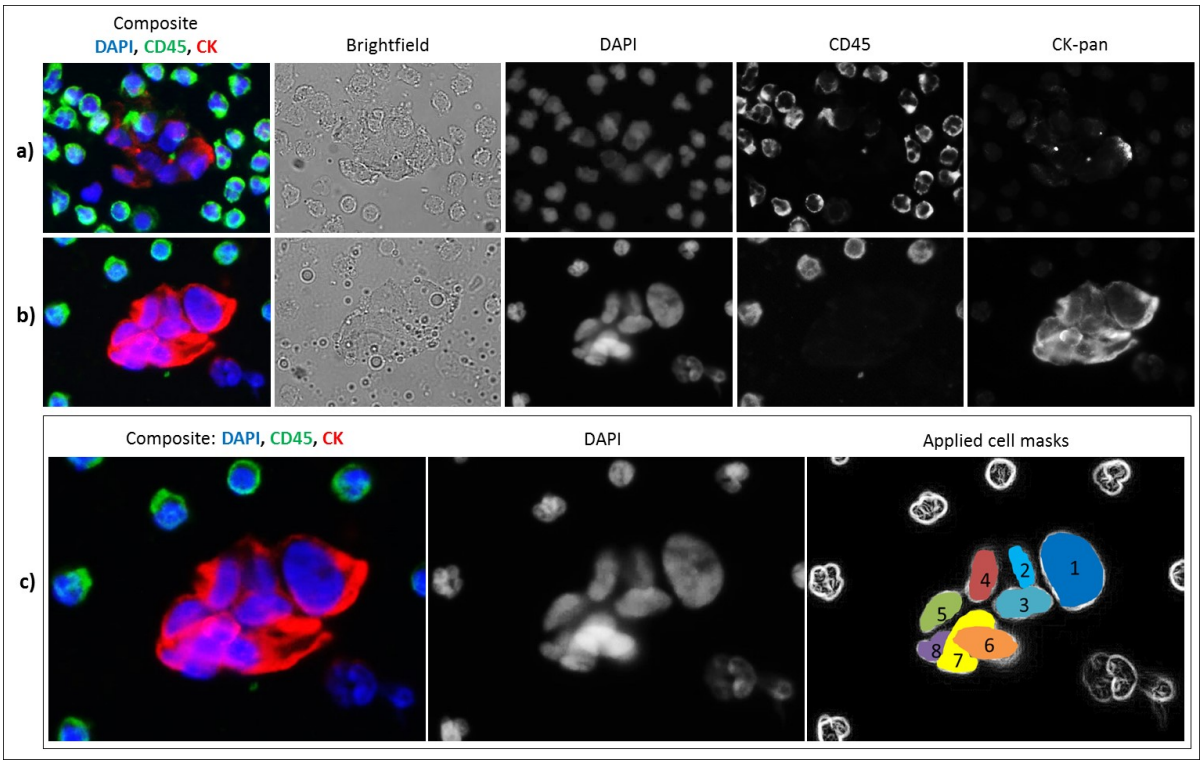

Figure 8: Heterogeneity within large HD-CTC clusters. Large clusters of HD-CTCs still show a variety of cell shapes and signal intensities as displayed in these two examples of clusters over six cells. In **a)** and **b)** the composite image of three channels (CK in red, CD45 in green and DAPI in blue) is shown on the left, followed by the brightfield image, the DAPI channel, the CD45 image and on the right the CK-pan signal in the TRITC channel. **a)** A cluster composed of nine HD-CTCs of similar size and rather low CK signal, **b)** cluster composed of eight HD-CTCs of varying sizes and high CK signals; **c)** application of single cell masks to the DAPI image to determine cell counts per cluster.

5.2 Evaluation of healthy donor samples

A total of ten healthy donors have been tested with the HD-SCA workflow. Enumeration results are summarized in **Table 4**. Analysis resulted in a specificity of 90% for a cut-off of 2 HD-CTCs/ml and 100% for a cut-off of 3 HD-CTCs/ml blood. No clusters were detected in any of the healthy donors, but other COI subtypes like CTC-LowCK and CTC-Small have been observed even with over 5 cells/ml (NBD-2, NBD-6 and NBD-10; **Table 4**). According to the detected amounts, the cut-offs for CTC-LowCK, to accomplish 100% specificity, were set at 8/ml, for CTC-Small as well and for CTC-cfDNA producing at 5/ml blood.

Table 4: Data of ten healthy blood donors for all detected cell categories

Volunteer ID	Gender/ Age	HD-CTC/ ml	CTC-LowCK/ ml	CTC-Small/ ml	CTC-cfDNA prod./ ml	Clusters/ ml
NBD-1	M/25	0.9	0.0	0.9	4.7	0.0
NBD-2	F/23	2.3	0.8	7.7	1.5	0.0
NBD-3	F/24	1.0	0.0	2.0	0.0	0.0
NBD-4	F/29	1.2	0.0	3.0	0.6	0.0
NBD-5	F/26	0.0	0.0	0.0	0.0	0.0
NBD-6	F/38	0.0	5.8	4.2	0.0	0.0
NBD-7	M/36	0.0	1.2	0.0	0.0	0.0
NBD-8	F/66	0.9	0.9	0.9	0.0	0.0
NBD-9	M/36	0.6	1.1	0.0	0.0	0.0
NBD-10	M/65	0	7.5	1.9	0	0

5.3 Enumeration data of HD-CTCs, CTC subcategories and CTCCs

For the pre-resection draws, 46 out of 47 were usable and only 39 patients out of 47 were available for follow-up draws. The eight missing follow-up draws mostly result from patients not returning to the clinic or draws taken outside of the defined time window (e.g. only two days after resection or over 1 year after resection).

5.3.1 Enumeration of HD-CTCs

Out of 46 patients, 27 had >2 HD-CTCs (58.7%) and 24 had > 3 HD-CTCs (52.2%) in the pre-resection draw. 19 patients (41.3%) and 22 (47.8%) respectively were negative for HD-CTCs.

In the follow-up draw (between 1 week and 5 months after surgery) we detected >2 HD-CTCs in 25 (64.1%), and >3 HD-CTCs in 20 (51.3%) patients. 14 (35.9%) and 19 (48.7%) patients respectively were negative for HD-CTCs in the follow-up draw. An overview of the patient cohort and according HD-CTC/ml counts are displayed including clinical data like disease status one year after surgery, age at surgery, sex and number of hepatic metastases in **Table 5**.

Table 5: HD-CTC enumeration data and clinical information of the entire CRC cohort

HD-CTC positive patients (>3HD-CTCs/ml blood) and their corresponding HD-CTCs/ml counts are marked in bold.

Patient ID	Sex	Age	Primary tumor site	No. Liver Mets	Status after 1 Year	HD-CTCs/ml Pre-res	HD-CTCs/ml Follow-Up
CRC201	F	66	rectum	1	Progression	1.2	0.00
CRC202	F	65	rectum	10	Progression	**5.6**	0.00
CRC203	F	63	ascending	8	Progression	0.0	N.A.
CRC204	F	47	sigmoideum	10	Stable	**210.1**	**3.83**
CRC205	M	68	transversum	3	Deceased	**32.4**	**5.43**
CRC206	F	65	sigmoideum	1	Progression	**28.3**	0.00
CRC208	M	81	transversum	10	Deceased	**287.1**	**14.82**
CRC209	M	68	rectum	1	Stable	**27.8**	0.00
CRC210	F	56	cecum	10	Deceased	0.0	**57.56**
CRC211	M	58	transversum	2	Progression	**94.5**	N.A.
CRC213	M	70	rectum	3	Progression	2.1	0.00
CRC214	F	65	cecum	1	Stable	**120.6**	1.33
CRC215	M	75	transversum	10	Stable	N.A.	**37.78**
CRC216	M	74	ascending	1	Stable	0.0	0.00
CRC218	M	55	rectum	1	Stable	0.0	0.00
CRC219	M	72	rectum	3	Stable	0.0	0.00
CRC221	M	76	rectum	1	Stable	0.0	**11.92**
CRC222	M	60	rectum	2	Stable	0.0	N.A.
CRC223	F	55	cecum	1	Stable	2.4	N.A.
CRC224	M	70	rectosigmoideum	7	Stable	0.0	N.A.
CRC225	M	84	sigmoideum	1	Stable	0.0	N.A.
CRC226	F	79	ascending/transv.	10	Deceased	2.8	**22.40**
CRC229	M	82	tranversum	1	Progression	**90.4**	2.08
CRC230	F	55	rectum	3	Stable	**85.3**	1.15
CRC232	M	76	sigmoideum	6	Stable	0.0	**6.07**
CRC234	M	67	ascending	1	Progression	0.0	2.44
CRC235	F	52	rectum	2	Deceased	1.9	**3.40**
CRC236	M	67	cecum	10	Progression	0.0	2.57
CRC237	F	41	rectosigmoideum	1	Stable	**35.0**	**4.35**
CRC239	M	49	sigmoideum	10	Deceased	**12.3**	0.00
CRC240	M	68	ascending	1	Stable	**14.7**	**12.00**
CRC241	F	55	rectosigmoideum	3	Stable	0.0	0.00
CRC243	F	81	cecum	10	Deceased	**24.6**	**265.47**
CRC244	F	73	cecum	2	Stable	1.0	**3.19**
CRC245	M	72	rectum	1	Stable	**10.8**	**5.00**
CRC246	F	35	rectum	2	Progression	**94.1**	0.00
CRC247	F	62	rectum	1	Progression	0.0	**3.42**
CRC248	M	60	rectum	N.A.	Progression	0.0	**20.80**
CRC249	M	64	transversum	1	Stable	**19.8**	N.A.
CRC251	M	50	rectum	1	Stable	**5.5**	**7.67**
CRC252	F	56	rectum	2	Progression	**3.8**	2.15
CRC253	F	68	sigmoideum	1	Stable	**3.2**	0.82
CRC255	M	64	rectum	1	Stable	**25.9**	2.99
CRC256	M	64	rectosigmoideum	2	Progression	**23.5**	**7.33**
CRC258	F	52	sigmoideum	1	Stable	1.4	N.A.
CRC259	F	58	ascending	10	Stable	**5.7**	**6.87**
CRC260	F	62	rectum	1	Stable	**158.6**	**17.70**

In **Figure 9** numbers for all HD-CTCs detected in pre-resection and the follow-up draws are visualized for each patient.

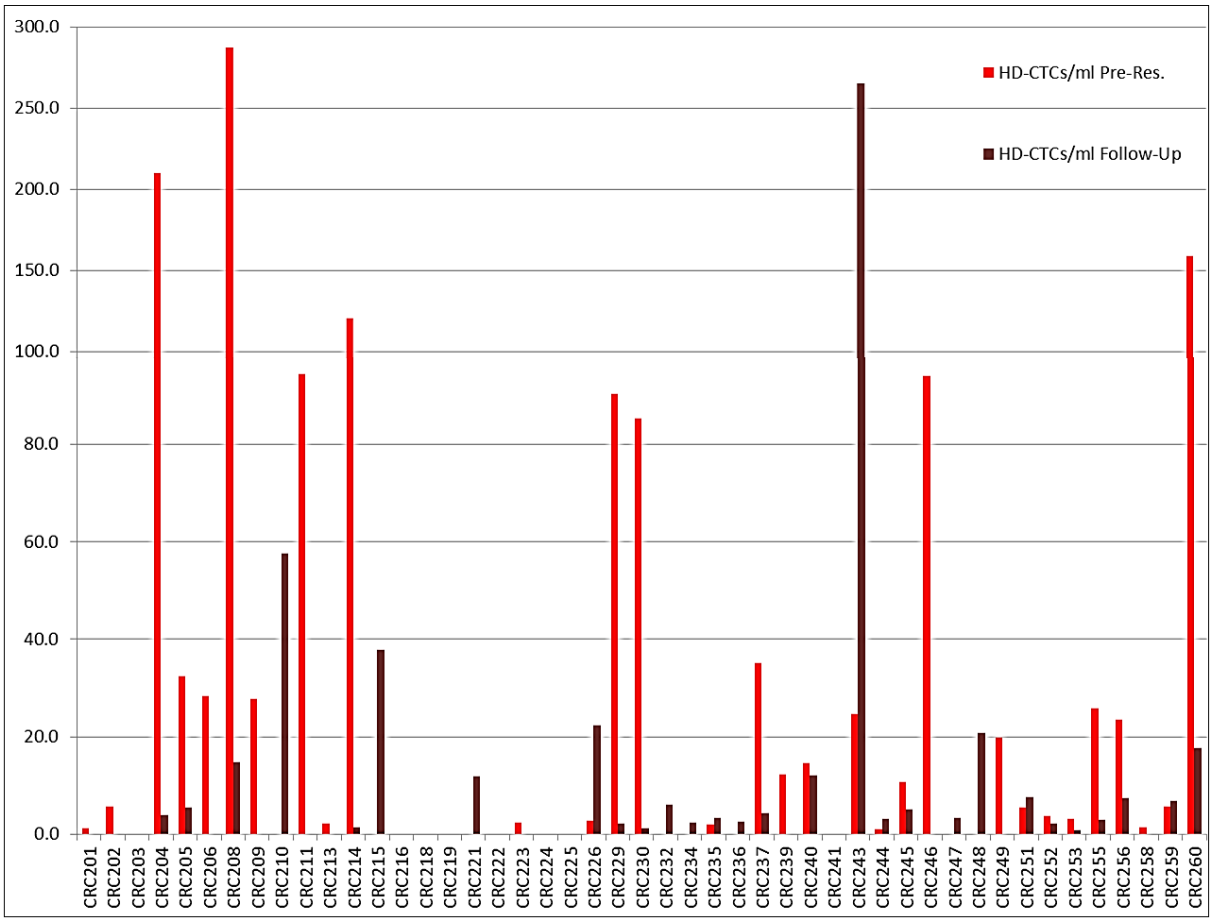

Figure 9: Enumeration data of the pre-resection and follow-up blood draw for all detected HD-CTCs. Displayed are all patients with the detected numbers of HD-CTCs for both the pre-resection draw (light-red) and the follow-up draw (dark red).

A comparison of average CTC counts/ml in the two blood draws per patient is shown in **Figure 11b** and indicates a higher amount of total averaged HD-CTCs in the pre-resection draw (31.14/ml) compared to the follow-up draw (13.65/ml).

5.3.2 Enumeration of subcategories of CTCs

Regarding average numbers/ml of the detected cells in CTC subcategories (shown in **Figure 11b**) we also observed a drop in the follow-up draw compared to the pre-resection draw for the CTC-Small and CTC-cfDNA producing cells. In the pre-resection draws an average number of 7.9 cells/ml were observed for CTC-Small and 6.0 cells/ml for CTC-cfDNA producing, compared to only 6.7 cells/ml and 3.1 cells/ml respectively in the follow-up draw. For CTC-LowCK cells there were an average of 6.4 cells/ml in pre-resection draws and 7.5 cells/ml in the follow-up draws. Therefore, CTC-LowCKs are the only cell group whose count does not decrease in the follow-up draws.

Enumeration data for all three subcategories for each patient are visualized in **Figure 10**. Using the threshold of >8 cells/ml blood, out of the 46 total pre-resection draws, 14 patients were positive for CTC-LowCK (30.4%) and 11 patients were positive for CTC-Small (23.9%). 13 patients showed >5 CTC-cfDNA producing cells (28.2%). No cells in the pre-resection draw were detected in 9 patients for CTC-LowCK (19.6%), 9 for CTC-Small (19.6%) and 12 patients for CTC-cfDNA producing cells (26.1%).

In the follow-up draws from 39 patients, 12 had >8 CTC-LowCK/ml (30.8%), 11 had >8 CTC-Small/ml (28.2%) and 9 >5 CTC-cfDNA producing cells/ml (23.1%).

Six patients (15.4%) had no CTC-LowCK cells, 10 patients (25.6%) had no CTC-Small cells and 12 patients (30.8%) no CTC-cfDNA producing cells in the follow-up draws.

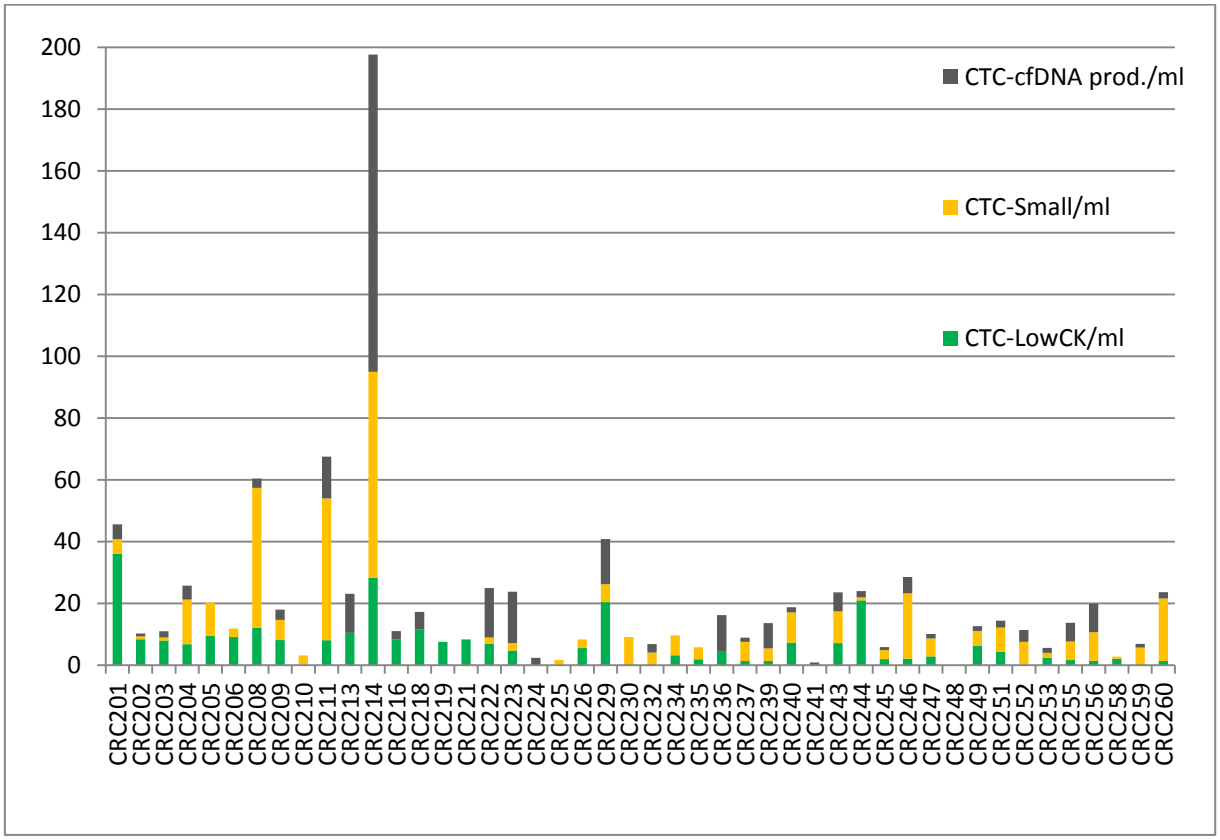

Figure 10: Enumeration data of the pre-resection blood draw for the three subcategories of CTCs. Displayed are all patients (except CRC215, where no analysis was possible for the pre-resection draw) with the detected number of cells for each listed category.

5.3.3 Enumeration of CTCCs

A total of 136 CTCCs were observed in the pre-resection draw across all patients. In **Figure 8c**, the determination of cell number per cluster through cell mask application was presented. The distribution of cluster sizes within the pre-resection draw of the entire cohort is displayed in **Figure**

11a. 50.7% were CTCCs of only two HD-CTCs, 33.8% contained between 3 and 5 HD-CTCs, 11.8% between 6 and 10 and only 3.7% of CTCCs contained more than 10 HD-CTCs. For all groups of CTCC sizes the counts are lower in the follow-up draws. The calculations for average clusters/ml resulted in 4.2 for the pre-resection draw and a drop to 1.8 clusters/ml for the follow-up draws.

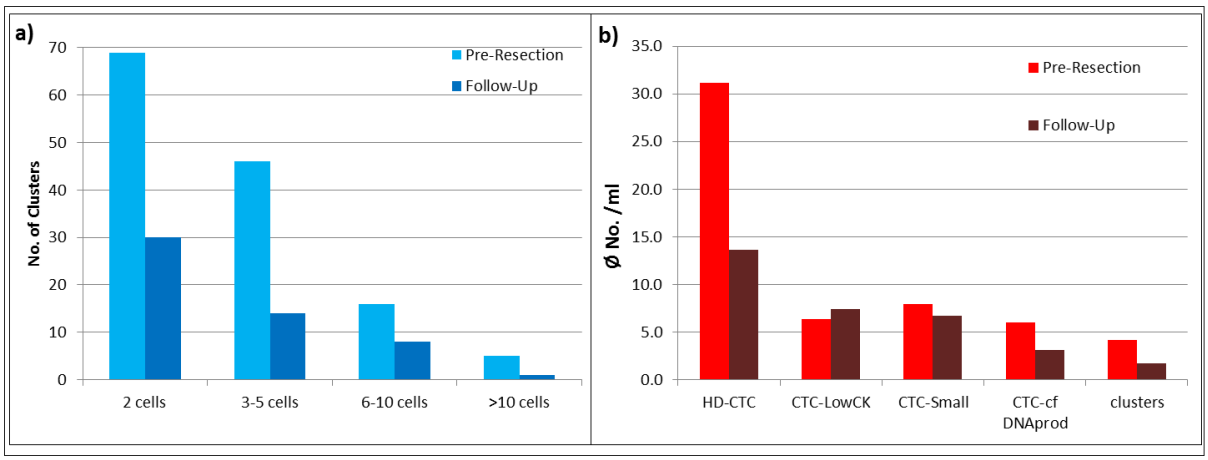

Figure 11: HD-CTC cluster sizes and average cell and cluster numbers for pre-resection and follow-up draws. Displayed are column diagrams of **a)** the distribution of total cluster counts (two analyzed slides/patient) sorted by cluster size (cell counts) for pre-resection and follow-up draw; **b)** total numbers of detected cell types/ml and clusters/ml blood in the entire CRC cohort for pre-resection and follow-up draws.

As each patient was evaluated, a draw was considered positive when at least one CTCC (=>2 HD-CTCs together) was detected on one of the two analyzed slides. 18 patients (39.1%) were CTCC positive from the 46 pre-resection draws and 8 patients (20.5%) out of 39 were positive for clusters in the follow-up draw. The distribution of CTCCs/ml is illustrated in **Figure 12**.

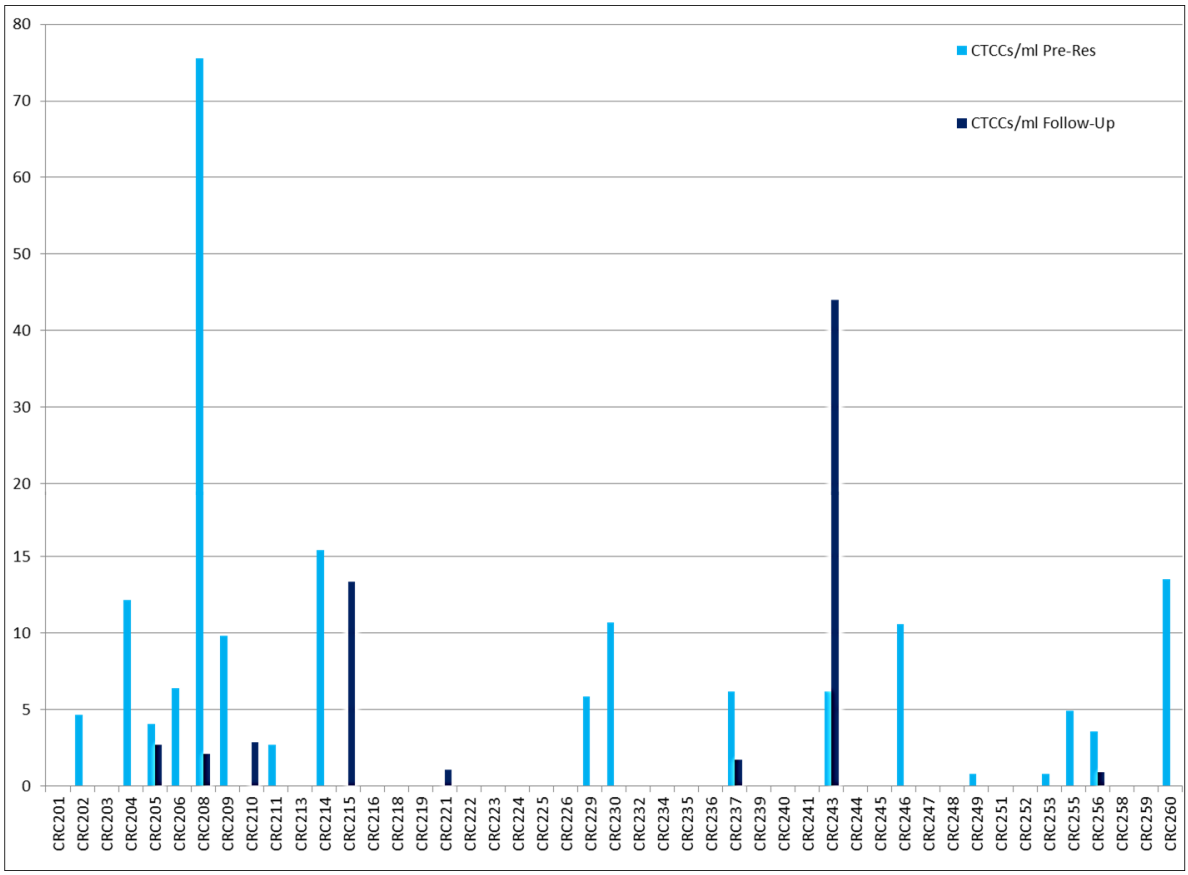

Figure 12: HD-CTC cluster counts of the pre-resection and follow-up draws. Enumeration data of all CTCCs/ml of blood detected in the draws of both time points from individual patients.

5.4 Associations of obtained data with survival

5.4.1 Association of clinical data with survival

In **Table 6** clinical characteristics of the patient cohort are summarized with corresponding significant p-values of their association with progression free survival (PFS) and overall survival (OS). Results with p≥0.05 are marked as non-significant (N.S.).

Table 6: Clinical characteristics of the cohort and their association with survival

Category	Groups	No.	%	Assoc. with OS	Assoc. with PFS
Gender	male	25	53.2	N.S.	N.S.
	female	22	46.8		
Age	30-50	5	10.6	N.S.	N.S.
	50-70	30	63.8		
	>70	12	25.5		
CRC Location	Left	29	61.7	**0.030**	**0.037**
	Right	10	21.3		
	Transvers	7	14.9		
	Left &Right	1	2.1		
Synchronous Disease	Yes	30	63.8	N.S.	N.S.
	No	16	34.0		
	N.A.	1	2.1		
Size of primary tumor	0.1 -3 cm	4	8.5	**0.002**	**0.005**
	3 -6 cm	24	51.1		
	> 6 cm	6	12.8		
	N.A.	13	27.7		
No. of hepatic metastases	1	21	44.7	**0.002**	N.S.
	2 - 8	15	31.9		
	> 8	10	21.3		
	N.A.	1	2.1		
Size of hepatic metastases	0.1 -3 cm	21	44.7	N.S.	N.S.
	3 -6 cm	10	21.3		
	> 6 cm	9	19.1		
	N.A.	7	14.9		
Location of hepatic metastases	Left	14	28.0	**0.003**	N.S.
	Right	21	42.0		
	All over	8	16.0		
	N.A.	4	8.0		
KRAS status	Mutated	10	21.3	N.S.	N.S.
	Wildtype	12	25.5		
	N.A.	25	53.2		
CEA > 5ng/ml	Yes	23	48.9	N.S.	N.S.
	No	16	34.0		
	N.A.	8	17.0		

There was an association between the location of the primary tumor and OS (p=0.030; Gehan-Wilcoxon) and PFS (p=0.037; Gehan-Wilcoxon). Also we found an association between the size of the primary tumor and OS (p=0.002; Univariable Cox) with a hazard rate (HR) of HR=1.879 (the risk of dying is increased by 87.9% with every centimeter of tumor size) and PFS (p=0.005; Univariable Cox)

with HR=1.478. Kaplan-Meier curves for associations with OS are displayed in **Figure 13**. For location of the primary tumor, patients with a left-sided CRC have the longest OS (**Figure 13a**), patients with transvers CRC the shortest OS. The OS of Patients with hepatic metastases differs significantly between patients with metastases in the left side of the liver, the right side or all over the liver (**Figure 13b**). For the hepatic metastases an association was detected between the location of the hepatic metastases with OS (p=0.003; Gehan-Wilcoxon). When patients were grouped into categories of 1 hepatic metastasis, 2-8 metastases and 9 or more metastases, statistics resulted in significant shorter OS the more metastases were observed (**Figure 13c**).

An automated threshold for primary tumor size using Kaplan-Meier curves resulted in a cut-off of 4.5 cm (**Figure 13d**). Patients with primary tumors >4.5 cm have a significant shorter OS and PFS.

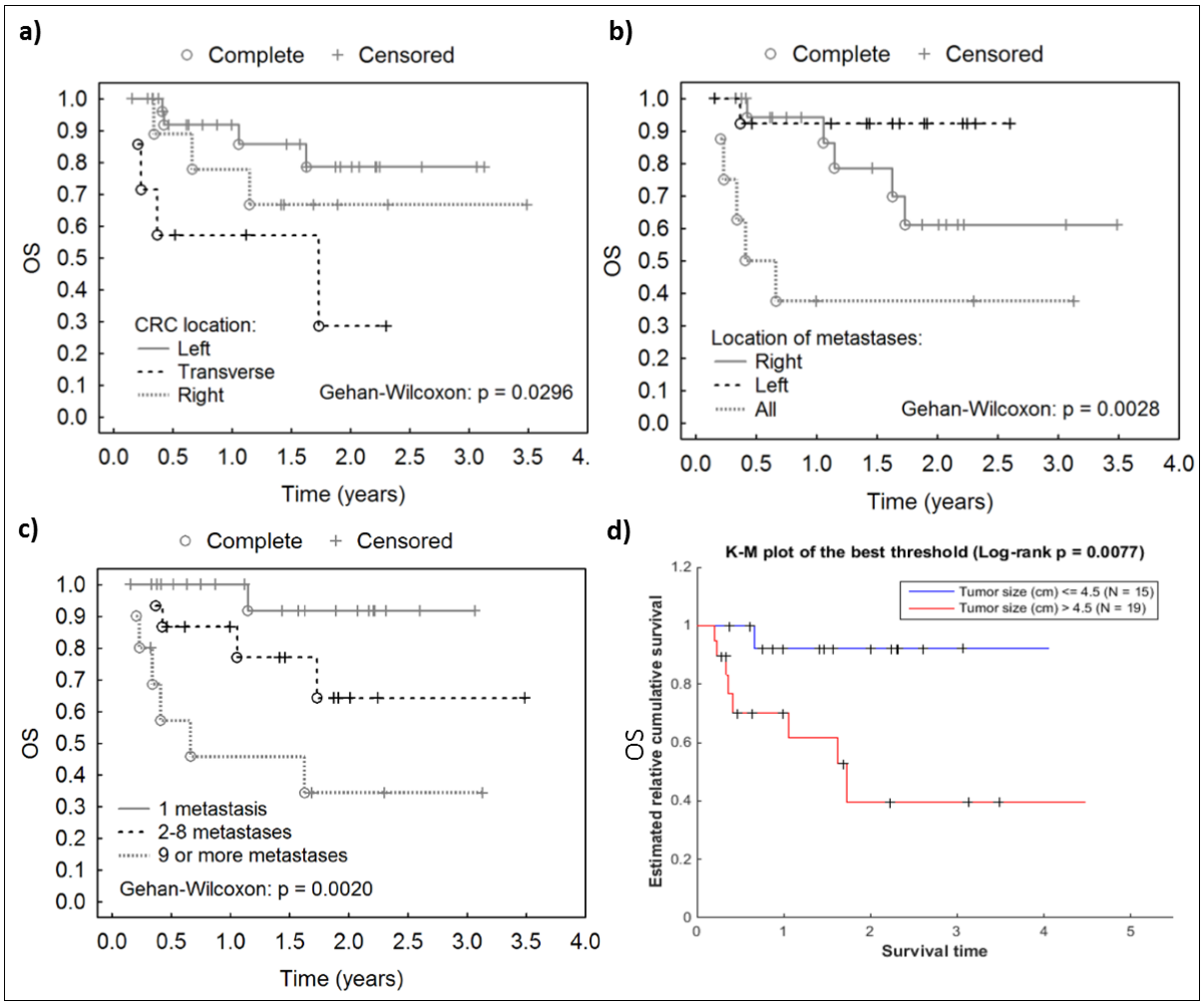

Figure 13: Kaplan-Meier curves for association between clinical cohort data and OS. a) Patients with primary tumors on the left side have the longest OS and patients with transvers CRC have the shortest OS of the cohort. **b)** CRC patients with hepatic metastases limited to the left side of the liver have the longest OS and patients with metastases all over the liver the shortest OS **c)** Patients with 9 or more hepatic metastases have the shortest OS. **d)** Optimized threshold for the tumor size shows a significant shorter OS for patients with primary tumors >4.5 cm.

5.4.2 Association of HD-CTC counts with survival

The enumeration data of chapter 5.2.2 was analyzed for associations with OS and PFS. There was no significant association with survival for the binary variables as shown in **Table 7**.

Table 7: Categorical HD-CTC variables and their association with survival

	Groups	No.	%	Assoc. with OS	Assoc. with PFS
> 2 HD-CTCs in Pre-Res	Yes	27	57.4	0.266	0.697
	No	19	40.4		
	N.A.	1	2.1		
> 3 HD-CTCs in Pre-Res	Yes	24	51.1	0.821	0.955
	No	22	46.8		
	N.A.	1	2.1		
> 2 HD-CTCs Follow-Up	Yes	24	51.1	0.379	0.113
	No	14	29.8		
	N.A.	9	19.1		
> 3 HD-CTCs Follow-Up	Yes	20	42.6	0.094	0.513
	No	18	38.3		
	N.A.	9	19.1		

Neither the HD-CTC positivity in the pre-resection draw nor in the follow-up blood draw was associated with survival (we tested thresholds of 2 and 3 cells/ml blood). For continuous variables (HD-CTC/ml blood) of the pre-resection draw and the follow-up draw, no association was detected for OS and PFS. A trend for being associated with OS (p=0.063; Univariable Cox) showed HD-CTC/ml blood in the follow-up draws.

5.4.3 Association of CTC subcategory counts with survival

We tested detected amounts of cells/ml of blood for all three subcategories of detected CTCs in the pre-resection and follow-up draw with OS and PFS and found an association of CTC-Small/ml in the follow-up draw with OS (p=0.040; Univariable Cox), with a HR=1.031. Using an automated threshold for this continuous variable, the Kaplan-Meier curve (**Figure 14**) shows that patients with >13.25 CTC-Small/ml of blood in the follow-up draw have a significant shorter OS than those patients with less CTC-Small/ml blood. After analysis of healthy donor samples, the thresholds of 8 CTC-Small/ml, 8 CTC-LowCK/ml and 5 CTC-cfDNA/ml producing were calculated. Applied to enumeration data of our cohort it resulted in significant association of 8 CTC-Small/ml blood with PFS (p=0.015; Gehan-Wilcoxon, **Figure 14b**).

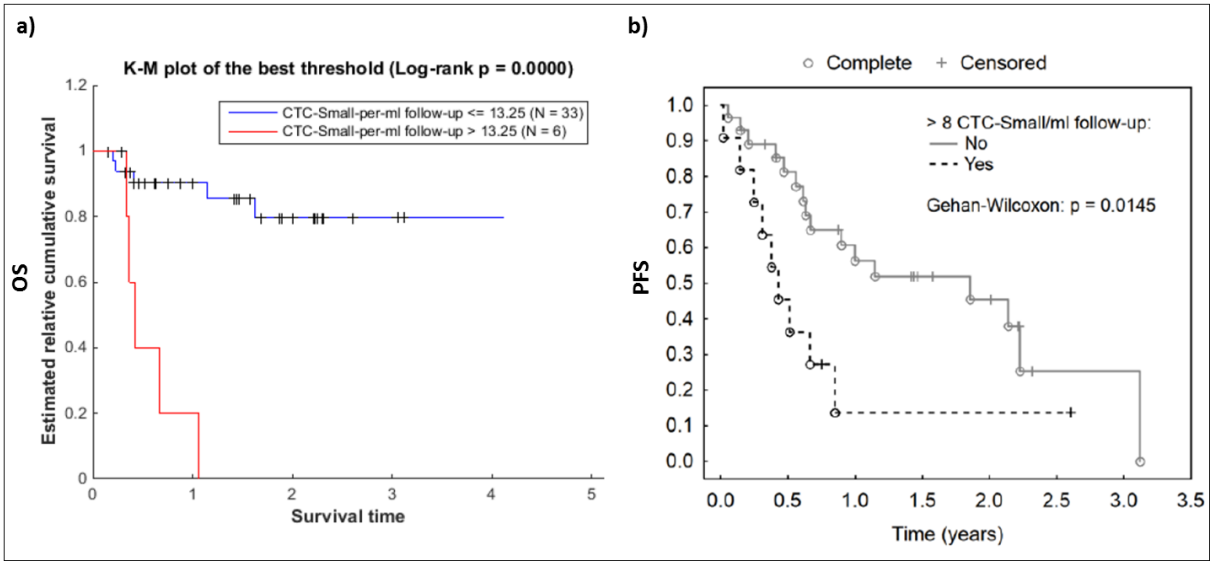

Figure 14: Association of CTC-Small counts/ml blood with OS and PFS. In **a)** an optimized threshold was applied for Kaplan-Meier curve for association of CTC-Small/ml blood in the follow up draw, **b)** shows the threshold of 8 CTC-Small/ml is associated to PFS in the follow-up draw.

5.4.4 Association of CTCCs with survival

All binary variables for clusters (positivity for clusters in pre-resection and follow-up) and continuous variables for cluster counts were tested for association with PFS and no association was significant.

Associations between binary cluster variables and survival are listed in **Table 8.**

On the other hand we found multiple enumeration data regarding CTCCs associated to OS.

Table 8: Association of binary CTCC variables with survival

Category	Groups	No.	%	Assoc. with OS	Assoc. with PFS
Clusters in Pre-Res	Yes	18	38.3	0.831	0.704
	No	28	59.6		
	N.A.	1	2.1		
Clusters in Follow-Up	Yes	8	17.0	**0.033**	0.315
	No	30	63.8		
	N.A.	9	19.1		
Clusters >6 cells max Pre-Res	Yes	9	50.0	0.624	0.235
	No	9	50.0		

Patients with CTCCs in the follow-up draw showed significant shorter OS (p=0.033; Gehan-Wilcoxon) and a Kaplan-Meier curve is presented in **Figure 15a**.

CTCCs/ml in the pre-resection draw were associated with OS as continuous variable (p=0.021; Univariable Cox) with a HR=1.062. The automated threshold for a Kaplan-Meier curve revealed that patients with a maximum cluster size >8 cells detected only in the pre-resection draw tend to have shorter OS (**Figure 15b**, p=0.059; Gehan-Wilcoxon), but only 3 patients had clusters with more than 8 cells.

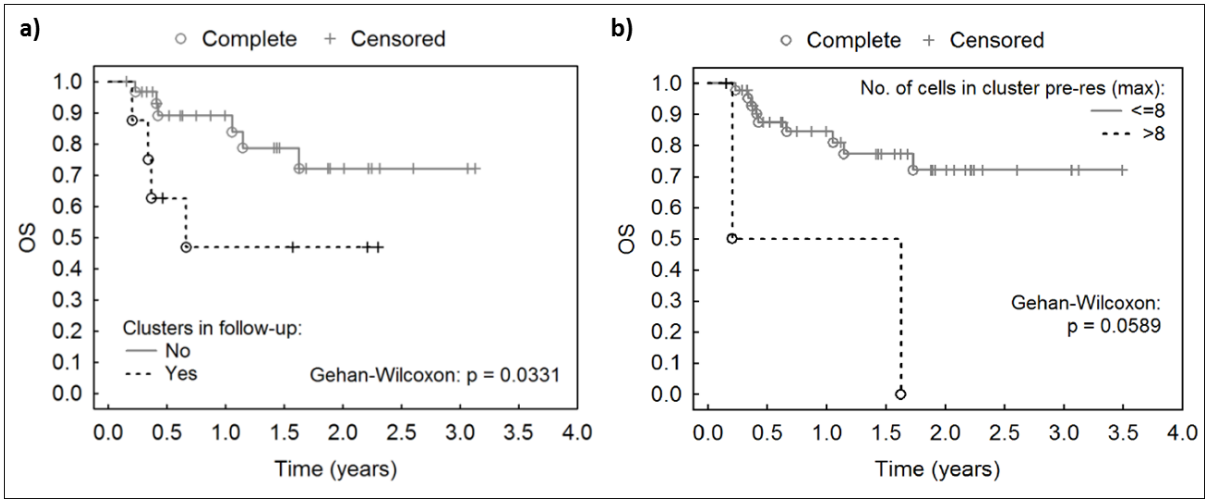

Figure 15: Association of CTCC variables with survival. a) Kaplan-Meier for the association CTCC positivity in the follow-up draw with OS **b)** Kaplan-Meier curve for the association of clusters containing >8 cells maximum in the pre-resection draws.

5.5 Association of HD-CTC and CTCC enumeration data with clinical characteristics

The tested clinical characteristics were *KRAS* mutation status (wildtype or mutated), CEA level >5 ng/ml, T, N, M, size of hepatic lesions and the primary tumor (in cm), location of hepatic metastases (left, right and all over the liver) and location of primary tumor (left, right and transverse). If not stated otherwise the results were non-significant for the mentioned variables. Differences between the resection type regarding cell count changes is examined in chapter 5.5.1.2.

5.5.1 Association of HD-CTCs counts with clinical characteristics

5.5.1.1 HD-CTC counts in association with clinical characteristics

The obtained HD-CTC counts per ml blood in the pre-resection draw showed a significant difference in patients depending on the primary tumor locations (p=0.032; Kruskal-Wallis ANOVA) with highest amounts of HD-CTCs/ml observed in patients with transverse tumors (**Figure 16a**). There was also a

difference observed between *KRAS* wildtype and *KRAS* mutated primary tumors and HD-CTC/ml in pre-resection (p=0.003; Mann-Whitney U, **Figure 16b**). In the 13 patients with *KRAS* wildtype, HD-CTC counts were mostly between 0 and 6 HD-CTCs/ml blood and only reached 10 HD-CTCs/ml in the pre-resection draw of one patient; whereas in *KRAS* mutant patients, only one is HD-CTC negative and two even have over 200 HD-CTCs/ml. HD-CTCs/ml in the follow up draw were not associated to any clinical characteristics tested.

The binary variables of HD-CTC positivity (>2 and >3 HD-CTCs/ml) have also shown to be associated to *KRAS* status (p=0.030 and p=0.027 respectively; Fisher's test).

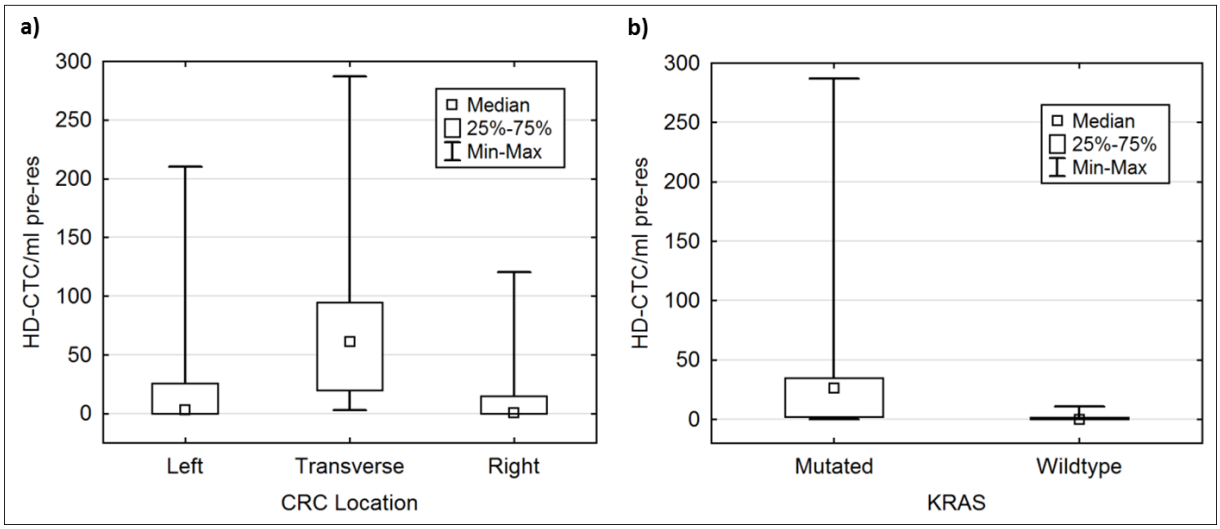

Figure 16: Association of HD-CTC counts in the pre-resection draw with tumor location and KRAS. Boxplot diagrams of **a)** HD-CTC/ml blood in the pre-resection draw in different primary tumor locations and **b)** HD-CTC/ml blood in patients with differing KRAS status.

5.5.1.2 Changes of HD-CTCs in association with resection type

After splitting the patient cohort by resection type, the change of HD-CTC counts depending on the type of resection was analyzed (**Figure 17**).

The HD-CTC counts drop significantly after resection of the primary tumor compared to changes after resection of hepatic metastases (p=0.025; Chi-Square test). Out of the 21 resections of hepatic metastases (with evaluated blood draws before surgery and in follow-up), only 5 patients showed a drop of >3 HD-CTCs/ml, with one sample being extremely high with 375.9 HD-CTCs/ml dropping down to 14.5 HD-CTCs/ml (**Figure 17**, left, sample cut off by scale). Within 20 resections of the primary tumor, in 6 comparisons the HD-CTCs decreased >80 cells/ml, but in one patient an increase of over 200 cells/ml after resection occurred (**Figure 17**, right). No significant drop in cell counts after a type of surgery was detected for the CTC subcategories or CTCCs.

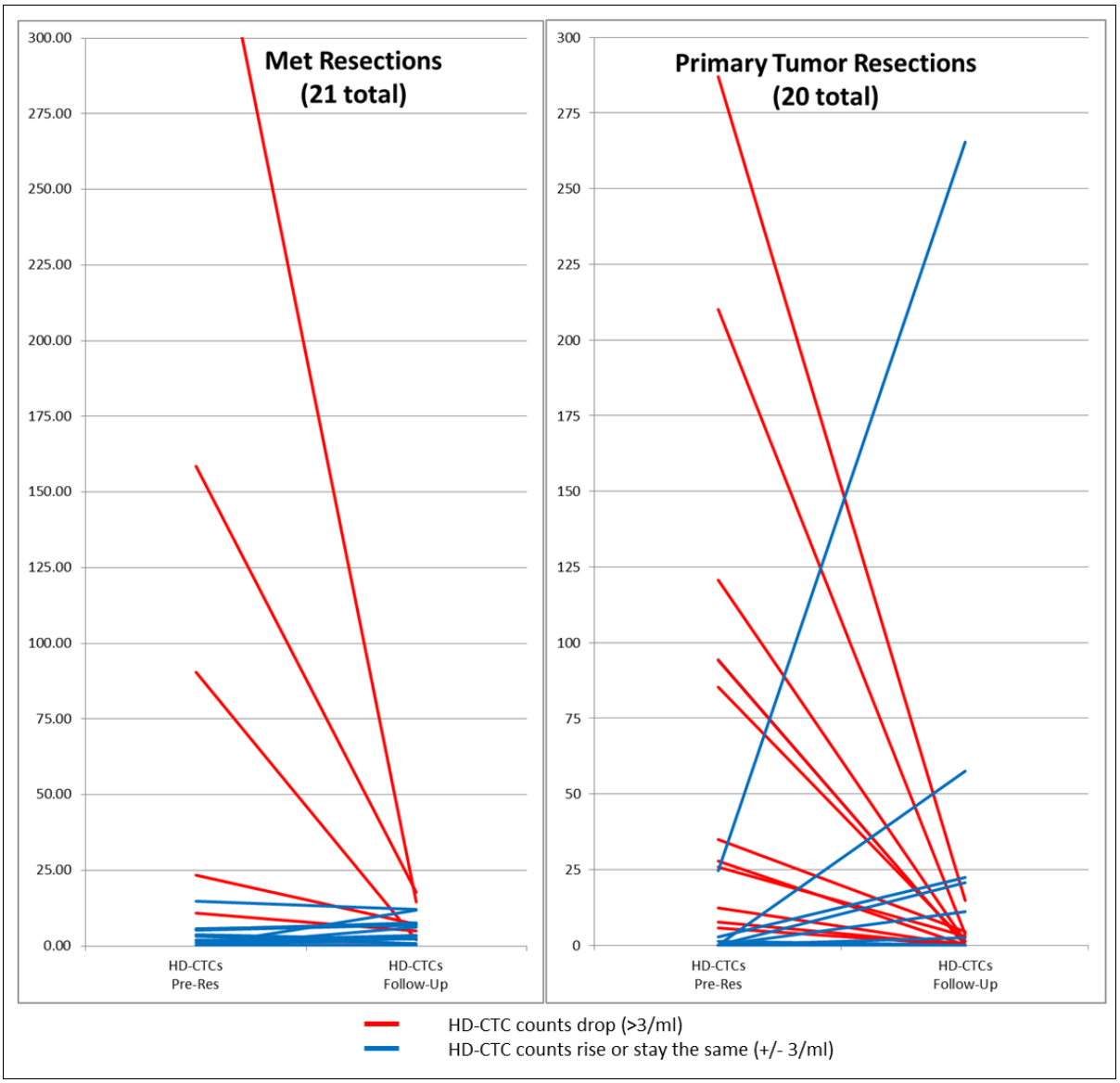

Figure 17: Development of HD-CTC counts depending on resection type. HD-CTC counts are displayed after resection of the hepatic metastases (left) and after resection of the primary tumor (right). The counts change significantly different depending on the resection type (p=0.025) and tend to drop more likely after resection of the primary tumor and stay mainly the same after resection of hepatic metastases.

5.5.2 Association of CTC subcategories with clinical characteristics

For CTC-cfDNA producing/ml in the pre-resection draw we found an association with the size of hepatic metastases (p=0.032; Spearman's), the larger the hepatic metastasis, the more CTC-cfDNA producing cells/ml. In the follow-up draw the threshold of 5 CTC-cfDNA producing cells/ml was associated with lymph node involvement (p=0.044; Mann-Whitney U) with >5 CTC-cfDNA producing cells being mainly in N2 patients and in none of the N0 patients.

For CTC-LowCK/ml in the pre-resection a significant varying number depending on the CRC location (p=0.038; Kruskal-Wallis, **Figure 18a**) was detected.

Counts of CTC-Small/ml blood in pre-resection draws show significantly differing numbers within patients with varying K*RAS* status (p=0.014; Mann-Whitney U), with higher CTC-Small/ml counts in pre-resection draws in patients with mutated *KRAS* CRC (**Figure 18b**). Numbers of CTC-Small in follow-up draws showed no association to *KRAS* status.

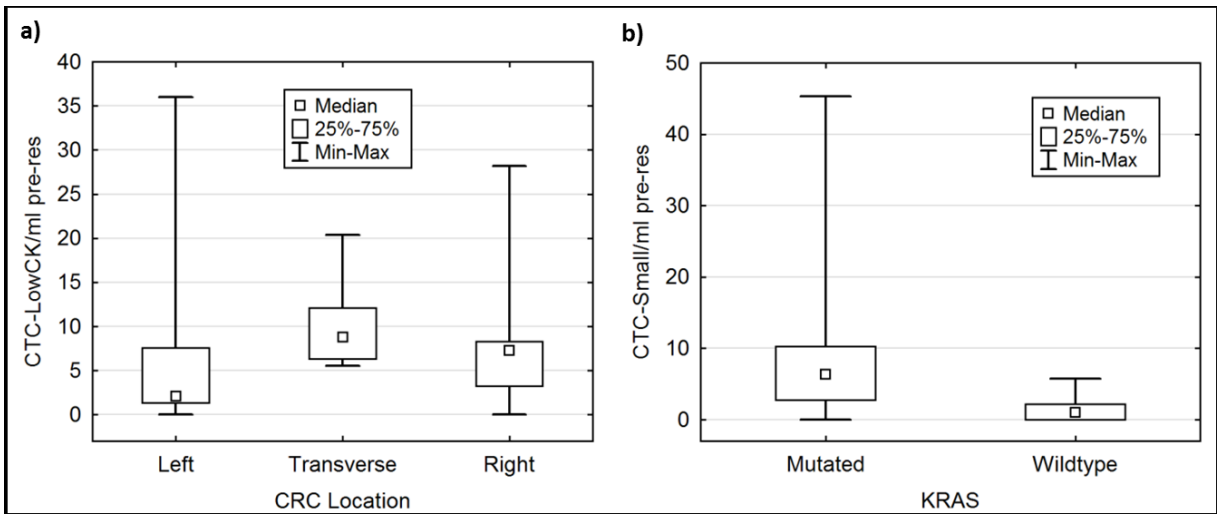

Figure 18: Association of CTC subcategories with tumor location and KRAS status. Boxplot diagrams of **a)** CTC-LowCK/ml in the pre-resection draw in association to CRC location and **b)** CTC-Small/ml blood in pre-resection draws and corresponding *KRAS* status.

5.5.3 Association of CTCCs with clinical characteristics

We observed no association between cluster positivity in pre-resection draws, or number of cells in clusters (mean or max) with size or location of the primary tumor or size of hepatic metastases. Looking at the metastatic status at the time of CRC diagnosis (M0 vs. M1), we detected a significantly higher average amount of cells within detected clusters in patients with M1 status at time of diagnosis (p=0.035; Mann-Whitney U, **Figure 19a**).

The amount of clusters/ml blood detected in the pre-resection draw has been significantly associated to the *KRAS* status of the patient's CRC (p=0.025; Mann-Whitney U, **Figure 19b**) with higher numbers of CTCCs/ml in the pre-resection draws of *KRAS* mutated patients.

Additionally, the CTCC counts after resection decreased differently depending on the location of the primary tumor (p=0.014; Chi-Square), with the least decrease in CTCC counts in right-sided CRC.

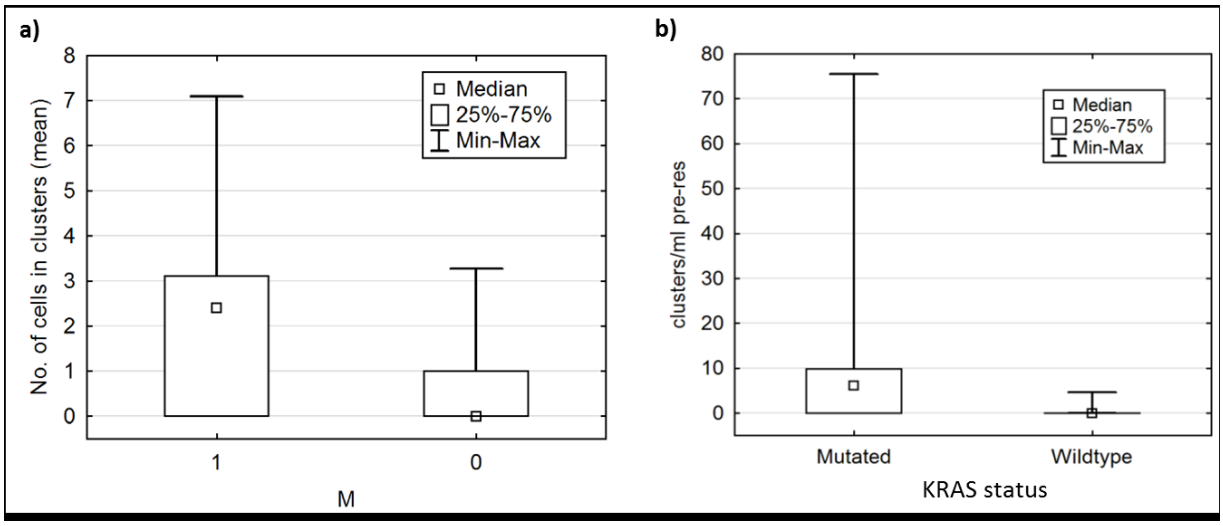

Figure 19: Association of CTCCs with metastasis and KRAS status. Displayed are boxplot diagrams of **a)** the average number of cells in clusters depending on the involvement of distant metastases at time of diagnosis **b)** the amount of CTCCs/ml blood in the pre-resection draw depending on the *KRAS* status of the patient's CRC.

5.5.4 Mutual correlations between clinical characteristics

The size of the primary tumor has been associated to the number of hepatic metastases (p=0.044; Spearman), and the number of hepatic metastases was associated to their location (p=0.001; Kruskal-Wallis, **Figure 20a**). Also associated to the location of hepatic metastases was infiltration of lymph nodes, the N status (p=0.004; Kruskal-Wallis, **Figure 20b**). No association was detected between metastases and *KRAS* status or the location of CRC and *KRAS* status.

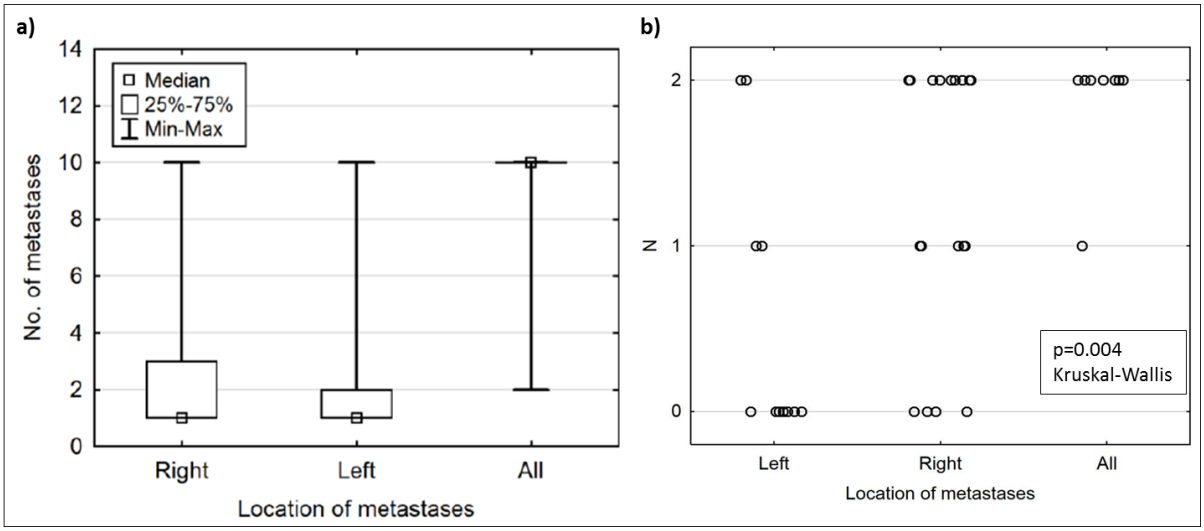

Figure 20: Associations between the location of hepatic metastases and lymph node status (N) and the number of metastases. The differing location of hepatic metastases showed significant associations with **a)** the number of hepatic metastases and **b)** the lymph node involvement (N).

5.6 Analysis of CNV profiles from CTCs and tissue touch preps

With single-cell CNV-profiling it became possible to detect clonality within CTCs. Unfortunately; no clear definition of clonality has been specified so far. For the purpose of our study, clonality was assessed as „two or more cells that share two or more genomic alterations" [206].

5.6.1 CNV profiles of HD-CTCs in CRC

A total of 136 HD-CTCs from the pre-resection draws of eleven patients have been analyzed. The clustered cells are displayed in **Figure 21**.

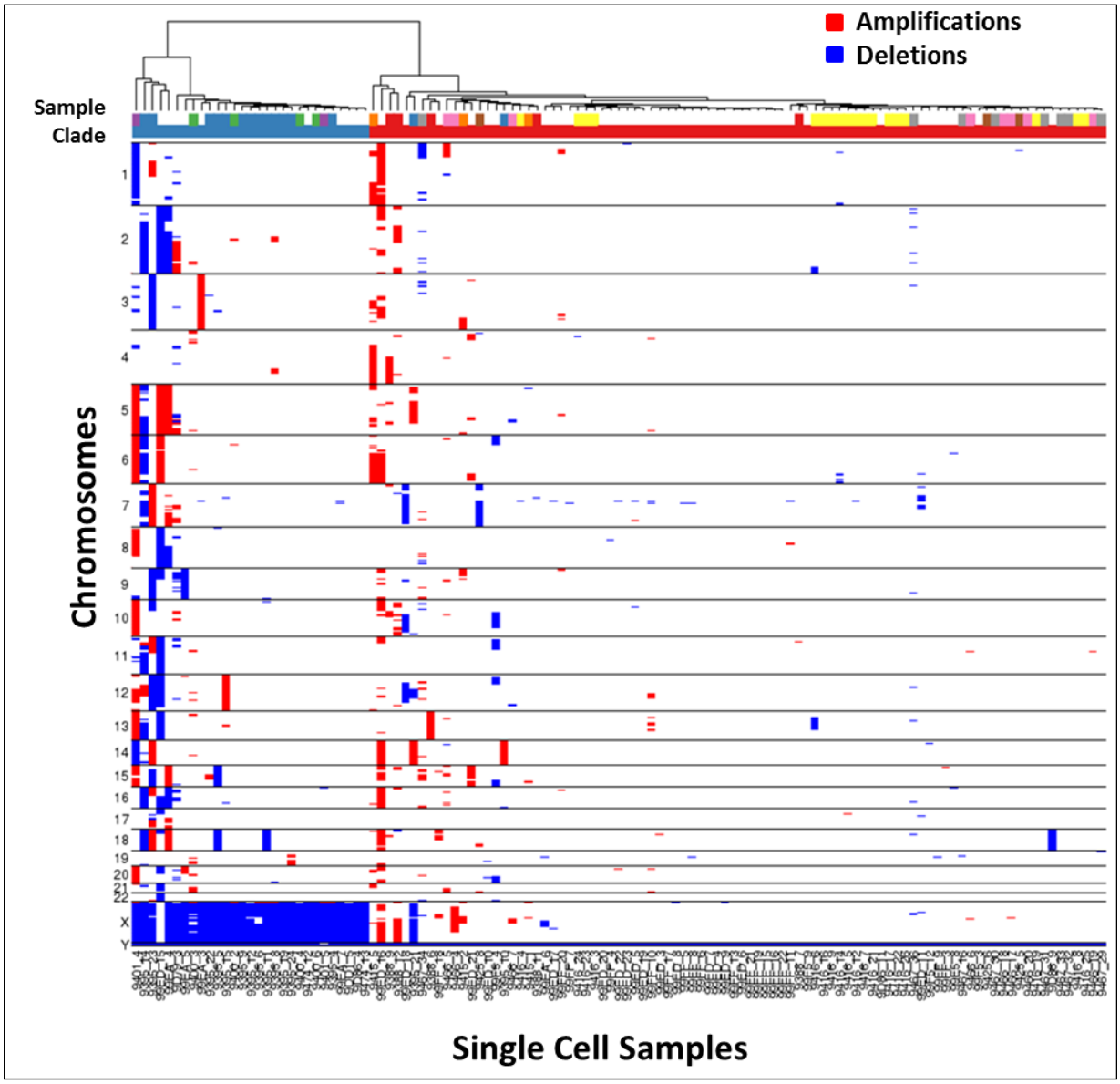

Figure 21: CNV profiles of all analyzed single HD-CTCs of pre-resection draws. Heatmap clustering (method ‚ward.D', distance method ‚manhattan' with 5k resolution) of 136 HD-CTC of pre-resection draws from 11 patients that showed no clonality.

CNV profiles separated per patient are illustrated in **Figure 22**. Analysis of specific alterations resulted in the detection of 21.3% (29 HD-CTCs) of the cells with partly deleted or amplified Chromosomes.

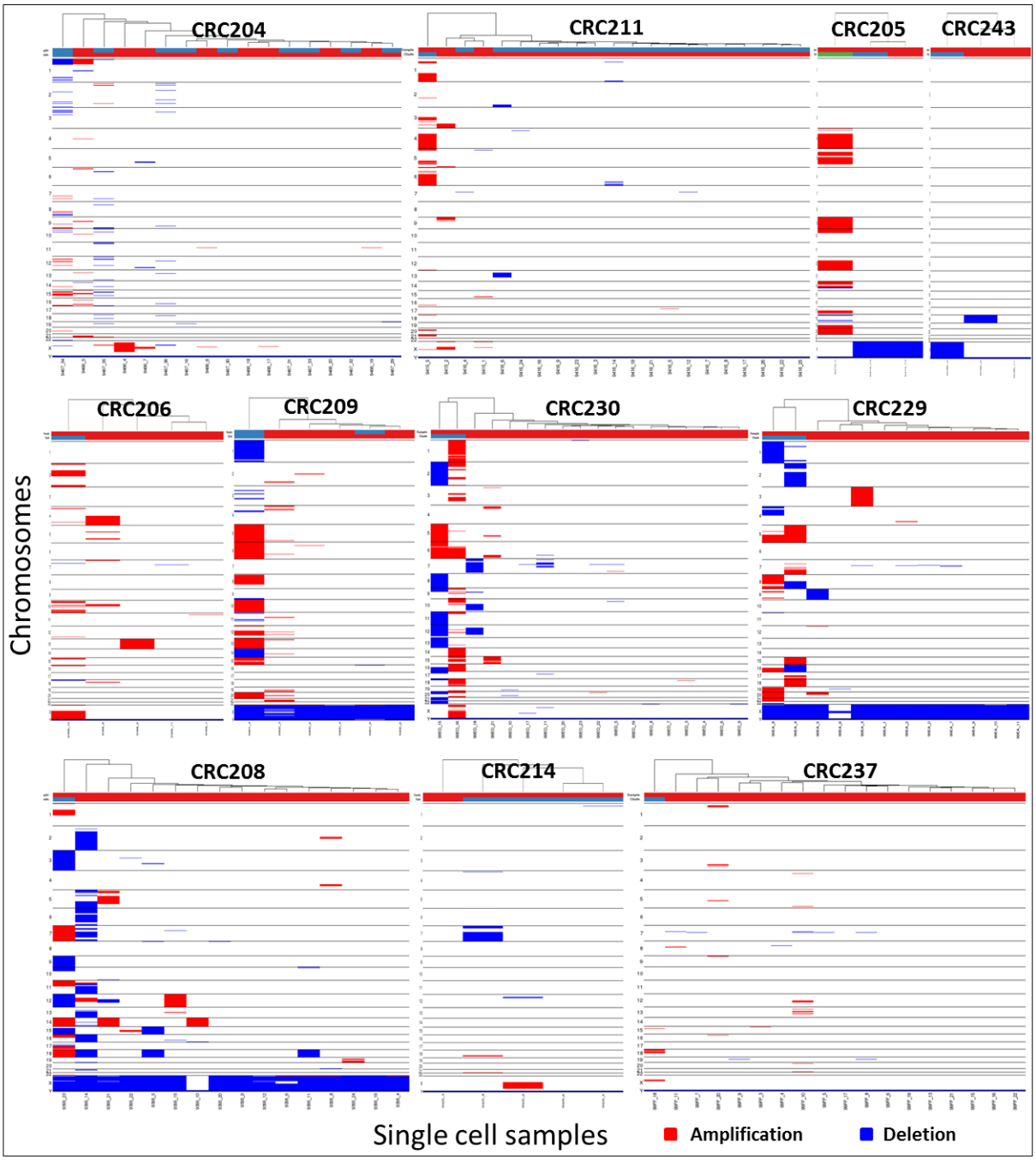

Figure 22: CNV profiles of HD-CTCs separated per patient. All analyzed single HD-CTCs from pre-resection draws of 11 patients in heatmaps (method ‚ward.D', distance method ‚manhattan' with 5k resolution) separated per patient.

HD-CTC clonality was detected, neither within particular patients nor within the HD-CTCs originating from different patients (to follow convergent changes in CRC cell genomes), so analysis of association of detected HD-CTC clones with survival was impossible. Clonality has been tested also for the cells from CTC subcategories, but their number was not sufficient for further analysis.

5.6.2 CNV profiles of single cells from CRC touch preparations

We analyzed a total of 126 single-cells isolated from CRC touch preps of 12 patients from our cohort. Ten out of 12 patients (83.3%) showed clonal profiles within the analyzed cells (**Figure 23**). Out of the 126 isolated cells, 87 cells (69%) were part of clonal profiles.

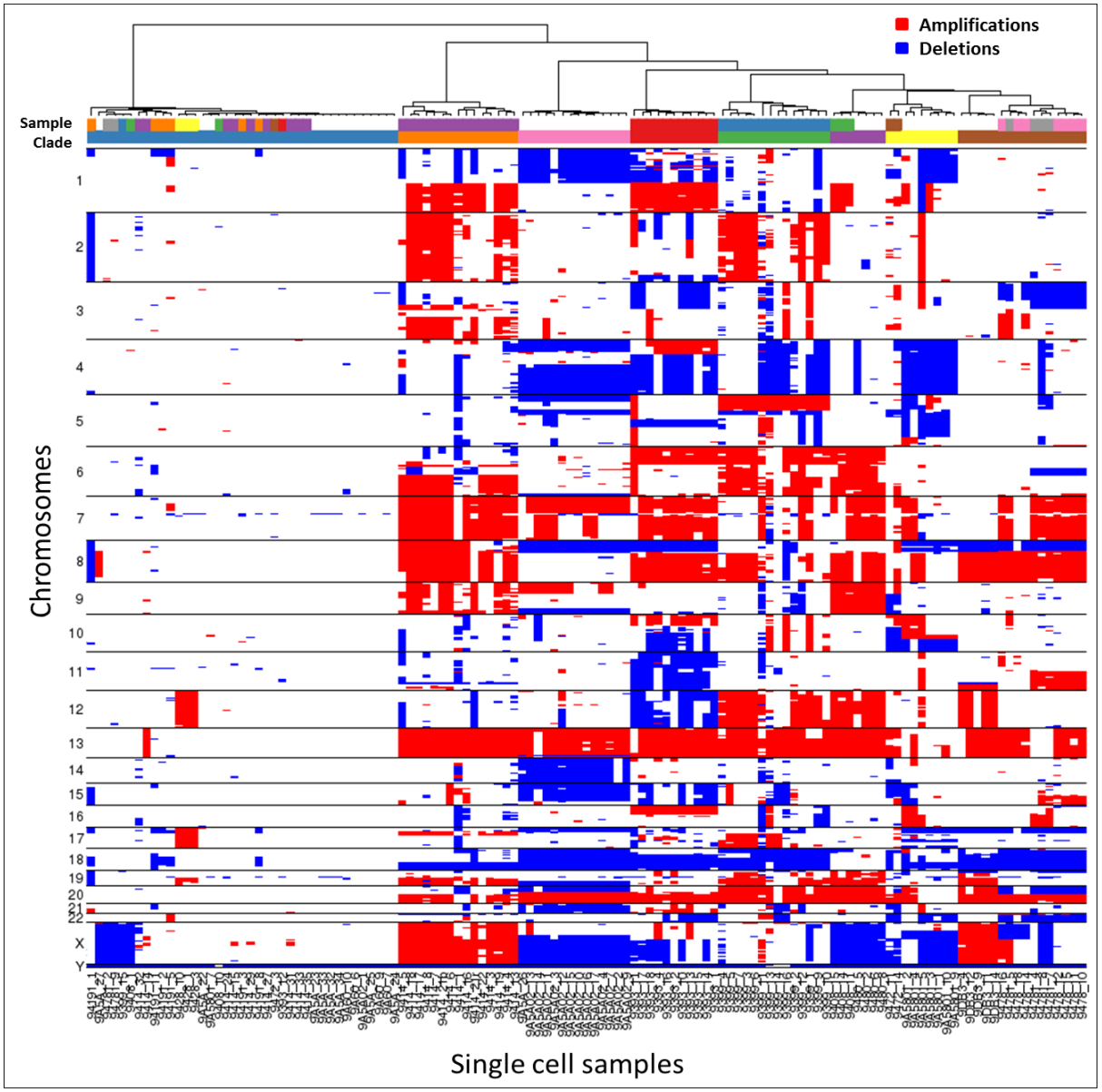

Figure 23: CNV profiles of all analyzed single cells from CRC touch preps. A total of 126 cells isolated from CRC tissue from 12 patients is displayed here in a heatmap (method ‚ward.D', distance method ‚manhattan' with 5k resolution) of 8 clades.

Only patients CRC211 and CRC237 had no clonal cells within their analyzed cells of CRC tissue (as shown in separate CNV profiles in **Figure 24**.

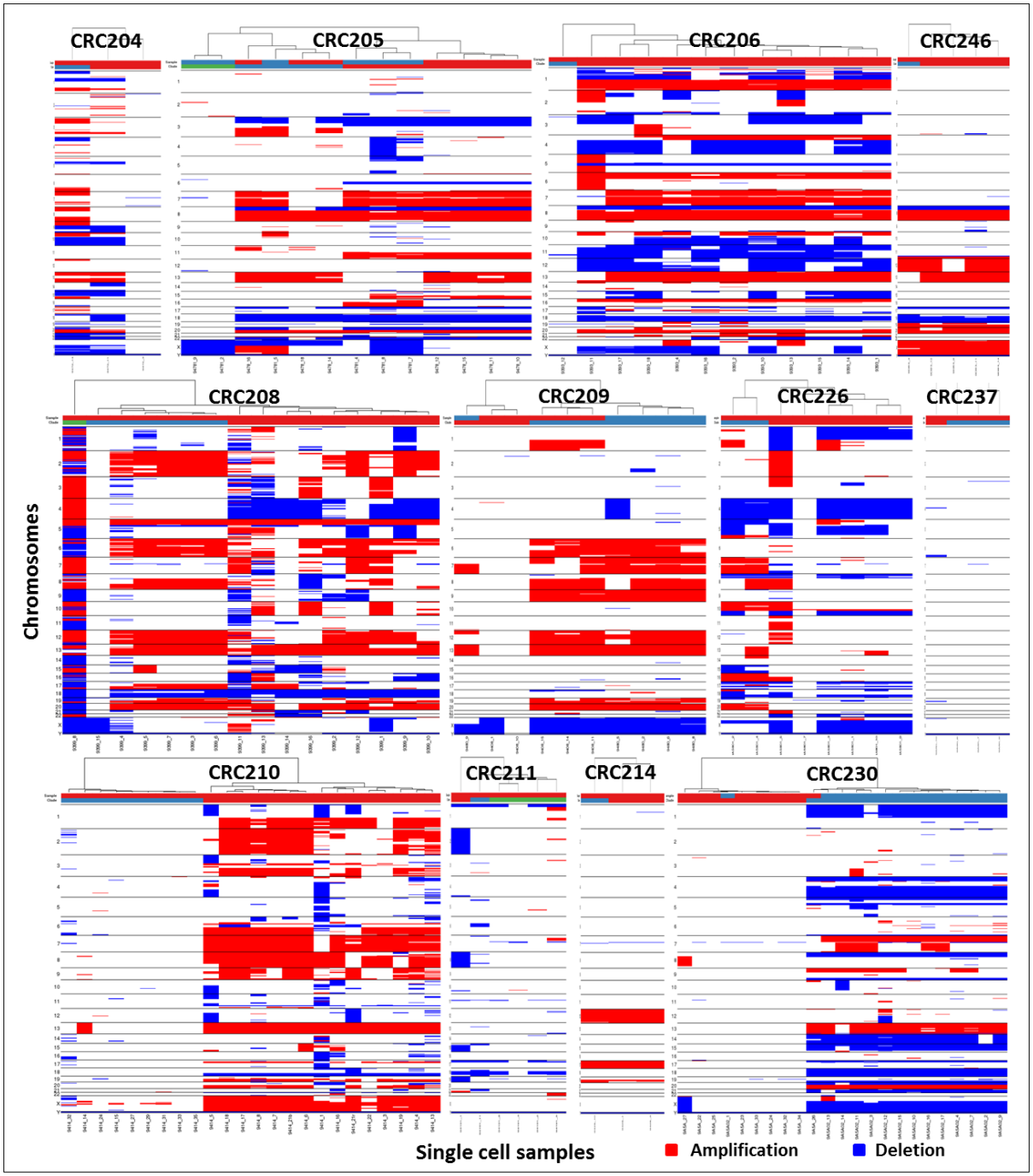

Figure 24: CNV profiles of single cells isolated from CRC tissue separated by patient. Shown are the CNV profiles from CRC tissue touch preps of 12 patients. Two patients (CRC211 and CRC237) did not show cells with clonal profiles. The other ten patients show at least two or more cells with similar alterations.

Looking at each patient separately, varying amounts of cells showed no or few alterations and were clustered in a different clade than the cells of the main clonal profile of the patient. In all ten patients with clonal profiles over 50% of the analyzed cells were clonal.

In case of the CRC touch prep from patient CRC206, only one cell (8.3%) differs from the main clone (**Figure 25**). Observed areas of amplification contain for example *NOTCH2*, *MUC1*, *MYC*, *ERCC4* and *TOP1*.

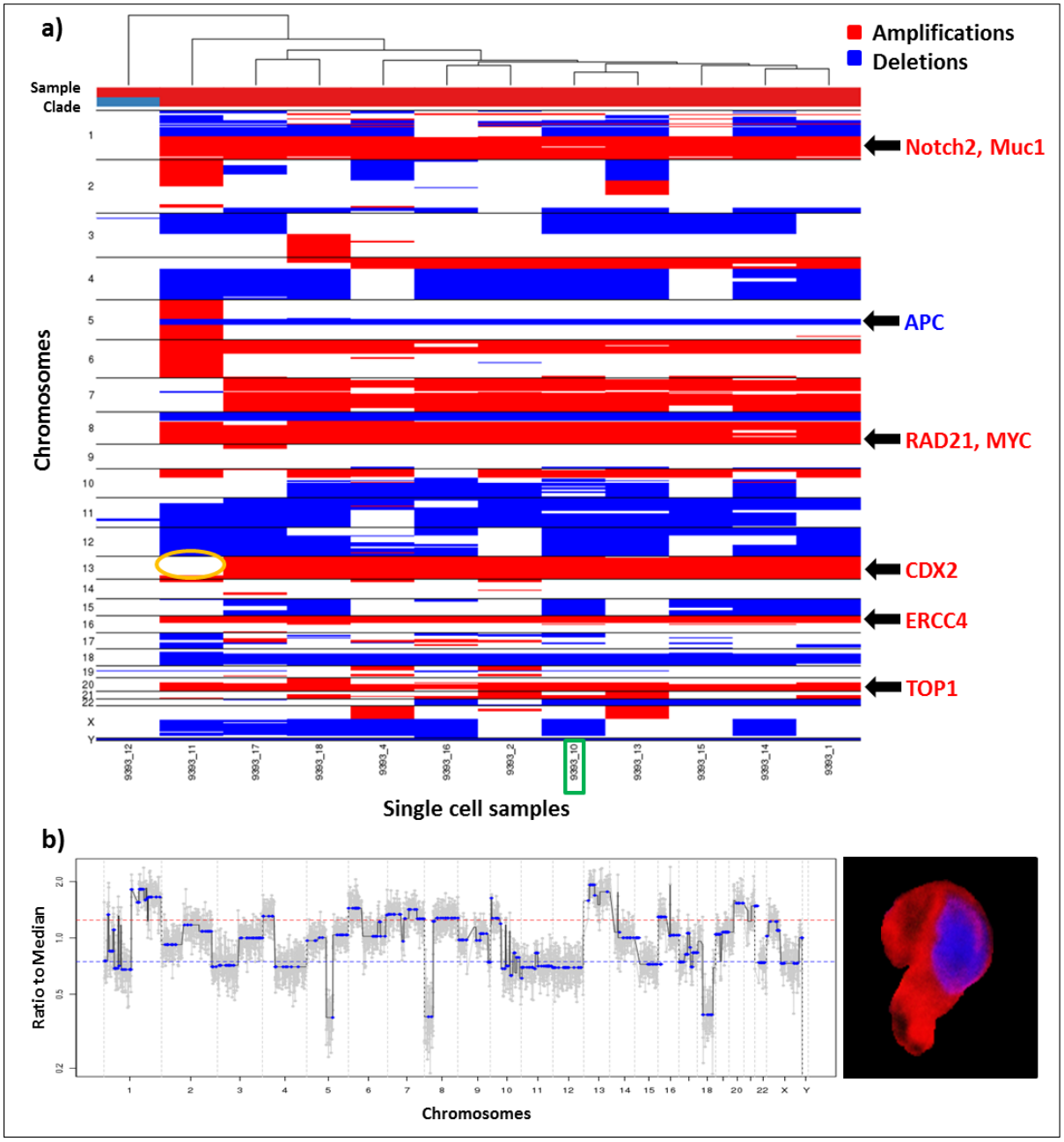

Figure 25: Heatmap of the analyzed single cells of the left sided primary tumor from patient CRC206. a) The heatmap shows 12 isolated single cells from a touch prep of a left sided CRC. Eleven out of twelve cells belong to one clone with one of the eleven cells showing one modification, the missing amplification of the *CDX2* containing region (marked with orange elipse). **b)** A single profile using the ratio median with the corresponding composite picture of the cell (red=CK-pan, blue=DAPI and green=CD45). The chosen cell is marked in the heatmap with the green rectangle.

An area of deletion on chromosome 5 contains *APC*. Some cells within a clone can show slight modifications in particular regions, here, for example the area of *CDX2* was not amplified in one cell. For better graphical visualization of the exact alterations of the regions one cell with it's corresponding CNV profile is displayed in **Figure 25b**.

5.6.3 CNV profiles of single cells from hepatic metastases

We analyzed a total of 37 cells from the hepatic metastases of 4 patients and observed clonality within each (100%) of the analyzed patients (**Figure 26**). Of the 37 cells, 32 (86.5%) were part of clonal profiles.

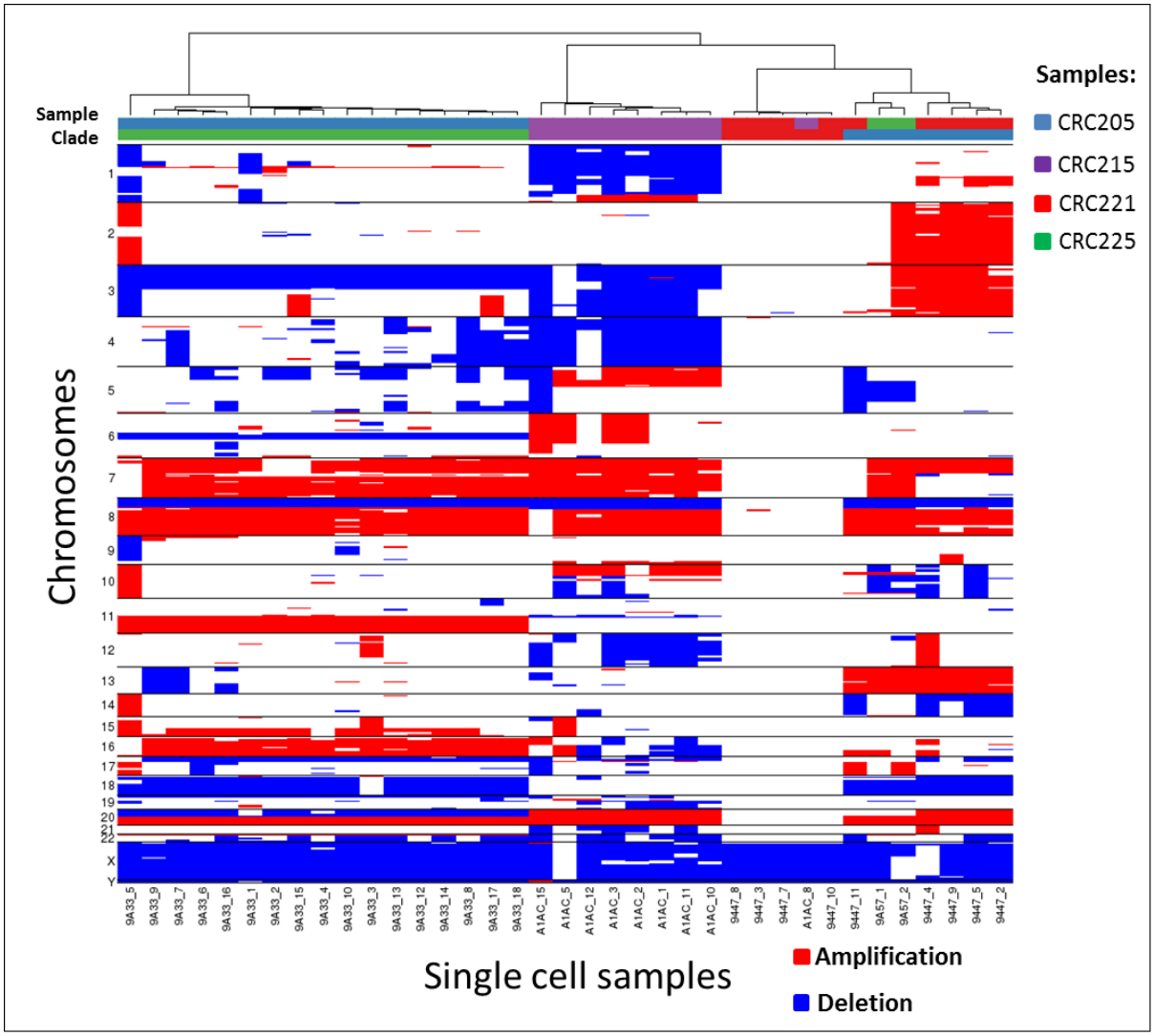

Figure 26: Overview of all CNV profiles of single cells from hepatic metastases. The CNV profiles of all analyzed single cells from the hepatic metastases of 4 CRC patients are displayed. Only 5 cells (red clade) are not clonal.

As an example, the heatmap of analyzed cells within the hepatic metastasis of patient CRC205 is displayed in **Figure 27**. Common amplifications observed were in regions containing *MET*, *BRAF*, *EGFR*, *MYC*, *RAD21*, *CCND1*, *TOP1* and *ERCC4* amongst others. Common deletions were found in regions containing *CTNNB1*, *RAF1*, *FOXP1* and *TP53*.

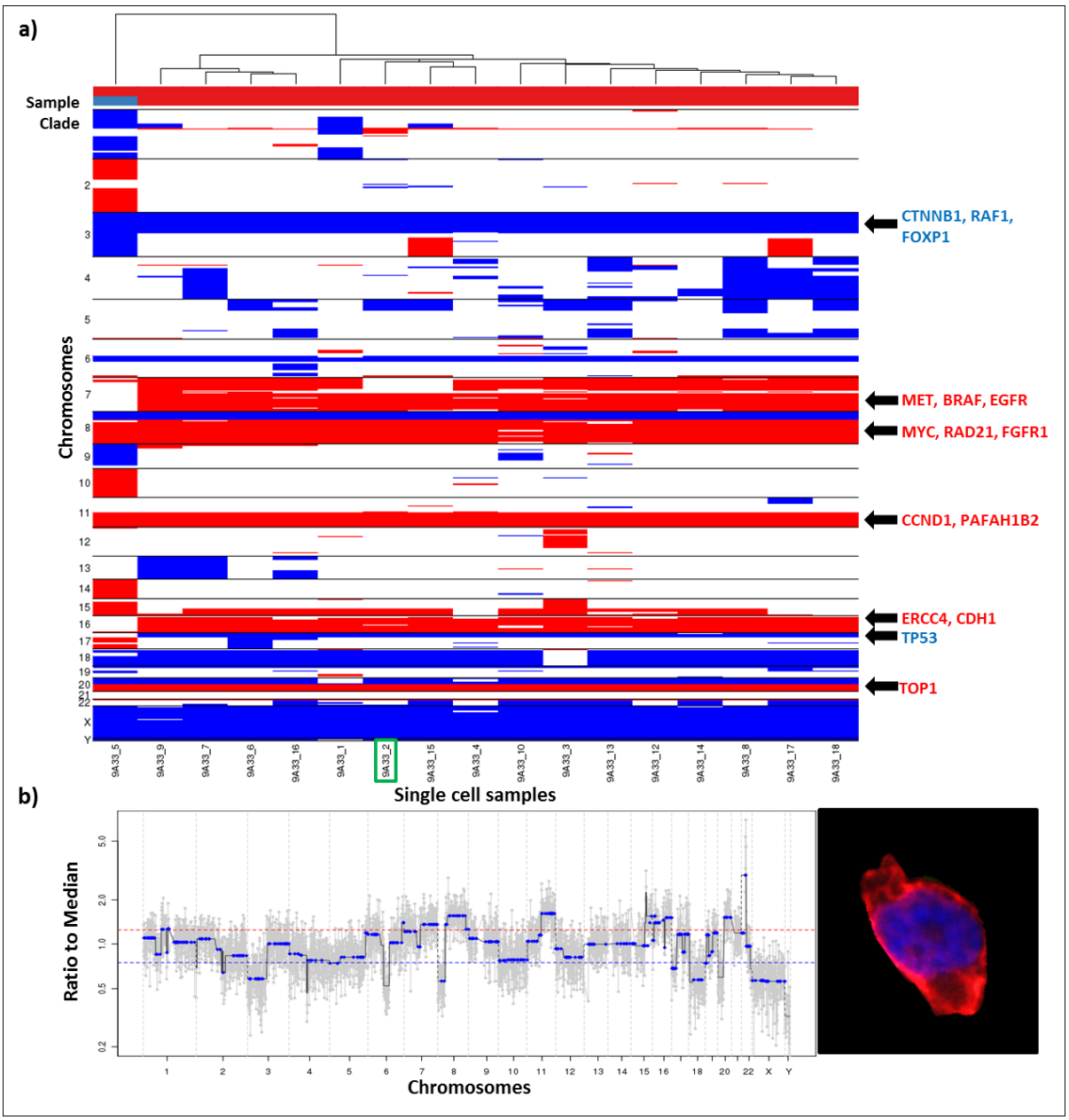

Figure 27: CNV-profiles of 17 cells from a hepatic metastasis of patient CRC205. CNV-profiles of **a)** all 17 single-cells from the hepatic metastasis of patient CRC205. 16 cells show perfectly clonal profiles and one cell (blue clade) possessing slight alterations like missing the amplification of *MET*, *BRAF* and *EGFR* regions. Marked with a green rectangle is the cell profile displayed in **b)** as a magnification of the clone together with the corresponding composite cell image(red=CK-pan, blue=DAPI and green=CD45). The chosen cell is marked in the heatmap with the green rectangle.

Only one (5.9%) out of 17 cells showed different aberrations from the detected main clone through e.g. additional amplification of chromosome 10, and normal copy numbers of the TP53 region (**Figure 27a**, first cell). The CNV profile of one of the cells of the detected clone is displayed in **Figure 27b** together with the 400X image of the corresponding cell before it was isolated from the microscopy slide.

5.6.4 Comparison of CNV profiles of touch preps and CTCs

We have analzyed CNV profiles of nine pairs of patients with HD-CTCs and matching CRC samples. As no CNV profiles of HD-CTCs were clonal, there was no clonal similarity detectable. The overview of analzyed CNV profiles of isolated single HD-CTCs and single cells from the CRC and hepatic metastasis touch preps from patient CRC205 are displayed in **Figure 28**.

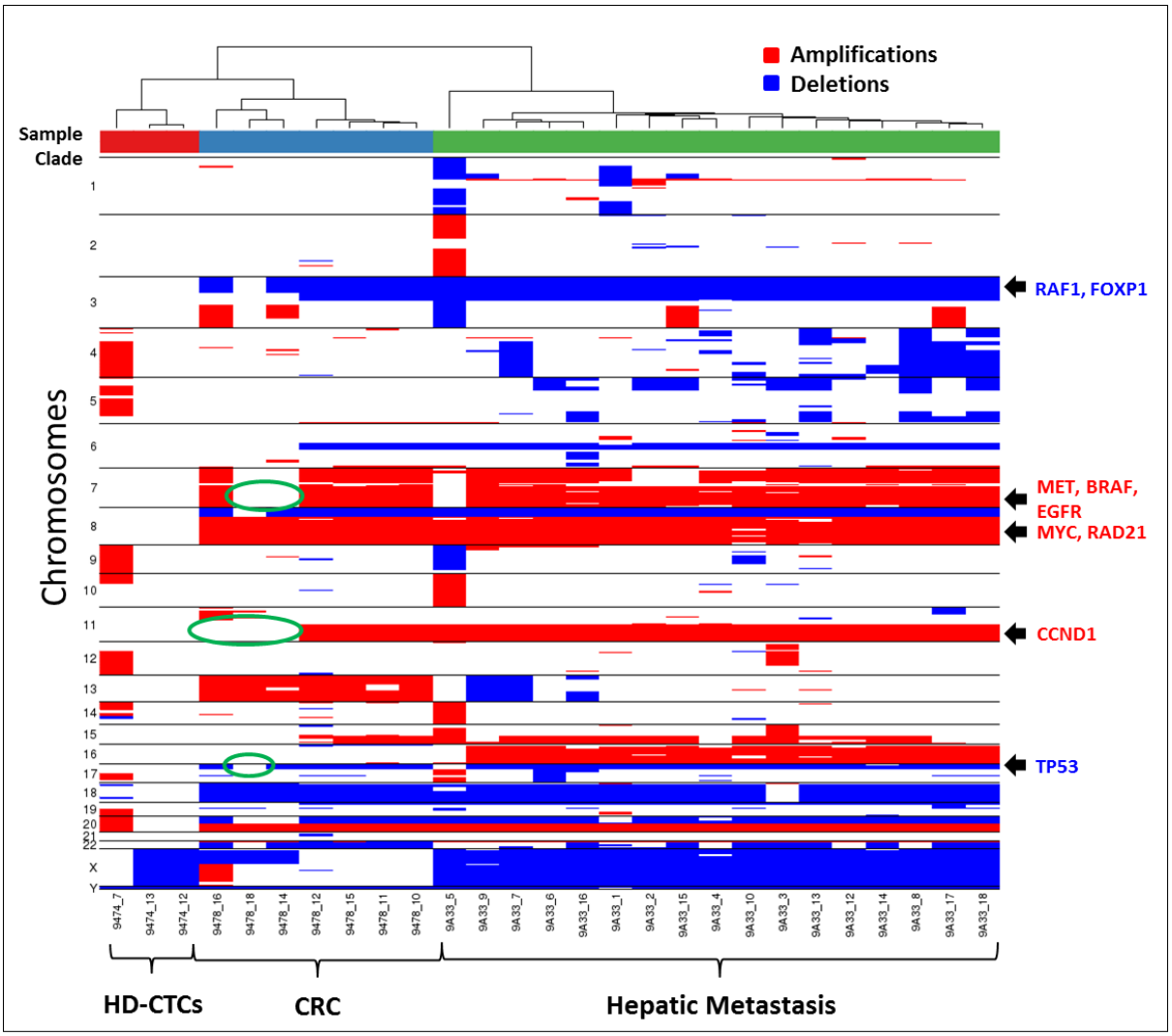

Figure 28: Comparison of CNV profiles of CTCs, single cells from CRC and the hepatic metastasis of patient CRC205. CNV profiles of HD-CTCs (red clade), isolated cells from CRC (blue clade) and the hepatic metastasis (green clade) of patient CRC205. Marked in green are regions within CRC cells that differ from the clone found in the hepatic metastasis.

The isolated single cells of the hepatic metastasis have been shown before (**Figure 27a**). In direct comparison to profiles from the corresponding CRC cells, the two sources are clustered in different clades and therefore vary (**Figure 28**, blue and red sample/clade). Some cells are matching the clone of the metastasis in multiple regions (like amplification of *MYC* region and chromosome 13 amplification), but three cells of the analyzed primary tumor cells are differing from the hepatic clone. In these three cells, *CCND1* amplification is missing in all of them, in two of these cells additionally the region containing *BRAF*, *EGFR* and *MET* are not amplified and in one cell the *TP53* region is not deleted.

In regard to the overall detected copy number alterations in the three different tumor cell sources, frequencies for altered regions were summarized in **Table 9**.

Table 9: Copy number alterations and frequencies of HD-CTCs and cells from CRC and hepatic metastasis tissue

Gene	Function	Type of alteration	CRC	Liver	HD-CTC
MYC	Transcription Factor	Amplification	**43.7%** (55/126)	**83.8%** (31/37)	**0.7%** (1/136)
MET	Proto-Oncogene	Amplification	**37.35%** (47/126)	**67.6%** (25/37)	**1.5%** (2/136)
FGFR1	Growth Factor Receptor	Deletion	**34.9%** (44/126)	**86.5%** (32/37)	**0.7%** (1/136)
CDX2	Transcription Factor	Amplification	**54%** (68/126)	**18.9%** (7/37)	**1.5%** (2/136)
APC	Tumor Suppressor	Deletion	**19.1%** (24/126)	**10.8%** (4/37)	**0%** (0/136)
Aneuploidy	—	Numerical change in a whole set of chromosomes	**73.8%** (98/126)	**86.5%** (32/37)	**11%** (15/136)

HD-CTCs showed the lowest frequency in every type of alteration with every mentioned region altered less than 2% except whole chromosome alteration which was observed in 11% of the HD-CTCs. Regions containing the genes *APC*, *MYC*, *MET*, *CDX2* and *FGFR1* have only been rearranged in up to two cells.

Within single cells of CRC tissue, 73.8% of cells showed aneuploidy (either deletion or amplification of entire chromosomes), 19.1% deletion of the *APC* gene region, 54% amplification of *CDX2* region, 34.9% deletion of *FGFR1* region, 37.4% amplification of *MET* region and 43.7% amplification of the *MYC* region.

Liver metastases tissue of four patients has been analyzed and 86.5% of the cells showed aneuploidy of entire chromosomes and deletion of *FGFR1* region, only 10.8% deletion of *APC* region, 18.9% amplification of *CDX2* region, 67.6% amplification of *MET* containing region and 83.8% showed amplifications of the *MYC* region.

Comparing copy number alterations in CRC tissue to liver tissue, alterations in *MYC*, *MET* and *FGFR1* regions increased excessively. Amplification of *CDX2* decreased (from 54% in CRC to 18.9%) and deletion of the *APC* region decreased as well. Alterations of entire chromosomes increased, but only from 73.8% in CRC cells to 86.5% in the liver tissue.

6 Discussion

CRC is a disease with high prevalence and mortality worldwide and highest mortality rates in Eastern Europe [211]. Enumeration of CTCs has been considered a promising marker for disease monitoring, survival prognosis and evaluation of treatment success [201, 212]. In our prospective observational study, an analysis of 47 AJCC stage IV CRC patients with hepatic metastases from the Czech Republic has been performed and CTCs and CTCCs have been detected and analyzed using the HD-SCA workflow, a non-enrichment approach for detection of the entire CTC population. Association with clinical parameters and survival has been analyzed and additionally CNV profiles of CTCs and corresponding tissue samples were assessed.

As in the result section (chapter 5), observed heterogeneity of CTCs will be addressed first, followed by enumeration data of all detected COI categories and, finally, analysis of obtained CNV profiles will be discussed.

6.1 Heterogeneity of CTCs in CRC

The existing studies on morphology of CTCs in CRC are limited. Many methods using magnetic bead separation produce either no images of the captured cells at all (AdnaTest®) or only low resolution images of the cells (MACS®MicroBeads, CellSearch®) [213–215]. In general studies on CTCs in CRC are not as prevalent as studies of CTCs in breast or lung cancer (PubMed search results using 'circulating tumor cells' + respective 'cancer' yield accordingly in 2979 and 2593 results as of June 20th 2018) with CRC showing only 1429 search results in PubMed.

Morphological features like size (in µm^2), nuclear to cytokeratin ratio and roundness have been analyzed by Ligthart et al. using the CellSearch® method [216], showing a high heterogeneity within CTCs from CRC. CTCs showed a mean total cell roundness of 1.5 (perfect roundness would result in 1) and a ratio between nuclear area and cytokeratin of 1, which indicated equal areas of DAPI and cytokeratin signal. They correlated a low nuclear to cytokeratin ratio (small DAPI signal with respect to CK) with a higher hazard for the patient in breast cancer. Results of size measurements in that study were biased by observed clusters which the system counts as one single cell, but high cytomorphological heterogeneity has been correlated to poor outcome [216]. In our cohort, 3001 HD-CTCs were analyzed for nuclear roundness and showed a median value of 0.7 which corresponds to a value of 1.42 using the calculation method of Ligthart et al. This does not give information about the entire cell, but at least for the nucleus it shows elliptical or elongated shapes and the high pleomorphic heterogeneity is conform with results of Ligthart et al. and Marrinucci et al. [210, 216]. For the CTC subcategories, the nuclear roundness was highest for CTC-Small cells and regarding size

or nuclear area this category was the most homogenous one. In contrast, the CTC-LowCK category showed the highest heterogeneity regarding nuclear area and one of the highest regarding nuclear roundness. This high heterogeneity in the CTC-LowCK group indicates that it consists of multiple unidentified cell types.

6.2 Healthy donors

The analysis of our healthy donor cohort resulted in similar results as in a published analysis from the HD-SCA method on healthy donors from 2012 [175]. Our average HD-CTC count in healthy donors was 0.63 cells/ml blood with a maximum of 2.3 cells/ml in one young female donor. Thus, we applied a cutoff of 3 HD-CTC/ml instead of 5 HD-CTCs/ml as used in former publications of this method regarding HD-CTCs from breast, prostate or pancreatic cancer. Compared to CellSearch® studies in CRC, this cutoff is still relatively high, as there ≥3 CTCs/7.5 ml of blood (0.4 CTCs/ml) are considered positive [214]. On the other hand an entire blood tube is analyzed in a CellSearch® analysis, whereas the HD-SCA method only uses two microscopy slides which contain approximately 1 ml of blood. The HD-SCA method may therefore offer a higher sensitivity compared to CellSearch®[175], but due to the low analyzed volume and the possibility of detecting other CK^{pos} cells released into the circulation, a higher threshold is applied.

6.3 Enumeration data

6.3.1 HD-CTCs enumeration

CTC detection rates in metastatic CRC were as low as in 26% of the patients using the CellSearch® platform [201], that was much lower than rates detected in other cancers like breast (61% CTC positivity; [217]) or prostate (57% CTC positivity; [218]). Detection rate of CTCs in our cohort of mCRC patients (52.2%) was similar to an optimized method by Gorges et al. that used the AdnaTest® in combination with the CellSearch® system to achieve a 50% positivity rate in a cohort of 38 metastatic CRC patients [214].

As patients enrolled in this study were stage IV CRC patients and therefore the disease had already spread to distant organs, it was expected to detect CTCs in a high percentage of cases. However, experimental data showed only 52.2% HD-CTC positive patients in the pre-resection draw. The relatively low CTC positivity rate could be explained through the anatomical position of the colon, which connects the blood vessels of the colon first over the mesenteric and portal vein with the liver, which may function as a sponge for CTCs and could be the reason for the liver being the main

metastatic site in CRC [219]. A similar position to the liver has the pancreas and a comparative study between CTCs detected in the portal vein with those detected in peripheral blood draws resulted in 100% positive results in the portal vein compared to 22.2% CTC positivity in the peripheral blood [220]. Therefore studies of CTCs in CRC using peripheral blood may be hindered by this fact and left with an already pre-selected CTC subpopulation that was able to pass the blood vessels in the liver. These cells may not possess the traits enabling extravasation and proliferation in distant tissue.

6.3.2 CTC subcategories enumeration

Compared to HD-CTCs, the cells of the other CTC subtypes have been found in more samples, but regarding the enumeration of healthy donors, the cutoff levels for positivity are higher than for HD-CTCs. After application of these cutoff levels, the other individual CTC subcategories did not result in a higher positivity rate than HD-CTCs. But when all counted cells/ml of all the CTC groups (including HD-CTCs) are added and a cut-off of 10 cells/ml is applied (according to the tested healthy cohort, this represents 90% specificity), 73.9% of patients are positive for COIs compared to 52.25% positivity for HD-CTCs alone in the pre-resection draw.

It has been shown before that CTCs can lose epithelial characteristics while undergoing EMT [221]. Therefore, a previous study using the CellSearch® system was perfomed capturing both – $EpCAM^{neg}$ and $EpCAM^{pos}$ cells in metastatic lung cancer patient blood, resulting in a higher overall detection rate of CTCs. However, the association with poor outcome was lost for the detected cohort of mixed CTCs compared to only $EpCAM^{pos}$ CTCs [222].

To better understand the COIs we have detected with the HD-SCA platform it will be necessary to apply multivariate analysis to study their phenotypes. Within the Kuhn laboratory first experiments have been performed using the HYPERION™ imaging system (Fluidigm Corporation, San Francisco, USA) for the detection of over 30 protein markers in parallel in one cell and assays have been validated for HD-CTCs detected in prostate cancer [223]. This allows detection of a combination of multiplex-protein markers that are tissue specific or therapy relevant as well as markers for EMT, stemness and other disease evolution relevant markers on the HD-SCA platform. Besides getting insight into multiple markers in HD-CTCs, cells of the CTC subcategories and CTCCs, it also allows the characterization of leukocytes, which could help to determine the patient's immune signature. Analyses like that may allow us to get an insight which molecular characteristics differ between the categories of HD-CTCs, CTC-LowCK and the CTC-Small category.

As most CTC detection methods are using epithelial markers to distinguish CTCs from surrounding WBCs, it would be of interest to evaluate if the here detected categories of HD-CTCs and CTC-Small

express EpCAM. Therefore, for future evaluations of CTCs detected with the HD-SCA method, the approach of combining these cell categories for enumeration and analysis as well as probable EpCAM staining could be considered.

6.3.3 CTCC enumeration

Our cohort had a relatively low CTCC count (39.1% positive pateints in pre-resection) compared to cluster counts in previously published studies. CTCC positivity rates in CRC patients have been as high as 68.8% in a study with 32 patients of different stages [215]. Cima et al. showed in 2016 that $CD45^{neg}$ -cell clusters (isolated from CRC patients through use of a microfiltration device in combination with immunofluorescent staining) expressing CK (CK8 and CK20), but no EpCAM are actually tumor derived endothelial cell clusters [204]. As discussed in **6.3.1**, this could also be the case in our results. However, even the detected endothelial cell clusters have only been present in CRC patients and not in healthy volunteers just as in our cohort. Cima et al. also stated that cluster counts are higher in treatment naïve patients and usually drop after resection of the primary tumor. Most patients included in our study have received treatment before the resection, and although the treatment ended at least 6 weeks before resection, it makes it difficult to estimate treatment influence to CTCC counts in our cohort.

6.4 Survival analysis

6.4.1 Association of clinical characteristics with survival

Our results are conform with previously published data that right sided metastatic CRC is associated with shorter OS [98]. Usually this observation is limited to *RAS*-wildtype patients. While in our cohort the analysis of survival based on CRC location was not adjusted to *KRAS* mutation status, only one patient with right-sided CRC was *KRAS* mutated. The worst prognosis in our cohort was detected for patients with transverse CRC. Studies usually separate the colon only in two locations; they often consider everything from the cecum to the splenic flexure as right-sided CRC and everything after the splenic flexure is considered left-sided. Our results show that probably the differentiation of the transverse colon may be valuable prognostic information. Also, as CRC location has been a valuable tool for predicting response to radiotherapy and chemotherapy for treatment of hepatic metastases [224], the transverse location by itself may offer more specific predictive potential for therapy response. It is not surprising that no correlation between lymph node involvement and survival is detectable, as all patients already developed distant metastases and those outweigh lymph node

involvement regarding association to survival [225]. Association of the location of hepatic metastases and OS may only be caused by the fact, that in case of multiple hepatic metastases those are spread over the entire liver; therefore, the number of metastases and the location are correlated as well (**Figure 20**) and the correlation with OS of the location is rather just the correlation of the amount of metastases with OS, therefore these two are not independent variables. The size of our cohort has not allowed evaluation of differences between involvement of left and right hepatic lobe regarding survival. Overall, the correlations between primary tumor size and amount of hepatic metastases with OS is in agreement with the literature [226, 227].

6.4.2 Association of HD-CTCs with survival

CTC enumeration has been established as a predictive and prognostic marker for PFS and OS in metastatic CRC [201, 212, 228]. These findings were established using the CellSearch® platform, which is based on immunomagnetic enrichment of EpCAM positive cells.

Interestingly, our results do not conform to these findings as we have detected neither significant association of numbers of HD-CTCs/ml blood before nor after resection to survival. This might be caused by the CTC detection method. So far, there are limited reports regarding CTCs detected in metastatic CRC patients by non-enrichment techniques. The study of Marrinucci et al. only included 5 patients analyzed by the HD-SCA method and the cohort was too small to correlate CTC numbers to survival. A recent meta-analysis including 16 studies regarding CTCs in CRC and their correlation with OS published between 2007 and 2016, also showed significant prognostic value of CTCs detected in CRC [229]. However, they stated in their results that four studies did not analyze association with OS and the remaining 12 (7 of which used CellSearch®) had to be adjusted to eliminate heterogeneity for association with OS by excluding non-CellSearch® methods. Another study from 2015 also pointed out that there was no difference of OS and PFS between groups of CTC positive vs. CTC negative patients in a cohort of 151 mCRC patients undergoing metastasectomy [230], even though they applied the CellSearch® system as well.

Another important and often ignored fact is, that circulating endothelial cells (CECs) are often increased in cancer patients [231], and it has been shown that human vascular endothelial cells, especially in malignant tumors, are expressing keratins similar to epithelia [232]. Therefore we cannot exclude the possibility of detecting a mixed population of CECs and CTCs with the HD-SCA method. This CTC mixture could be similar to cells detected in the previously mentioned CellSearch® study in lung cancer where this detected mixed population of $EpCAM^{pos}$ and $EpCAM^{neg}$ cells was also not correlated to survival [222].

To distinguish between CECs and HD-CTCs, the HD-SCA workflow has recently been adjusted and the platelet endothelial cell adhesion molecule marker CD31 has been added to the workflow. This will allow future analysis of both populations seperately, which may especially be interesting for CRC research as HD-CTCs detected in these cohorts showed the lowest signal SDOM for CK-pan marker compared to prostate and breast HD-CTCs.

According the possibility of detecting endothelial cells as well as "real" CTCs, our cohort could consist of a mixture of cells containing also cells similar to $EpCAM^{neg}$ Overall the missing correlation of our detected HD-CTC counts with survival might represent potential limitation of the HD-SCA method, or reflect detection of a broader, but not as prognostic CTC population. However, as our cohort was relatively small, further research will be needed.

6.4.3 Association of CTC subcategories with survival

As the only CTC subcategory with association to OS and PFS, CTC-Small cells may represent the cell population usually detected by EpCAM-based CTC enrichment techniques. When comparing the morphological characteristics of published data of circulating endothelial cells [233, 234], they mostly resemble the detected HD-CTC category (very large nucleus, large heterogeneity in size and shape, with cytoplasmic appendix-like extensions). The CTC-Small category possessed the highest roundness in our cohort (**Figure 7**, page 46) and this morphology, including a size just slightly bigger than a WBC is often displayed in papers as CTC properties associated to cancer patient survival [213]. This would be conforming to our data of CTC-Small association with OS and PFS. In the study of Ligthart et al. it was discovered that higher counts of CTCs and CTCs with a roundness close to one are more dangerous for the patient than elongated cells, also that small CTCs in breast cancer are more dangerous than large CTCs [216]. This confirms our findings that the CTC-Small subcategory might be the CTC population with the highest importance for disease development.

Regarding the CTC-cfDNA producing cells, it was not expected to find correlations with survival as these cells are probably undergoing apoptosis, but they might contribute to circulating tumor DNA (ctDNA) in the blood which has shown promising results as a biomarker for patient monitoring or therapeutic resistance [47].

As the CTC-LowCK cells are defined as CK^{neg} and $CD45^{neg}$ but with enlarged nuclei, they might as well be similar to the $EpCAM^{neg}$ cells detected in the CellSearch® study in lung cancer, which could explain their missing association to patient survival. On the other hand a study by Pecot et al. showed that only CK^{neg} CTCs detected with a microfluidic platform were associated to shorter PFS in ovarian cancer patients, but only if they were also aneuploid [235]. The major issue with this cell category is

that there is not enough information about what particular cell type is forming this group and it is highly possible that it consists of cells of various origins. To answer this question, experiments with multiplex protein analysis (as discussed in 6.3.2) will be used to further characterize the CTC-LowCK phenotype.

6.4.4 Association of CTCCs with survival

Based on our results, the size of CTCCs detected in the pre-resection draw is associated to OS. It seems that if in a patient's blood a CTCC containing more than 8 cells is detected, OS survival will be shorter compared to patients with smaller CTCCs. Unfortunately, only three patients possessed clusters larger than 8 cells, therefore more data should be acquired before reliable conclusions can be drawn.

In the follow-up draw the presence of at least one CTCC is a promising marker for shorter OS. In CRC, CTCCs have been detected and described and once also associated to reduced OS [215, 236, 237].

Other publications have observed CTCCs in breast, prostate or lung cancer and identified CTCCs as promising markers of survival. In a publication from Zurita et al. in metastatic castration-resistant prostate cancer (mCRPC), it was reported that higher numbers of CTCCs in bone marrow samples and within those clusters their size was significantly correlated to PFS and OS [238]. In non-small cell lung cancer (NSCLC), Carlsson et al. have shown as well that CTCCs exceed the detected CTCs in utility for patient monitoring and diagnosis of stage I NSCLC [239]. This might be linked to the possibility that CTCCs might act as metastatic drivers. Aceto et al. have shown CTCCs to be precursors of metastases in breast cancer and their presence in CRC patients was associated with shorter PFS [240].

A possible explanation for this correlation could be first of all the size itself. The higher metastatic potential and chance of survival of CTCCs may be caused by their close association to other cell types as fibroblasts, platelets and endothelial cells [161]. Therefore a large CTCC may just bring their own "soil" and enhance the potential to extravasate and then proliferate in distant tissue [241]. After a CTCC has entered the vasculature, either by active or passive mechanisms, it's risk for apoptosis is lower than for CTCs and they are observed to clog blood vessels which may cause venous thromboembolism, a common cause of cancer related death, which could explain their association to OS [240, 242].

6.5 Association of enumeration data with clinical characteristics

6.5.1 Association of HD-CTCs with clinical characteristics

In our data the transverse colon CRC has been associated with shedding the most HD-CTCs/ml in the pre-resection draw. This could be explained through the special anatomical character of the transverse colon; unlike to the descending colon and the ascending colon, the transverse colon is mobile as it is encased by the peritoneum and blood is supplied from two different arteries (superior and inferior mesenteric artery). This increased exposure to movement and presence of multiple blood supplies may cause tumors in this area to shed a larger amount of cells, which is supported by many reports stating higher numbers of CTCs in right-sided CRC, which usually group the cecum, ascending and transverse part of the colon [243].

HD-CTC counts have also been significantly higher in patients with *KRAS* mutated tumors compared to *KRAS* wildtype tumors. As *KRAS* is a GTPase that transmits signals to the nucleus, acting as a switch for signaling networks associated to cell differentiation, survival, migration and growth, it plays a large role in CRC development and is a regulator of mesenchymal features in cancer [243, 244]. As mesenchymal features and the process of EMT have been proposed as one of the major contributors to tumor cell intravasation into the vasculature [245], higher HD-CTC counts in *KRAS* mutated tumors could be the consequence of this switch to a mobile, mesenchymal phenotype. These mesenchymal-like cells may disrupt vessels of the vasculature and cause shedding of endothelial cells into the circulation. And as discussed before, evidence suspects that HD-CTCs may represent detected endothelial cells in the bloodstream. Another reason for less stabile capillaries in *KRAS* mutated CRC may be faster tumor growth caused by increased tumor aggressiveness and shorter OS in early CRC stages that has been associated with *KRAS* mutated CRC [246, 247].

HD-CTCs have been the only category of cells that significantly decreased in numbers after resection of the primary tumor. Additionally, no association was detected between HD-CTC counts and number or size of hepatic metastases. This data may point out that the primary tumor is the main source of HD-CTCs in CRC stage IV patients, despite the anatomical challenge of cells having to pass through the portal vein and the liver. Hepatic metastases on the other hand do not bare this cell filtration problem, but cell numbers released from metastases seem to be lower. This could be cause by the small size of hepatic metastases or the changed phenotype of the re-seeded cells that have been proposed to have undergone mesenchymal to epithelial transition [161]. To proof that the primary tumor is the main source of CTC shedding, a larger control group would be needed that had underwent surgery of the primary tumor with only hepatic metastases present and on the other hand patients that underwent resection of hepatic metastases with primary CRC present at time of blood draws. In our study this cohort was heterogeneous and we were only able to measure changes

in COI numbers depending on the surgery type, not taking into consideration if a possible source of COIs is still present.

6.5.2 Association of CTC subcategories with clinical characteristics

Much like HD-CTC counts, the amounts of CTC-Small cells in the pre-resection draws were significantly higher in patients with *KRAS* mutated tumors. This evidence might show that these two cell categories could be closer related in phenotype than the two are related to the CTC-LowCK or CTC-cfDNA producing cells. On the other hand, as discussed before, the *KRAS* mutated tumors may have more disrupted capillary walls caused by cells of a more mobile and mesenchymal phenotype, therefore releasing more endothelial cells. Also, the possession of more mesenchymal-like cells leads to more ‚real' CTCs actively intravasating into the vasculature [245].

The category of CTC-cfDNA producing cells has shown association to the size of hepatic metastases. The larger the metastases, the more cells are found that have the morphology of a CTC undergoing apoptosis. Allen et al. have shown before that high amounts of apoptotic cells amongst detected CTCs are associated to the presence of hepatic metastases, whereas CTCs were not [248]. Now our data suggests that the metastatic load also influences the amount of apoptotic CTCs in the blood. These cells might represent dying liver cells. The higher metastatic load may cause pressure on the liver parenchym and cause liver cells to undergo apoptosis.

On the other hand, a study from 2002 of Backus et al. analyzed the protein markers of apoptosis and showed that these were more abundant in the primary CRC tumor than in hepatic metastases [249]. Although there is no direct explanation for our observations, the apoptotic cells could also be a late consequence of neoadjuvant treatment. After resection, >5 CTC-cfDNA producing cells were associated to higher lymph node involvement, therefore more apoptotic cells are observed in patients with further developed disease.

Cells of the CTC-LowCK category were, like HD-CTCs, also more prevalent in transverse CRC. This extensive shedding may be caused by the same reasons as discussed in 6.5.1, related to the exposed anatomical position of the transverse colon.

6.5.3 Association of CTCCs with clinical characteristics

For CTCCs, this study showed no association with CRC characteristics, except that after resection, CTCC counts decreased the least in right-sided CRC. As right-sided CRC is known to be more aggressive with high prevalence of MSI, *BRAF* mutations and CIMP, clusters could be another sign of

CRC aggressiveness. It has been discussed how clusters of tumor cells or tumor associated cells are entering the blood stream. Besides pieces of the tumor breaking of in a passive manner, they are also actively growing inside vessels and detaching from the tumor. This process is also called “tumor budding” and has been observed in CRC. This phenomenon has been described as tumor cells or cell clusters with stem cell properties (ability to re-differentiate and proliferate) at the invasive front of the tumor and has been correlated to vascular and lymphatic invasion as well as distant metastases [147]. The amount of cells in a CTCC was also significantly higher in M1 patients compared to M0 and the amount of detected CTCCs has been significantly higher in *KRAS* mutated patients. These findings support the theory that clusters are related to highly chromosomal instable CRC as the *KRAS* mutation is one of the key events in the development of CIN in CRC [250]. It also has to be mentioned that all patients with M1 status have therefore been diagnosed with synchronous disease which implies that the disease load developed over a longer time without detection and the tumor might have had more time to gain higher CIN. One surprising observation in this study is the lack of association between HD-CTCs or CTC-Small cells with number, status or size of hepatic metastases. The fact that HD-CTCs were associated to the primary CRC and decreased with its resection, leads to the conclusion that they are mainly shedded by the primary CRC. CTCCs were shown to be strongly associated with hepatic metastases, but data is not sufficient enough to conclude if they are causing hepatic metastases or rather originate from them.

If CTCCs and especially the size of CTCCs are the result of hepatic metastases or the cause has to be investigated further. One promising tool will be the use of multiplex protein detection by using the HYPERION™ technique [223], as discussed in 6.3.2.

Our cohort and the detected numbers for CTCCs were too small to analyze changes in CTCC counts depending on the type of surgery.

6.6 CNV profiles

Single CTCs from various cancers have recently been analyzed for CNV. Clonal profiles (common alterations within a set of single cells) within detected CTCs have been reported for prostate cancer [188], breast cancer [251], melanoma [252] and lung cancer [253]. Often clonal development was able to uncover temporal disease development and acquisition of amplifications.

6.6.1 CNV profiles of HD-CTCs

In our data, clonality in HD-CTCs was neither detected within individual patients, nor amongst cells of all analyzed 11 patients while searching for convergent genomic changes. One reason may be the fact, that the captured cells have passed through the liver and are collected from peripheral blood as discussed in 6.3.1. Therefore cells from the tumor that had acquired major alterations may have already seeded in the liver.

On the other hand these findings are supporting the aforementioned theory that the detected group of HD-CTCs are representing tumor derived $EpCAM^{neg}/CD45^{neg}$ CECs. This cell type has been analyzed by Cima et al. and did not mirror mutations and chromosomal abnormalities of the primary tumor [204]. Their study also proved by principal component analysis that CECs were associated to the tumor tissue and were prevalent in CRC patients. Using the *FOLH1* gene, which is specifically expressed in tumor vasculature, but not in healthy blood vessels, they were able to show that these CECs might be directly released from tumor vasculature.

In a review from A. Dudley it was stated that tumor blood vessels possess poor stability, cells are only loosely attached and the morphology of the tumor endothelial cells is described as of irregular size and shape with long cytoplasmic projections, which is similar to our findings in the HD-CTC category and could explain CEC cells detected in the blood stream [254]. Endothelial cells derive partly from already existing vessels or *de novo* from mesenchymal stem cells and already VEGFA expression is sufficient to induce blood vessel formation [254].

Taking these findings into consideration there might be the possibility that the detected HD-CTCs actually represent (at least partially) these CECs. Further analyses, using CD31 as additional fluorescence marker or multiplex protein detection are prepared to answer this question.

On the other hand, studies have been published using the HD-SCA method showing successful detection of tumor related clonal profiles in detected HD-CTCs. However, these findings were only shown in other cancers like prostate and melanoma [188, 252] and in CTCs detected in bone marrow of a prostate cancer patient [206]. In these cancers though, additional cancer specific markers have been used for identification of CTCs, like AR in prostate cancer and CSPG4 expression in melanoma.

Another contradictory publication exists showing genetic abnormalities in tumor derived endothelial cells in renal cell carcinoma, however, these cells were isolated from tissue sections and were not in the circulation [255].

For future experiments it would be interesting to focus on CNV profiling of the CTC-Small category and also to add a tumor specific marker to ensure the origin of HD-CTCs detected in CRC patients. On

the other hand, CEC can provide us with information about the tumor vasculature and its changes during treatment or disease evolution.

6.6.2 CNV profiles in tissue samples compared to those of HD-CTCs

Common alteration have been observed within the CRC tissue cells of one patient as well as within cells isolated from multiple patients. Amplifications of similar regions (e.g. the *MYC* containing region) have been observed in 43.7% of the analyzed cells and numerical changes in a whole set of chromosomes even in 73.8% of cells from CRC tissue.

Li et al. have also discovered common clonal profiles in single cells from CRC tissues using reference component analysis [256]. As CRC tumors share common pathways of molecular development, common alterations within the genome could be expected. But as tumor tissue is composed of multiple associated cell types as macrophages [257], stromal cells [258] and endothelial cells [254], some cells analyzed without showing clonal or altered CNV profiles may belong to one of these tumor associated cell categories.

Based on our data there is a high similarity between CNV profiles of CRC tissue cells and cells isolated from corresponding hepatic metastases. In addition, a clear evolution from the primary tumor to metastasis is visible when special regions are analyzed. For the *MYC* containing region on chromosome 8 amplifications were gained in cells from hepatic metastases (43.7% in CRC compared to 83.8% of cells in hepatic metastasis tissue). A similar gain in hepatic metastases was observed for amplifications of the region containing *MET* (37.4% to 67.6%) and deletions containing *FGFR1* (34.9% to 86.5%). This observation for elevated *MET* amplification in hepatic metastases compared to mCRC tissue was also observed by Zeng et al. [259], and later Raghav et al. reported that this amplification gain might be a response to anti-EGFR therapy [260]. Bardelli et al. showed that the amplification gain of *MET* then finally leads to resistance to anti-EGFR therapy [261].

For *FGFR1* the most common alteration reported in 42% of cancers is *FGFR1* amplification [262], and has been associated with worse prognosis in lung cancer. However, these observations did not include studies of CRC. And additionally it has been observed that *FGFR1* amplifications are mostly detected in early stages of cancer, suggesting a key role for initiation of tumor development [263]. Therefore our observation of higher frequency of *FGFR1* deletions may correspond to disease evolution from localized disease to distant metastasis and may be conform to former observations. These changes in hepatic tissue may mirror the necessary chromosomal changes for successful seeding in distant organs.

For the *APC* gene region a decrease of deletions was observed when the tumor developed liver metastases. *APC* is a known tumor suppressor gene and its protein is a key negative regulator of the Wnt signaling pathway, which controls cell proliferation [264]. *APC* deletions have been identified as a common cause of familial adenomatous polyposis (FAP), which only accounts for about 1-2% of CRC cases [265]. More common are mutations of *APC* , which is observed in more than 80% of sporadic CRC and functions as a known initiator of CRC development [264]. As *APC* is one of the initiators of CRC, it could be concluded that loss of *APC* function is in later stages not required, especially not crucial for metastasation. This would explain our observed decreased in *APC* deletions in hepatic lesions. On the other hand, the group of patients tested for CNV profiles of hepatic metastases was limited to 4 patients and differed from the before tested group tested for alterations in CRC tissue. Liver lesion cells were not tested for two patients with major *APC* deletions (CRC206 and CRC226); this could have biased the numbers for this rare deletion.

CDX2 is an intestine-specific transcription factor and its expression is used as a sensitive marker for intestinal carcinomas [266]. Studies of patients with resected CRC revealed, that those with stage II and III CRC and CDX2 positive tumors had significant longer OS [267]. Subtil et al. showed that *CDX2* gene amplifications in sporadic CRC were not causing higher CDX2 expression and were not associated to survival [268]. The here observed decrease of amplifications to a diploid state in the *CDX2* containing region in cells of hepatic metastases may be due to the organ-specific character of this marker, and seeding in a different tissue may be followed by reduction of *CDX2* amplification.

Overall, high heterogeneity of CNVs and existence of multiple clones among individual cells within a single tumor has been observed in various cancers before [188, 269]. This phenomenon could cause CT failure as one clone might be more sensitive than another [270]. This is why through the last years many studies have pointed out that single cell analysis might be beneficial for the patient compared to bulk analysis. As we had access to CTCs in the blood and tumor cells from tissue, we aimed to link clones from the tissue to CTC phenotype associated to the hepatic metastases, but could not find any clonality in the blood. For proper statistical comparison of clones in the primary tumor to those in hepatic metastases the sample size was too small, but it became one of the goals for a future project.

7 Conclusions

Based on our data it is most likely that the detected category of HD-CTCs in CRC consists of mostly tumor associated CECs. This was backed by the results of our CNV data as HD-CTCs showed no clonality and less than 2% of general alterations observed in the tissue cells isolated from CRC.

In contrast, the CTC subcategory of CTC-Small cells showed a more round and less heterogenic morphology and was associated to OS with a significant threshold of 8 cells/ml. Cell counts for both categories, HD-CTCs and CTC-Small, were elevated in *KRAS* mutated CRC.

Results for detected CTCCs were most interesting and novel, showing that size matters. The number of cells per CTCC was associated to OS and significantly elevated in M1 CRC patients. The number of CTCCs/ml was significantly elevated in the pre-resection draws of *KRAS* mutated CRCs. This makes CTCCs a promising biomarker for CRC patients and a probable driver of metastasation.

Taking all results into consideration, the detected category of HD-CTCs have to be analyzed for endothelial origin and in contrast has the category of CTC-Small cells be highly considered as the 'real' CTC category. For further enumeration studies we would apply the updated HD-SCA detection with detection of CD31 signal inclusion. As the analysis of association with survival was successful in the category of CTC-Small cells, these cells should be in the focus of future studies.

Compared to other cancers like breast and prostate, the heterogeneity of detected COIs seems elevated in CRC, especially the number of cells similar to endothelial cells. This phenomenon may be caused by the unique location and blood supply situation of the colon and has to be taken into consideration for future studies. Discussions with surgeons about possible blood draws from the portal vein illustrated that this is barely feasible as it causes additional hazard for the patient.

The use of CK markers instead of EpCAM might be an obstacle due to parallel expression in endothelial cells. On the other hand it can allow the detection of an important tumor associated cell subpopulation if an additional differentiation marker for endothelial cells (e.g. CD31) is applied.

Regarding the detected CTCC, we would focus specifically on these in future projects and the next step could be their multiplex profiling to decipher protein expression and the cell phenotypes of individual cells assembling a CTCC.

As there was no clonality detected within HD-CTCs in the CRC patients of this cohort, this is just another confirmation that this subpopulation was rather composed of tumor derived endothelial cells than CTCs. In the future we will focus on CNV profiling and multiplex protein detection of CTC-Small cells and CTCCs.

Findings of evolving clones from cells of the primary CRC compared to hepatic metastatic tissue shows that this method is a promising tool to monitor disease evolution and may give insight in the temporal changes in genomic alterations necessary for CRC exacerbation.

8 Literature

1. Malvezzi M, Carioli G, Bertuccio P, et al (2017) European cancer mortality predictions for the year 2017, with focus on lung cancer. Ann Oncol 28:1117–1123 . doi: 10.1093/annonc/mdx033

2. Ait Ouakrim D, Pizot C, Boniol M, et al (2015) Trends in colorectal cancer mortality in Europe: retrospective analysis of the WHO mortality database. BMJ h4970 . doi: 10.1136/bmj.h4970

3. Yamagishi H, Kuroda H, Imai Y, Hiraishi H (2016) Molecular pathogenesis of sporadic colorectal cancers. Chin J Cancer 35: . doi: 10.1186/s40880-015-0066-y

4. Issa J-PJ, Shen L, Toyota M (2005) CIMP, at Last. Gastroenterology 129:1121–1124 . doi: 10.1053/j.gastro.2005.07.040

5. Armaghany T, Wilson JD, Chu Q, Mills G (2012) Genetic alterations in colorectal cancer. Gastrointest Cancer Res GCR 5:19–27

6. Grady WM, Markowitz SD (2015) The Molecular Pathogenesis of Colorectal Cancer and Its Potential Application to Colorectal Cancer Screening. Dig Dis Sci 60:762–772 . doi: 10.1007/s10620-014-3444-4

7. Romiti A (2014) Circulating Tumor Cells Count Predicts Survival in Colorectal Cancer Patients. J Gastrointestin Liver Dis 23: . doi: 10.15403/jgld.2014.1121.233.arom1

8. Ferlay J, Steliarova-Foucher E, Lortet-Tieulent J, et al (2013) Cancer incidence and mortality patterns in Europe: Estimates for 40 countries in 2012. Eur J Cancer 49:1374–1403 . doi: 10.1016/j.ejca.2012.12.027

9. Siegel RL, Miller KD, Jemal A (2017) Cancer statistics, 2017. CA Cancer J Clin 67:7–30 . doi: 10.3322/caac.21387

10. What Are the Survival Rates for Colorectal Cancer, by Stage? https://www.cancer.org/cancer/colon-rectal-cancer/detection-diagnosis-staging/survival-rates.html. Accessed 2 Feb 2018

11. Can Colorectal Polyps and Cancer Be Found Early? https://www.cancer.org/cancer/colon-rectal-cancer/detection-diagnosis-staging/detection.html. Accessed 2 Feb 2018

12. Brenner H, Hoffmeister M, Brenner G, et al (2009) Expected reduction of colorectal cancer incidence within 8 years after introduction of the German screening colonoscopy programme: Estimates based on 1,875,708 screening colonoscopies. Eur J Cancer 45:2027–2033 . doi: 10.1016/j.ejca.2009.02.017

13. Brenner H, Stock C, Hoffmeister M (2014) Effect of screening sigmoidoscopy and screening colonoscopy on colorectal cancer incidence and mortality: systematic review and meta-analysis of randomised controlled trials and observational studies. BMJ 348:g2467–g2467 . doi: 10.1136/bmj.g2467

14. World Cancer Research Fund International (2017) Continuous Update Project Report: Diet, nutrition, physical activity and colorectal cancer

15. Pan P, Yu J, Wang L-S (2018) Colon Cancer. Surg Oncol Clin N Am 27:243–267 . doi: 10.1016/j.soc.2017.11.002

16. Leitzmann M, Powers H, Anderson AS, et al (2015) European Code against Cancer 4th Edition: Physical activity and cancer. Cancer Epidemiol 39:S46–S55 . doi: 10.1016/j.canep.2015.03.009

17. Norat T, Scoccianti C, Boutron-Ruault M-C, et al (2015) European Code against Cancer 4th Edition: Diet and cancer. Cancer Epidemiol 39:S56–S66 . doi: 10.1016/j.canep.2014.12.016

18. Kang H, Shibata D (2013) Direct Measurements of Human Colon Crypt Stem Cell Niche Genetic Fidelity: The Role of Chance in Non-Darwinian Mutation Selection. Front Oncol 3: . doi: 10.3389/fonc.2013.00264

19. Huels DJ, Sansom OJ (2015) Stem vs non-stem cell origin of colorectal cancer. Br J Cancer 113:1–5 . doi: 10.1038/bjc.2015.214

20. Lopez-Garcia C, Klein AM, Simons BD, Winton DJ (2010) Intestinal Stem Cell Replacement Follows a Pattern of Neutral Drift. Science 330:822–825 . doi: 10.1126/science.1196236

21. Snippert HJ, Schepers AG, van Es JH, et al (2014) Biased competition between Lgr5 intestinal stem cells driven by oncogenic mutation induces clonal expansion. EMBO Rep 15:62–69 . doi: 10.1002/embr.201337799

22. Cho KR, Vogelstein B (1992) Genetic alterations in the adenoma--carcinoma sequence. Cancer 70:1727–1731

23. Weinberg RA (2014) The biology of cancer, Second edition. Garland Science, Taylor & Francis Group, New York

24. Ionov Y, Peinado MA, Malkhosyan S, et al (1993) Ubiquitous somatic mutations in simple repeated sequences reveal a new mechanism for colonic carcinogenesis. Nature 363:558–561 . doi: 10.1038/363558a0

25. Grady WM (2004) Genomic instability and colon cancer. Cancer Metastasis Rev 23:11–27

26. Boland CR, Thibodeau SN, Hamilton SR, et al (1998) A National Cancer Institute Workshop on Microsatellite Instability for cancer detection and familial predisposition: development of international criteria for the determination of microsatellite instability in colorectal cancer. Cancer Res 58:5248–5257

27. Issa J-P (2014) Aging and epigenetic drift: a vicious cycle. J Clin Invest 124:24–29 . doi: 10.1172/JCI69735

28. Tahara T, Yamamoto E, Madireddi P, et al (2014) Colorectal Carcinomas With CpG Island Methylator Phenotype 1 Frequently Contain Mutations in Chromatin Regulators. Gastroenterology 146:530-538.e5 . doi: 10.1053/j.gastro.2013.10.060

29. Bae JM, Kim JH, Kwak Y, et al (2017) Distinct clinical outcomes of two CIMP-positive colorectal cancer subtypes based on a revised CIMP classification system. Br J Cancer 116:1012–1020 . doi: 10.1038/bjc.2017.52

30. Geiersbach KB, Samowitz WS (2011) Microsatellite Instability and Colorectal Cancer. Arch Pathol Lab Med 135:1269–1277 . doi: 10.5858/arpa.2011-0035-RA

31. Grady WM, Pritchard CC (2014) Molecular Alterations and Biomarkers in Colorectal Cancer. Toxicol Pathol 42:124–139 . doi: 10.1177/0192623313505155

32. Ma H, Brosens LAA, Offerhaus GJA, et al (2018) Pathology and genetics of hereditary colorectal cancer. Pathology (Phila) 50:49–59 . doi: 10.1016/j.pathol.2017.09.004

33. Parsons MT, Buchanan DD, Thompson B, et al (2012) Correlation of tumour BRAF mutations and *MLH1* methylation with germline mismatch repair (MMR) gene mutation status: a literature review assessing utility of tumour features for MMR variant classification. J Med Genet 49:151–157 . doi: 10.1136/jmedgenet-2011-100714

34. Moreira L, Balaguer F, Lindor N, et al (2012) Identification of Lynch Syndrome Among Patients With Colorectal Cancer. JAMA 308:1555 . doi: 10.1001/jama.2012.13088

35. Engel C, Rahner N, Schulmann K, et al (2010) Efficacy of Annual Colonoscopic Surveillance in Individuals With Hereditary Nonpolyposis Colorectal Cancer. Clin Gastroenterol Hepatol 8:174–182 . doi: 10.1016/j.cgh.2009.10.003

36. Kinzler KW, Vogelstein B (1996) Lessons from hereditary colorectal cancer. Cell 87:159–170

37. Zavoral M, Suchanek S, Zavada F, et al (2009) Colorectal cancer screening in Europe. World J Gastroenterol 15:5907–5915

38. Bevan R, Lee TJ, Nickerson C, et al (2014) Non-neoplastic findings at colonoscopy after positive faecal occult blood testing: Data from the English Bowel Cancer Screening Programme. J Med Screen 21:89–94 . doi: 10.1177/0969141314528889

39. (2000) Recommendations on cancer screening in the European union. Advisory Committee on Cancer Prevention. Eur J Cancer Oxf Engl 1990 36:1473–1478

40. Lieberman DA (2009) Screening for Colorectal Cancer. N Engl J Med 361:1179–1187 . doi: 10.1056/NEJMcp0902176

41. Byrd RL, Whitney Boggs H, Slagle GW, Cole PA (1989) Reliability of colonoscopy: Dis Colon Rectum 32:1023–1025 . doi: 10.1007/BF02553873

42. Rutter CM, Johnson E, Miglioretti DL, et al (2012) Adverse events after screening and follow-up colonoscopy. Cancer Causes Control 23:289–296 . doi: 10.1007/s10552-011-9878-5

43. Regge D, Iussich G, Senore C, et al (2014) Population screening for colorectal cancer by flexible sigmoidoscopy or CT colonography: study protocol for a multicenter randomized trial. Trials 15:97 . doi: 10.1186/1745-6215-15-97

44. Spada C, Stoker J, Alarcon O, et al (2015) Clinical indications for computed tomographic colonography: European Society of Gastrointestinal Endoscopy (ESGE) and European Society of Gastrointestinal and Abdominal Radiology (ESGAR) Guideline. Eur Radiol 25:331–345 . doi: 10.1007/s00330-014-3435-z

45. Dickinson BT, Kisiel J, Ahlquist DA, Grady WM (2015) Molecular markers for colorectal cancer screening. Gut 64:1485–1494 . doi: 10.1136/gutjnl-2014-308075

46. Imperiale TF, Ransohoff DF, Itzkowitz SH, et al (2014) Multitarget Stool DNA Testing for Colorectal-Cancer Screening. N Engl J Med 370:1287–1297 . doi: 10.1056/NEJMoa1311194

47. Moati E, Taly V, Didelot A, et al (2018) Role of circulating tumor DNA in the management of patients with colorectal cancer. Clin Res Hepatol Gastroenterol. doi: 10.1016/j.clinre.2018.03.002

48. Yang Y, Junjie P, Sanjun C, Ma Y (2017) Long non-coding RNAs in Colorectal Cancer: Progression and Future Directions. J Cancer 8:3212–3225 . doi: 10.7150/jca.19794

49. Eslamizadeh S, Heidari M, Agah S, et al (2018) The Role of MicroRNA Signature as Diagnostic Biomarkers in Different Clinical Stages of Colorectal Cancer. Cell J Yakhteh. doi: 10.22074/cellj.2018.5366

50. Wikberg ML, Myte R, Palmqvist R, et al (2018) Plasma miRNA can detect colorectal cancer, but how early? Cancer Med. doi: 10.1002/cam4.1398

51. Hench IB, Hench J, Tolnay M (2018) Liquid Biopsy in Clinical Management of Breast, Lung, and Colorectal Cancer. Front Med 5: . doi: 10.3389/fmed.2018.00009

52. Stintzing S, Tejpar S, Gibbs P, et al (2017) Understanding the role of primary tumour localisation in colorectal cancer treatment and outcomes. Eur J Cancer Oxf Engl 1990 84:69–80 . doi: 10.1016/j.ejca.2017.07.016

53. Weiss JM, Pfau PR, O'Connor ES, et al (2011) Mortality by Stage for Right- Versus Left-Sided Colon Cancer: Analysis of Surveillance, Epidemiology, and End Results–Medicare Data. J Clin Oncol 29:4401–4409 . doi: 10.1200/JCO.2011.36.4414

54. Loupakis F, Yang D, Yau L, et al (2015) Primary Tumor Location as a Prognostic Factor in Metastatic Colorectal Cancer. JNCI J Natl Cancer Inst 107: . doi: 10.1093/jnci/dju427

55. Grimminger PP, Shi M, Barrett C, et al (2012) TS and ERCC-1 mRNA expressions and clinical outcome in patients with metastatic colon cancer in CONFIRM-1 and -2 clinical trials. Pharmacogenomics J 12:404–411 . doi: 10.1038/tpj.2011.29

56. Thomas DS, Fourkala E-O, Apostolidou S, et al (2015) Evaluation of serum CEA, CYFRA21-1 and CA125 for the early detection of colorectal cancer using longitudinal preclinical samples. Br J Cancer 113:268–274 . doi: 10.1038/bjc.2015.202

57. Mondal S, Sinha S, Mukhopadhyay M, et al (2014) Diagnostic and prognostic significance of different mucin expression, preoperative CEA, and CA-125 in colorectal carcinoma: A clinicopathological study. J Nat Sci Biol Med 5:404 . doi: 10.4103/0976-9668.136207

58. Shaib W, Mahajan R, El-Rayes B (2013) Markers of resistance to anti-EGFR therapy in colorectal cancer. J Gastrointest Oncol 4:308–318 . doi: 10.3978/j.issn.2078-6891.2013.029

59. Yuza K, Nagahashi M, Watanabe S, et al (2017) Hypermutation and microsatellite instability in gastrointestinal cancers. Oncotarget 8: . doi: 10.18632/oncotarget.22783

60. Müller MF, Ibrahim AEK, Arends MJ (2016) Molecular pathological classification of colorectal cancer. Virchows Arch 469:125–134 . doi: 10.1007/s00428-016-1956-3

61. Zarkavelis G (2017) Current and future biomarkers in colorectal cancer. Ann Gastroenterol. doi: 10.20524/aog.2017.0191

62. Guinney J, Dienstmann R, Wang X, et al (2015) The consensus molecular subtypes of colorectal cancer. Nat Med 21:1350–1356 . doi: 10.1038/nm.3967

63. Kufe DW, Holland JF, Frei E, American Cancer Society (2003) Cancer medicine 6, 6th ed. BC Decker, Hamilton, Ont. ; Lewiston, NY

64. Colon Cancer Treatment. In: Natl. Cancer Inst. https://www.cancer.gov/types/colorectal/hp/colon-treatment-pdq#section/_105. Accessed 19 Apr 2018

65. Patrlj L, Kopljar M, Kliček R, et al (2014) The surgical treatment of patients with colorectal cancer and liver metastases in the setting of the "liver first" approach. Hepatobiliary Surg Nutr 3:324–329 . doi: 10.3978/j.issn.2304-3881.2014.09.12

66. Kye B-H, Cho H-M (2014) Overview of Radiation Therapy for Treating Rectal Cancer. Ann Coloproctology 30:165 . doi: 10.3393/ac.2014.30.4.165

67. Radiation Therapy for Colorectal Cancer. https://www.cancer.org/cancer/colon-rectal-cancer/treating/radiation-therapy.html. Accessed 23 May 2018

68. Chemotherapy for Colorectal Cancer. https://www.cancer.org/cancer/colon-rectal-cancer/treating/chemotherapy.html. Accessed 19 Apr 2018

69. NCCN Guidelines for Patients® | Colon Cancer. https://www.nccn.org/patients/guidelines/colon/index.html. Accessed 23 May 2018

70. Chu E (2007) Clinical Colorectal Cancer: "Ode to 5-Fluorouracil." Clin Colorectal Cancer 6:609 . doi: 10.3816/CCC.2007.n.029

71. Parker JB, Stivers JT (2011) Dynamics of Uracil and 5-Fluorouracil in DNA. Biochemistry (Mosc) 50:612–617 . doi: 10.1021/bi101536k

72. Gustavsson B, Carlsson G, Machover D, et al (2015) A Review of the Evolution of Systemic Chemotherapy in the Management of Colorectal Cancer. Clin Colorectal Cancer 14:1–10 . doi: 10.1016/j.clcc.2014.11.002

73. Waxman S, Bruckner H (1982) The enhancement of 5-fluorouracil anti-metabolic activity by leucovorin, menadione and alpha-tocopherol. Eur J Cancer Clin Oncol 18:685–692

74. Pan X, Wang C, Wang F, et al (2011) Development of 5-Fluorouracil Derivatives as Anticancer Agents. Curr Med Chem 18:4538–4556 . doi: 10.2174/092986711797287584

75. Fujita K (2015) Irinotecan, a key chemotherapeutic drug for metastatic colorectal cancer. World J Gastroenterol 21:12234 . doi: 10.3748/wjg.v21.i43.12234

76. McWhinney SR, Goldberg RM, McLeod HL (2009) Platinum neurotoxicity pharmacogenetics. Mol Cancer Ther 8:10–16 . doi: 10.1158/1535-7163.MCT-08-0840

77. Zhang S, Lovejoy KS, Shima JE, et al (2006) Organic Cation Transporters Are Determinants of Oxaliplatin Cytotoxicity. Cancer Res 66:8847–8857 . doi: 10.1158/0008-5472.CAN-06-0769

78. Johnstone TC, Park GY, Lippard SJ (2014) Understanding and improving platinum anticancer drugs--phenanthriplatin. Anticancer Res 34:471–476

79. Battaglin F, Puccini A, Intini R, et al (2018) The role of tumor angiogenesis as a therapeutic target in colorectal cancer. Expert Rev Anticancer Ther 18:251–266 . doi: 10.1080/14737140.2018.1428092

80. Linnekamp JF, Wang X, Medema JP, Vermeulen L (2015) Colorectal Cancer Heterogeneity and Targeted Therapy: A Case for Molecular Disease Subtypes. Cancer Res 75:245–249 . doi: 10.1158/0008-5472.CAN-14-2240

81. Herbst RS (2004) Review of epidermal growth factor receptor biology. Int J Radiat Oncol 59:S21–S26 . doi: 10.1016/j.ijrobp.2003.11.041

82. Harris M (2004) Monoclonal antibodies as therapeutic agents for cancer. Lancet Oncol 5:292–302 . doi: 10.1016/S1470-2045(04)01467-6

83. Roock WD, Vriendt VD, Normanno N, et al (2011) KRAS, BRAF, PIK3CA, and PTEN mutations: implications for targeted therapies in metastatic colorectal cancer. Lancet Oncol 12:594–603 . doi: 10.1016/S1470-2045(10)70209-6

84. Tian S, Simon I, Moreno V, et al (2013) A combined oncogenic pathway signature of *BRAF* , *KRAS* and *PI3KCA* mutation improves colorectal cancer classification and cetuximab treatment prediction. Gut 62:540–549 . doi: 10.1136/gutjnl-2012-302423

85. De Roock W, Claes B, Bernasconi D, et al (2010) Effects of KRAS, BRAF, NRAS, and PIK3CA mutations on the efficacy of cetuximab plus chemotherapy in chemotherapy-refractory metastatic colorectal cancer: a retrospective consortium analysis. Lancet Oncol 11:753–762 . doi: 10.1016/S1470-2045(10)70130-3

86. Zhao B, Wang L, Qiu H, et al (2017) Mechanisms of resistance to anti-EGFR therapy in colorectal cancer. Oncotarget 8: . doi: 10.18632/oncotarget.14012

87. Le DT, Uram JN, Wang H, et al (2015) PD-1 Blockade in Tumors with Mismatch-Repair Deficiency. N Engl J Med 372:2509–2520 . doi: 10.1056/NEJMoa1500596

88. Research C for DE and Approved Drugs - FDA grants nivolumab accelerated approval for MSI-H or dMMR colorectal cancer. https://www.fda.gov/Drugs/InformationOnDrugs/ApprovedDrugs/ucm569366.htm. Accessed 20 Apr 2018

89. Commissioner O of the Press Announcements - FDA approves first cancer treatment for any solid tumor with a specific genetic feature. https://www.fda.gov/newsevents/newsroom/pressannouncements/ucm560167.htm. Accessed 23 May 2018

90. Seow H, Yip WK, Fifis T (2016) Advances in targeted and immunobased therapies for colorectal cancer in the genomic era. OncoTargets Ther 1899 . doi: 10.2147/OTT.S95101

91. Gang W, Wang J-J, Guan R, et al (2018) Strategy to targeting the immune resistance and novel therapy in colorectal cancer. Cancer Med. doi: 10.1002/cam4.1386

92. Baretti M, Azad NS (2018) The role of epigenetic therapies in colorectal cancer. Curr Probl Cancer. doi: 10.1016/j.currproblcancer.2018.03.001

93. Dhaliwal A, Vlachostergios PJ, Oikonomou KG, Moshenyat Y (2015) Fecal DNA testing for colorectal cancer screening: Molecular targets and perspectives. World J Gastrointest Oncol 7:178 . doi: 10.4251/wjgo.v7.i10.178

94. Bosch LJW, Carvalho B, Fijneman RJA, et al (2011) Molecular Tests for Colorectal Cancer Screening. Clin Colorectal Cancer 10:8–23 . doi: 10.3816/CCC.2011.n.002

95. Wang Q, Huang Z, Ni S, et al (2012) Plasma miR-601 and miR-760 Are Novel Biomarkers for the Early Detection of Colorectal Cancer. PLoS ONE 7:e44398 . doi: 10.1371/journal.pone.0044398

96. Giráldez MD, Lozano JJ, Ramírez G, et al (2013) Circulating MicroRNAs as Biomarkers of Colorectal Cancer: Results From a Genome-Wide Profiling and Validation Study. Clin Gastroenterol Hepatol 11:681-688.e3 . doi: 10.1016/j.cgh.2012.12.009

97. Sartore-Bianchi A, Trusolino L, Martino C, et al (2016) Dual-targeted therapy with trastuzumab and lapatinib in treatment-refractory, KRAS codon 12/13 wild-type, HER2-positive metastatic colorectal cancer (HERACLES): a proof-of-concept, multicentre, open-label, phase 2 trial. Lancet Oncol 17:738–746 . doi: 10.1016/S1470-2045(16)00150-9

98. Boeckx N, Koukakis R, Op de Beeck K, et al (2017) Primary tumor sidedness has an impact on prognosis and treatment outcome in metastatic colorectal cancer: results from two randomized first-line panitumumab studies. Ann Oncol 28:1862–1868 . doi: 10.1093/annonc/mdx119

99. Brulé SY, Jonker DJ, Karapetis CS, et al (2015) Location of colon cancer (right-sided versus left-sided) as a prognostic factor and a predictor of benefit from cetuximab in NCIC CO.17. Eur J Cancer 51:1405–1414 . doi: 10.1016/j.ejca.2015.03.015

100. Missiaglia E, Jacobs B, D'Ario G, et al (2014) Distal and proximal colon cancers differ in terms of molecular, pathological, and clinical features. Ann Oncol 25:1995–2001 . doi: 10.1093/annonc/mdu275

101. Popat S, Matakidou A, Houlston RS (2004) Thymidylate Synthase Expression and Prognosis in Colorectal Cancer: A Systematic Review and Meta-Analysis. J Clin Oncol 22:529–536 . doi: 10.1200/JCO.2004.05.064

102. Jensen NF, Smith DH, Nygård SB, et al (2012) Predictive biomarkers with potential of converting conventional chemotherapy to targeted therapy in patients with metastatic colorectal cancer. Scand J Gastroenterol 47:340–355 . doi: 10.3109/00365521.2012.640835

103. Braun MS, Richman SD, Quirke P, et al (2008) Predictive Biomarkers of Chemotherapy Efficacy in Colorectal Cancer: Results From the UK MRC FOCUS Trial. J Clin Oncol 26:2690–2698 . doi: 10.1200/JCO.2007.15.5580

104. Basbug M, Arikanoglu Z, Bulbuller N, et al (2011) Prognostic value of preoperative CEA and CA 19-9 levels in patients with colorectal cancer. Hepatogastroenterology 58:400–405

105. Richman SD, Seymour MT, Chambers P, et al (2009) *KRAS* and *BRAF* Mutations in Advanced Colorectal Cancer Are Associated With Poor Prognosis but Do Not Preclude Benefit From Oxaliplatin or Irinotecan: Results From the MRC FOCUS Trial. J Clin Oncol 27:5931–5937 . doi: 10.1200/JCO.2009.22.4295

106. Kim S-H, Kwon H-C, Oh SY, et al (2009) Prognostic Value of ERCC1, Thymidylate Synthase, and Glutathione S-Transferase π for 5-FU/Oxaliplatin Chemotherapy in Advanced Colorectal Cancer: Am J Clin Oncol 32:38–43 . doi: 10.1097/COC.0b013e31817be58e

107. Polyak K (2011) Heterogeneity in breast cancer. J Clin Invest 121:3786–3788 . doi: 10.1172/JCI60534

108. El Bairi K, Tariq K, Himri I, et al (2018) Decoding colorectal cancer epigenomics. Cancer Genet 220:49–76 . doi: 10.1016/j.cancergen.2017.11.001

109. Burrell RA, McGranahan N, Bartek J, Swanton C (2013) The causes and consequences of genetic heterogeneity in cancer evolution. Nature 501:338–345 . doi: 10.1038/nature12625

110. Babayan A, Hannemann J, Spötter J, et al (2013) Heterogeneity of estrogen receptor expression in circulating tumor cells from metastatic breast cancer patients. PloS One 8:e75038 . doi: 10.1371/journal.pone.0075038

111. Zhang C, Guan Y, Sun Y, et al (2016) Tumor heterogeneity and circulating tumor cells. Cancer Lett. doi: 10.1016/j.canlet.2016.02.024

112. de Bruin EC, McGranahan N, Mitter R, et al (2014) Spatial and temporal diversity in genomic instability processes defines lung cancer evolution. Science 346:251–256 . doi: 10.1126/science.1253462

113. Oh H-S, Chung H-J, Kim H-K, Choi J-S (2007) Differences in Overall Survival When Colorectal Cancer Patients are Stratified into New TNM Staging Strategy. Cancer Res Treat 39:61 . doi: 10.4143/crt.2007.39.2.61

114. Riihimäki M, Hemminki A, Sundquist J, Hemminki K (2016) Patterns of metastasis in colon and rectal cancer. Sci Rep 6: . doi: 10.1038/srep29765

115. Hardingham JE, Kotasek D, Farmer B, et al (1993) Immunobead-PCR: a technique for the detection of circulating tumor cells using immunomagnetic beads and the polymerase chain reaction. Cancer Res 53:3455–3458

116. Tsavellas G, Patel H, Allen-Mersh TG (2001) Detection and clinical significance of occult tumour cells in colorectal cancer. Br J Surg 88:1307–1320 . doi: 10.1046/j.0007-1323.2001.01863.x

117. Bork U, Rahbari NN, Schölch S, et al (2015) Circulating tumour cells and outcome in non-metastatic colorectal cancer: a prospective study. Br J Cancer 112:1306–1313 . doi: 10.1038/bjc.2015.88

118. Praharaj PP, Bhutia SK, Nagrath S, et al (2018) Circulating tumor cell-derived organoids: Current challenges and promises in medical research and precision medicine. Biochim Biophys Acta BBA - Rev Cancer 1869:117–127 . doi: 10.1016/j.bbcan.2017.12.005

119. Miller MC, Doyle GV, Terstappen LWMM (2010) Significance of Circulating Tumor Cells Detected by the CellSearch System in Patients with Metastatic Breast Colorectal and Prostate Cancer. J Oncol 2010:617421 . doi: 10.1155/2010/617421

120. Lu S-H, Tsai W-S, Chang Y-H, et al (2016) Identifying Cancer Origin Using Circulating Tumor Cells. Cancer Biol Ther 00–00 . doi: 10.1080/15384047.2016.1141839

121. Nadal R, Lorente JA, Rosell R, Serrano MJ (2013) Relevance of molecular characterization of circulating tumor cells in breast cancer in the era of targeted therapies. Expert Rev Mol Diagn 13:295–307 . doi: 10.1586/erm.13.7

122. Gasch C, Plummer PN, Jovanovic L, et al (2015) Heterogeneity of miR-10b expression in circulating tumor cells. Sci Rep 5:15980 . doi: 10.1038/srep15980

123. Schramm A, Friedl TWP, Schochter F, et al (2016) Therapeutic intervention based on circulating tumor cell phenotype in metastatic breast cancer: concept of the DETECT study program. Arch Gynecol Obstet 293:271–281 . doi: 10.1007/s00404-015-3879-7

124. Masuda T, Hayashi N, Iguchi T, et al (2016) Clinical and biological significance of circulating tumor cells in cancer. Mol Oncol 10:408–417 . doi: 10.1016/j.molonc.2016.01.010

125. Harouaka RA, Nisic M, Zheng S-Y (2013) Circulating Tumor Cell Enrichment Based on Physical Properties. J Lab Autom 18:455–468 . doi: 10.1177/2211068213494391

126. Shapiro HM, Schildkraut ER, Curbelo R, et al (1976) Combined blood cell counting and classification with fluorochrome stains and flow instrumentation. J Histochem Cytochem Off J Histochem Soc 24:396–401

127. Shaw Bagnall J, Byun S, Begum S, et al (2015) Deformability of Tumor Cells versus Blood Cells. Sci Rep 5:18542 . doi: 10.1038/srep18542

128. Suresh S (2007) Biomechanics and biophysics of cancer cells☆. Acta Biomater 3:413–438 . doi: 10.1016/j.actbio.2007.04.002

129. Pethig R (2010) Dielectrophoresis: Status of the theory, technology, and applications. Biomicrofluidics 4:022811 . doi: 10.1063/1.3456626

130. Ponder E (1942) The relation between red blood cell density and corpuscular hemoglobin concentration. J Biol Chem 333–338

131. Phillips KG, Velasco CR, Li J, et al (2012) Optical quantification of cellular mass, volume, and density of circulating tumor cells identified in an ovarian cancer patient. Front Oncol 2:72 . doi: 10.3389/fonc.2012.00072

132. Noman MZ, Messai Y, Muret J, et al (2014) Crosstalk between CTC, Immune System and Hypoxic Tumor Microenvironment. Cancer Microenviron 7:153–160 . doi: 10.1007/s12307-014-0157-3

133. Kalluri R, Weinberg RA (2009) The basics of epithelial-mesenchymal transition. J Clin Invest 119:1420–1428 . doi: 10.1172/JCI39104

134. Pietilä M, Ivaska J, Mani SA (2016) Whom to blame for metastasis, the epithelial–mesenchymal transition or the tumor microenvironment? Cancer Lett. doi: 10.1016/j.canlet.2015.12.033

135. Labelle M, Begum S, Hynes RO (2011) Direct Signaling between Platelets and Cancer Cells Induces an Epithelial-Mesenchymal-Like Transition and Promotes Metastasis. Cancer Cell 20:576–590 . doi: 10.1016/j.ccr.2011.09.009

136. Laberge R-M, Awad P, Campisi J, Desprez P-Y (2012) Epithelial-Mesenchymal Transition Induced by Senescent Fibroblasts. Cancer Microenviron 5:39–44 . doi: 10.1007/s12307-011-0069-4

137. Condeelis J, Pollard JW (2006) Macrophages: obligate partners for tumor cell migration, invasion, and metastasis. Cell 124:263–266 . doi: 10.1016/j.cell.2006.01.007

138. Liu Z-J, Semenza GL, Zhang H-F (2015) Hypoxia-inducible factor 1 and breast cancer metastasis. J Zhejiang Univ Sci B 16:32–43 . doi: 10.1631/jzus.B1400221

139. Yeo CD, Kang N, Choi SY, et al (2017) The role of hypoxia on the acquisition of epithelial-mesenchymal transition and cancer stemness: a possible link to epigenetic regulation. Korean J Intern Med 32:589–599 . doi: 10.3904/kjim.2016.302

140. Hazan RB, Qiao R, Keren R, et al (2004) Cadherin switch in tumor progression. Ann N Y Acad Sci 1014:155–163

141. Martin TA, Ye L, Sanders AJ, et al (2013) Cancer Invasion and Metastasis: Molecular and Cellular Perspective. In: Metastatic Cancer: Clinical and Biological Perspectives. Landes Bioscience

142. Chang JT, Mani SA (2013) Sheep, wolf, or werewolf: Cancer stem cells and the epithelial-to-mesenchymal transition. Cancer Lett 341:16–23 . doi: 10.1016/j.canlet.2013.03.004

143. Shibue T, Brooks MW, Weinberg RA (2013) An Integrin-Linked Machinery of Cytoskeletal Regulation that Enables Experimental Tumor Initiation and Metastatic Colonization. Cancer Cell 24:481–498 . doi: 10.1016/j.ccr.2013.08.012

144. Tian X, Liu Z, Niu B, et al (2011) E-Cadherin/ β -Catenin Complex and the Epithelial Barrier. J Biomed Biotechnol 2011:1–6 . doi: 10.1155/2011/567305

145. Sleeman JP, Thiery JP (2011) SnapShot: The Epithelial-Mesenchymal Transition. Cell 145:162-162.e1 . doi: 10.1016/j.cell.2011.03.029

146. Prall F (2007) Tumour budding in colorectal carcinoma. Histopathology 50:151–162 . doi: 10.1111/j.1365-2559.2006.02551.x

147. Giger OT, Comtesse SCM, Lugli A, et al (2012) Intra-tumoral budding in preoperative biopsy specimens predicts lymph node and distant metastasis in patients with colorectal cancer. Mod Pathol 25:1048–1053 . doi: 10.1038/modpathol.2012.56

148. Bedke J, Heide J, Ribback S, et al (2018) Microvascular and lymphovascular tumour invasion are associated with poor prognosis and metastatic spread in renal cell carcinoma: a validation study in clinical practice. BJU Int 121:84–92 . doi: 10.1111/bju.13984

149. Lim S-B, Yu CS, Jang SJ, et al (2010) Prognostic Significance of Lymphovascular Invasion in Sporadic Colorectal Cancer: Dis Colon Rectum 53:377–384 . doi: 10.1007/DCR.0b013e3181cf8ae5

150. Zhe X, Cher ML, Bonfil RD (2011) Circulating tumor cells: finding the needle in the haystack. Am J Cancer Res 1:740–751

151. Chang YS, di Tomaso E, McDonald DM, et al (2000) Mosaic blood vessels in tumors: frequency of cancer cells in contact with flowing blood. Proc Natl Acad Sci U S A 97:14608–14613 . doi: 10.1073/pnas.97.26.14608

152. Frisch SM, Francis H (1994) Disruption of epithelial cell-matrix interactions induces apoptosis. J Cell Biol 124:619–626

153. Lambert AW, Pattabiraman DR, Weinberg RA (2017) Emerging Biological Principles of Metastasis. Cell 168:670–691 . doi: 10.1016/j.cell.2016.11.037

154. Bockhorn M, Roberge S, Sousa C, et al (2004) Differential gene expression in metastasizing cells shed from kidney tumors. Cancer Res 64:2469–2473

155. Meng S (2004) Circulating Tumor Cells in Patients with Breast Cancer Dormancy. Clin Cancer Res 10:8152–8162 . doi: 10.1158/1078-0432.CCR-04-1110

156. Chaffer CL, Weinberg RA (2011) A Perspective on Cancer Cell Metastasis. Science 331:1559–1564 . doi: 10.1126/science.1203543

157. Pantel K, Speicher MR (2015) The biology of circulating tumor cells. Oncogene. doi: 10.1038/onc.2015.192

158. Yao D, Dai C, Peng S (2011) Mechanism of the Mesenchymal-Epithelial Transition and Its Relationship with Metastatic Tumor Formation. Mol Cancer Res 9:1608–1620 . doi: 10.1158/1541-7786.MCR-10-0568

159. Engell HC (1955) Cancer cells in the circulating blood; a clinical study on the occurrence of cancer cells in the peripheral blood and in venous blood draining the tumour area at operation. Acta Chir Scand Suppl 201:1–70

160. Cristofanilli M, Hayes DF, Budd GT, et al (2005) Circulating tumor cells: a novel prognostic factor for newly diagnosed metastatic breast cancer. J Clin Oncol Off J Am Soc Clin Oncol 23:1420–1430 . doi: 10.1200/JCO.2005.08.140

161. Thiele J-A, Bethel K, Králíčková M, Kuhn P (2017) Circulating Tumor Cells: Fluid Surrogates of Solid Tumors. Annu Rev Pathol Mech Dis 12:419–447 . doi: 10.1146/annurev-pathol-052016-100256

162. Nagrath S, Sequist LV, Maheswaran S, et al (2007) Isolation of rare circulating tumour cells in cancer patients by microchip technology. Nature 450:1235–1239 . doi: 10.1038/nature06385

163. Talasaz AH, Powell AA, Huber DE, et al (2009) Isolating highly enriched populations of circulating epithelial cells and other rare cells from blood using a magnetic sweeper device. Proc Natl Acad Sci 106:3970–3975 . doi: 10.1073/pnas.0813188106

164. Saucedo-Zeni N, Mewes S, Niestroj R, et al (2012) A novel method for the in vivo isolation of circulating tumor cells from peripheral blood of cancer patients using a functionalized and structured medical wire. Int J Oncol 41:1241–1250 . doi: 10.3892/ijo.2012.1557

165. Aktas B, Tewes M, Fehm T, et al (2009) Stem cell and epithelial-mesenchymal transition markers are frequently overexpressed in circulating tumor cells of metastatic breast cancer patients. Breast Cancer Res 11: . doi: 10.1186/bcr2333

166. Allard WJ, Matera J, Miller MC, et al (2004) Tumor cells circulate in the peripheral blood of all major carcinomas but not in healthy subjects or patients with nonmalignant diseases. Clin Cancer Res Off J Am Assoc Cancer Res 10:6897–6904 . doi: 10.1158/1078-0432.CCR-04-0378

167. Yin J, Wang Y, Yin H, et al (2015) Circulating Tumor Cells Enriched by the Depletion of Leukocytes with Bi-Antibodies in Non-Small Cell Lung Cancer: Potential Clinical Application. PLOS ONE 10:e0137076 . doi: 10.1371/journal.pone.0137076

168. Baccelli I, Schneeweiss A, Riethdorf S, et al (2013) Identification of a population of blood circulating tumor cells from breast cancer patients that initiates metastasis in a xenograft assay. Nat Biotechnol 31:539–544 . doi: 10.1038/nbt.2576

169. Harouaka R, Kang Z, Zheng S-Y, Cao L (2014) Circulating tumor cells: Advances in isolation and analysis, and challenges for clinical applications. Pharmacol Ther 141:209–221 . doi: 10.1016/j.pharmthera.2013.10.004

170. Baker MK, Mikhitarian K, Osta W, et al (2003) Molecular detection of breast cancer cells in the peripheral blood of advanced-stage breast cancer patients using multimarker real-time reverse transcription-polymerase chain reaction and a novel porous barrier density gradient centrifugation technology. Clin Cancer Res Off J Am Assoc Cancer Res 9:4865–4871

171. Chinen LTD, de Carvalho FM, Rocha BMM, et al (2013) Cytokeratin-based CTC counting unrelated to clinical follow up. J Thorac Dis 5:593–599 . doi: 10.3978/j.issn.2072-1439.2013.09.18

172. Alix-Panabières C (2012) EPISPOT assay: detection of viable DTCs/CTCs in solid tumor patients. Recent Results Cancer Res Fortschritte Krebsforsch Prog Dans Rech Sur Cancer 195:69–76 . doi: 10.1007/978-3-642-28160-0_6

173. Pizon M, Zimon D, Carl S, et al (2013) Heterogeneity of circulating epithelial tumour cells from individual patients with respect to expression profiles and clonal growth (sphere formation) in breast cancer. Ecancermedicalscience 7:343 . doi: 10.3332/ecancer.2013.343

174. Wu S, Liu S, Liu Z, et al (2015) Classification of circulating tumor cells by epithelial-mesenchymal transition markers. PloS One 10:e0123976 . doi: 10.1371/journal.pone.0123976

175. Marrinucci D, Bethel K, Kolatkar A, et al (2012) Fluid biopsy in patients with metastatic prostate, pancreatic and breast cancers. Phys Biol 9:016003 . doi: 10.1088/1478-3975/9/1/016003

176. Hwang WL, Pleskow HM, Miyamoto DT (2018) Molecular analysis of circulating tumors cells: Biomarkers beyond enumeration. Adv Drug Deliv Rev. doi: 10.1016/j.addr.2018.01.003

177. Williams ES, Rodriquez-Bravo V, Chippada-Venkata U, et al (2015) Generation of Prostate Cancer Patient Derived Xenograft Models from Circulating Tumor Cells. J Vis Exp. doi: 10.3791/53182

178. Kolostova K, Spicka J, Matkowski R, Bobek V (2015) Isolation, primary culture, morphological and molecular characterization of circulating tumor cells in gynecological cancers. Am J Transl Res 7:1203–1213

179. Khoo BL, Lee SC, Kumar P, et al (2015) Short-term expansion of breast circulating cancer cells predicts response to anti-cancer therapy. Oncotarget 6:15578–15593 . doi: 10.18632/oncotarget.3903

180. Yu M, Bardia A, Aceto N, et al (2014) Ex vivo culture of circulating breast tumor cells for individualized testing of drug susceptibility. Science 345:216–220 . doi: 10.1126/science.1253533

181. Fehm T, Müller V, Aktas B, et al (2010) HER2 status of circulating tumor cells in patients with metastatic breast cancer: a prospective, multicenter trial. Breast Cancer Res Treat 124:403–412 . doi: 10.1007/s10549-010-1163-x

182. Yan W-T, Cui X, Chen Q, et al (2017) Circulating tumor cell status monitors the treatment responses in breast cancer patients: a meta-analysis. Sci Rep 7:43464 . doi: 10.1038/srep43464

183. Metzker ML (2010) Sequencing technologies — the next generation. Nat Rev Genet 11:31–46 . doi: 10.1038/nrg2626

184. Baslan T, Hicks J (2014) Single cell sequencing approaches for complex biological systems. Curr Opin Genet Dev 26:59–65 . doi: 10.1016/j.gde.2014.06.004

185. Gasch C, Bauernhofer T, Pichler M, et al (2013) Heterogeneity of Epidermal Growth Factor Receptor Status and Mutations of KRAS/PIK3CA in Circulating Tumor Cells of Patients with Colorectal Cancer. Clin Chem 59:252–260 . doi: 10.1373/clinchem.2012.188557

186. Polzer B, Medoro G, Pasch S, et al (2014) Molecular profiling of single circulating tumor cells with diagnostic intention. EMBO Mol Med 6:1371–1386 . doi: 10.15252/emmm.201404033

187. Heitzer E, Auer M, Gasch C, et al (2013) Complex tumor genomes inferred from single circulating tumor cells by array-CGH and next-generation sequencing. Cancer Res 73:2965–2975 . doi: 10.1158/0008-5472.CAN-12-4140

188. Dago AE, Stepansky A, Carlsson A, et al (2014) Rapid Phenotypic and Genomic Change in Response to Therapeutic Pressure in Prostate Cancer Inferred by High Content Analysis of Single Circulating Tumor Cells. PLoS ONE 9:e101777 . doi: 10.1371/journal.pone.0101777

189. Alix-Panabieres C, Pantel K (2016) Clinical Applications of Circulating Tumor Cells and Circulating Tumor DNA as Liquid Biopsy. Cancer Discov. doi: 10.1158/2159-8290.CD-15-1483

190. Cann GM, Gulzar ZG, Cooper S, et al (2012) mRNA-Seq of single prostate cancer circulating tumor cells reveals recapitulation of gene expression and pathways found in prostate cancer. PloS One 7:e49144 . doi: 10.1371/journal.pone.0049144

191. Pailler E, Adam J, Barthélémy A, et al (2013) Detection of circulating tumor cells harboring a unique ALK rearrangement in ALK-positive non-small-cell lung cancer. J Clin Oncol Off J Am Soc Clin Oncol 31:2273–2281 . doi: 10.1200/JCO.2012.44.5932

192. Steinestel J, Luedeke M, Arndt A, et al (2015) Detecting predictive androgen receptor modifications in circulating prostate cancer cells. Oncotarget. doi: 10.18632/oncotarget.3925

193. Pailler E, Auger N, Lindsay CR, et al (2015) High level of chromosomal instability in circulating tumor cells of ROS1-rearranged non-small-cell lung cancer. Ann Oncol. doi: 10.1093/annonc/mdv165

194. Antonarakis ES, Lu C, Luber B, et al (2015) Androgen Receptor Splice Variant 7 and Efficacy of Taxane Chemotherapy in Patients With Metastatic Castration-Resistant Prostate Cancer. JAMA Oncol 1:582–591 . doi: 10.1001/jamaoncol.2015.1341

195. Wallwiener M, Riethdorf S, Hartkopf AD, et al (2014) Serial enumeration of circulating tumor cells predicts treatment response and prognosis in metastatic breast cancer: a prospective study in 393 patients. BMC Cancer 14:512 . doi: 10.1186/1471-2407-14-512

196. Smerage JB, Barlow WE, Hortobagyi GN, et al (2014) Circulating Tumor Cells and Response to Chemotherapy in Metastatic Breast Cancer: SWOG S0500. J Clin Oncol 32:3483–3489 . doi: 10.1200/JCO.2014.56.2561

197. Antonarakis ES, Lu C, Wang H, et al (2014) AR-V7 and resistance to enzalutamide and abiraterone in prostate cancer. N Engl J Med 371:1028–1038 . doi: 10.1056/NEJMoa1315815

198. Thalgott M, Rack B, Horn T, et al (2015) Detection of Circulating Tumor Cells in Locally Advanced High-risk Prostate Cancer During Neoadjuvant Chemotherapy and Radical Prostatectomy. Anticancer Res 35:5679–5685

199. Gazzaniga P, de Berardinis E, Raimondi C, et al (2014) Circulating tumor cells detection has independent prognostic impact in high-risk non-muscle invasive bladder cancer. Int J Cancer 135:1978–1982 . doi: 10.1002/ijc.28830

200. Rack B, Schindlbeck C, Jückstock J, et al (2014) Circulating tumor cells predict survival in early average-to-high risk breast cancer patients. J Natl Cancer Inst 106: . doi: 10.1093/jnci/dju066

201. Cohen SJ, Punt CJA, Iannotti N, et al (2008) Relationship of circulating tumor cells to tumor response, progression-free survival, and overall survival in patients with metastatic colorectal cancer. J Clin Oncol Off J Am Soc Clin Oncol 26:3213–3221 . doi: 10.1200/JCO.2007.15.8923

202. Grover PK, Cummins AG, Price TJ, et al (2014) Circulating tumour cells: the evolving concept and the inadequacy of their enrichment by EpCAM-based methodology for basic and clinical cancer research. Ann Oncol 25:1506–1516 . doi: 10.1093/annonc/mdu018

203. Giuliano M, Shaikh A, Lo HC, et al (2018) Perspective on Circulating Tumor Cell Clusters: Why It Takes a Village to Metastasize. Cancer Res 78:845–852 . doi: 10.1158/0008-5472.CAN-17-2748

204. Cima I, Kong SL, Sengupta D, et al (2016) Tumor-derived circulating endothelial cell clusters in colorectal cancer. Sci Transl Med 8:345ra89-345ra89 . doi: 10.1126/scitranslmed.aad7369

205. Carter L, Rothwell DG, Mesquita B, et al (2017) Molecular analysis of circulating tumor cells identifies distinct copy-number profiles in patients with chemosensitive and chemorefractory small-cell lung cancer. Nat Med 23:114–119 . doi: 10.1038/nm.4239

206. Malihi PD, Morikado M, Welter L, et al (2018) Clonal diversity revealed by morphoproteomic and copy number profiles of single prostate cancer cells at diagnosis. Converg Sci Phys Oncol 4:015003 . doi: 10.1088/2057-1739/aaa00b

207. Baslan T, Kendall J, Rodgers L, et al (2012) Genome-wide copy number analysis of single cells. Nat Protoc 7:1024–1041 . doi: 10.1038/nprot.2012.039

208. Navin N, Kendall J, Troge J, et al (2011) Tumour evolution inferred by single-cell sequencing. Nature 472:90–94 . doi: 10.1038/nature09807

209. Venkatraman ES, Olshen AB (2007) A faster circular binary segmentation algorithm for the analysis of array CGH data. Bioinformatics 23:657–663 . doi: 10.1093/bioinformatics/btl646

210. Marrinucci D, Bethel K, Lazar D, et al (2010) Cytomorphology of Circulating Colorectal Tumor Cells: A Small Case Series. J Oncol 2010:1–7 . doi: 10.1155/2010/861341

211. Gandomani HS, Yousefi SM, Aghajani M, et al (2017) Colorectal cancer in the world: incidence, mortality and risk factors. Biomed Res Ther 4:1656 . doi: 10.15419/bmrat.v4i10.372

212. Matsusaka S, Suenaga M, Mishima Y, et al (2011) Circulating tumor cells as a surrogate marker for determining response to chemotherapy in Japanese patients with metastatic colorectal cancer. Cancer Sci 102:1188–1192 . doi: 10.1111/j.1349-7006.2011.01926.x

213. Hardingham JE, Grover P, Winter M, et al (2015) Detection and Clinical Significance of Circulating Tumor Cells in Colorectal Cancer--20 Years of Progress. Mol Med Camb Mass 21 Suppl 1:S25-31 . doi: 10.2119/molmed.2015.00149

214. Gorges TM, Stein A, Quidde J, et al (2016) Improved Detection of Circulating Tumor Cells in Metastatic Colorectal Cancer by the Combination of the CellSearch® System and the AdnaTest®. PLOS ONE 11:e0155126 . doi: 10.1371/journal.pone.0155126

215. Molnar B, Ladanyi A, Tanko L, et al (2001) Circulating tumor cell clusters in the peripheral blood of colorectal cancer patients. Clin Cancer Res Off J Am Assoc Cancer Res 7:4080–4085

216. Ligthart ST, Coumans FAW, Bidard F-C, et al (2013) Circulating Tumor Cells Count and Morphological Features in Breast, Colorectal and Prostate Cancer. PLoS ONE 8:e67148 . doi: 10.1371/journal.pone.0067148

217. Cristofanilli M, Budd GT, Ellis MJ, et al (2004) Circulating Tumor Cells, Disease Progression, and Survival in Metastatic Breast Cancer. N Engl J Med 351:781–791 . doi: 10.1056/NEJMoa040766

218. de Bono JS, Scher HI, Montgomery RB, et al (2008) Circulating Tumor Cells Predict Survival Benefit from Treatment in Metastatic Castration-Resistant Prostate Cancer. Clin Cancer Res 14:6302–6309 . doi: 10.1158/1078-0432.CCR-08-0872

219. Sheth KR, Clary BM (2005) Management of Hepatic Metastases from Colorectal Cancer. Clin Colon Rectal Surg 18:215–223 . doi: 10.1055/s-2005-916282

220. Catenacci DVT, Chapman CG, Xu P, et al (2015) Acquisition of Portal Venous Circulating Tumor Cells From Patients With Pancreaticobiliary Cancers by Endoscopic Ultrasound. Gastroenterology 149:1794-1803.e4 . doi: 10.1053/j.gastro.2015.08.050

221. Hyun K-A, Koo G-B, Han H, et al (2016) Epithelial-to-mesenchymal transition leads to loss of EpCAM and different physical properties in circulating tumor cells from metastatic breast cancer. Oncotarget 7: . doi: 10.18632/oncotarget.8250

222. Wit S de, Dalum G van, Lenferink ATM, et al (2015) The detection of EpCAM+ and EpCAM– circulating tumor cells. Sci Rep 5:12270

223. Gerdtsson E, Pore M, Thiele J-A, et al (2018) Multiplex protein detection on circulating tumor cells from liquid biopsies using imaging mass cytometry. Converg Sci Phys Oncol 4:015002 . doi: 10.1088/2057-1739/aaa013

224. Doi H, Uemoto K, Suzuki O, et al (2017) Effect of primary tumor location and tumor size on the response to radiotherapy for liver metastases from colorectal cancer. Oncol Lett 14:453–460 . doi: 10.3892/ol.2017.6167

225. Yuan H, Dong Q, Zheng B, et al (2017) Lymphovascular invasion is a high risk factor for stage I/II colorectal cancer: a systematic review and meta-analysis. Oncotarget 8: . doi: 10.18632/oncotarget.15425

226. Saha S, Shaik M, Johnston G, et al (2015) Tumor size predicts long-term survival in colon cancer: an analysis of the National Cancer Data Base. Am J Surg 209:570–574 . doi: 10.1016/j.amjsurg.2014.12.008

227. Engstrand J, Nilsson H, Strömberg C, et al (2018) Colorectal cancer liver metastases – a population-based study on incidence, management and survival. BMC Cancer 18: . doi: 10.1186/s12885-017-3925-x

228. Groot Koerkamp B, Rahbari NN, Büchler MW, et al (2013) Circulating Tumor Cells and Prognosis of Patients with Resectable Colorectal Liver Metastases or Widespread Metastatic Colorectal Cancer: A Meta-Analysis. Ann Surg Oncol 20:2156–2165 . doi: 10.1245/s10434-013-2907-8

229. Zou K, Yang S, Zheng L, et al (2016) Prognostic Role of the Circulating Tumor Cells Detected by Cytological Methods in Gastric Cancer: A Meta-Analysis. BioMed Res Int 2016:1–10 . doi: 10.1155/2016/2765464

230. Lalmahomed ZS, Mostert B, Onstenk W, et al (2015) Prognostic value of circulating tumour cells for early recurrence after resection of colorectal liver metastases. Br J Cancer 112:556–561 . doi: 10.1038/bjc.2014.651

231. Beerepoot LV, Mehra N, Vermaat JSP, et al (2004) Increased levels of viable circulating endothelial cells are an indicator of progressive disease in cancer patients. Ann Oncol 15:139–145 . doi: 10.1093/annonc/mdh017

232. Miettinen M, Fetsch JF (2000) Distribution of keratins in normal endothelial cells and a spectrum of vascular tumors: Implications in tumor diagnosis. Hum Pathol 31:1062–1067 . doi: 10.1053/hupa.2000.9843

233. Bethel K, Luttgen MS, Damani S, et al (2014) Fluid phase biopsy for detection and characterization of circulating endothelial cells in myocardial infarction. Phys Biol 11:016002 . doi: 10.1088/1478-3975/11/1/016002

234. Rigolin GM (2006) Neoplastic circulating endothelial cells in multiple myeloma with 13q14 deletion. Blood 107:2531–2535 . doi: 10.1182/blood-2005-04-1768

235. Pecot CV, Bischoff FZ, Lin YG, et al (2011) Clinical relevance of cytokeratin-negative circulating tumor cells. J Clin Oncol 29:e21101–e21101 . doi: 10.1200/jco.2011.29.15_suppl.e21101

236. Divella R, Daniele A, Abbate I, et al (2014) The presence of clustered circulating tumor cells (CTCs) and circulating cytokines define an aggressive phenotype in metastatic colorectal cancer. Cancer Causes Control 25:1531–1541 . doi: 10.1007/s10552-014-0457-4

237. Cho EH, Wendel M, Luttgen M, et al (2012) Characterization of circulating tumor cell aggregates identified in patients with epithelial tumors. Phys Biol 9:016001 . doi: 10.1088/1478-3975/9/1/016001

238. Zurita AJ, Carlsson A, Troncoso P, et al (2016) Abstract 4966: High-definition single cell analysis (HD-SCA) reveals enrichment in androgen receptor (AR) expression in tumor cell clusters in bone marrow and blood of metastatic castration-resistant prostate cancer (mCRPC) patients. Cancer Res 76:4966–4966 . doi: 10.1158/1538-7445.AM2016-4966

239. Carlsson A, Nair VS, Luttgen MS, et al (2014) Circulating Tumor Microemboli Diagnostics for Patients with Non–Small-Cell Lung Cancer. J Thorac Oncol 9:1111–1119 . doi: 10.1097/JTO.0000000000000235

240. Aceto N, Bardia A, Miyamoto DT, et al (2014) Circulating Tumor Cell Clusters Are Oligoclonal Precursors of Breast Cancer Metastasis. Cell 158:1110–1122 . doi: 10.1016/j.cell.2014.07.013

241. Ribatti D, Mangialardi G, Vacca A (2006) Stephen Paget and the 'seed and soil' theory of metastatic dissemination. Clin Exp Med 6:145–149 . doi: 10.1007/s10238-006-0117-4

242. Khorana AA, Francis CW, Culakova E, et al (2007) Thromboembolism is a leading cause of death in cancer patients receiving outpatient chemotherapy. J Thromb Haemost JTH 5:632–634 . doi: 10.1111/j.1538-7836.2007.02374.x

243. Arnold D, Lueza B, Douillard J-Y, et al (2017) Prognostic and predictive value of primary tumour side in patients with RAS wild-type metastatic colorectal cancer treated with chemotherapy and EGFR directed antibodies in six randomized trials†. Ann Oncol 28:1713–1729 . doi: 10.1093/annonc/mdx175

244. Shelygin YA, Pospekhova NI, Shubin VP, et al (2014) Epithelial-Mesenchymal Transition and Somatic Alteration in Colorectal Cancer with and without Peritoneal Carcinomatosis. BioMed Res Int 2014:1–7 . doi: 10.1155/2014/629496

245. Thiery JP (2002) Epithelial–mesenchymal transitions in tumour progression. Nat Rev Cancer 2:442–454 . doi: 10.1038/nrc822

246. Jančík S, Drábek J, Radzioch D, Hajdúch M (2010) Clinical Relevance of KRAS in Human Cancers. J Biomed Biotechnol 2010:1–13 . doi: 10.1155/2010/150960

247. Dinu D, Dobre M, Panaitescu E, et al (2014) Prognostic significance of KRAS gene mutations in colorectal cancer--preliminary study. J Med Life 7:581–587

248. Allen JEE, Saroya BS, Kunkel M, et al (2014) Apoptotic circulating tumor cells (CTCs) in the peripheral blood of metastatic colorectal cancer patients are associated with liver metastasis but not CTCs. Oncotarget 5: . doi: 10.18632/oncotarget.1524

249. Backus HHJ, Van Groeningen CJ, Vos W, et al (2002) Differential expression of cell cycle and apoptosis related proteins in colorectal mucosa, primary colon tumours, and liver metastases. J Clin Pathol 55:206–211

250. Pino MS, Chung DC (2010) The Chromosomal Instability Pathway in Colon Cancer. Gastroenterology 138:2059–2072 . doi: 10.1053/j.gastro.2009.12.065

251. Neves RPL, Raba K, Schmidt O, et al (2014) Genomic High-Resolution Profiling of Single CKpos/CD45neg Flow-Sorting Purified Circulating Tumor Cells from Patients with Metastatic Breast Cancer. Clin Chem. doi: 10.1373/clinchem.2014.222331

252. Ruiz C, Li J, Luttgen MS, et al (2015) Limited genomic heterogeneity of circulating melanoma cells in advanced stage patients. Phys Biol 12:016008 . doi: 10.1088/1478-3975/12/1/016008

253. Ni X, Zhuo M, Su Z, et al (2013) Reproducible copy number variation patterns among single circulating tumor cells of lung cancer patients. Proc Natl Acad Sci U S A 110:21083–21088 . doi: 10.1073/pnas.1320659110

254. Dudley AC (2012) Tumor Endothelial Cells. Cold Spring Harb Perspect Med 2:a006536–a006536 . doi: 10.1101/cshperspect.a006536

255. Akino T, Hida K, Hida Y, et al (2009) Cytogenetic Abnormalities of Tumor-Associated Endothelial Cells in Human Malignant Tumors. Am J Pathol 175:2657–2667 . doi: 10.2353/ajpath.2009.090202

256. Li H, Courtois ET, Sengupta D, et al (2017) Reference component analysis of single-cell transcriptomes elucidates cellular heterogeneity in human colorectal tumors. Nat Genet 49:708

257. Noy R, Pollard JW (2014) Tumor-Associated Macrophages: From Mechanisms to Therapy. Immunity 41:49–61 . doi: 10.1016/j.immuni.2014.06.010

258. Bussard KM, Mutkus L, Stumpf K, et al (2016) Tumor-associated stromal cells as key contributors to the tumor microenvironment. Breast Cancer Res 18: . doi: 10.1186/s13058-016-0740-2

259. Zeng Z-S, Weiser MR, Kuntz E, et al (2008) c-Met gene amplification is associated with advanced stage colorectal cancer and liver metastases. Cancer Lett 265:258–269 . doi: 10.1016/j.canlet.2008.02.049

260. Raghav K, Morris V, Tang C, et al (2016) MET amplification in metastatic colorectal cancer: an acquired response to EGFR inhibition, not a *de novo* phenomenon. Oncotarget 7: . doi: 10.18632/oncotarget.10559

261. Bardelli A, Corso S, Bertotti A, et al (2013) Amplification of the *MET* Receptor Drives Resistance to Anti-EGFR Therapies in Colorectal Cancer. Cancer Discov 3:658–673 . doi: 10.1158/2159-8290.CD-12-0558

262. Helsten T, Elkin S, Arthur E, et al (2016) The FGFR Landscape in Cancer: Analysis of 4,853 Tumors by Next-Generation Sequencing. Clin Cancer Res 22:259–267 . doi: 10.1158/1078-0432.CCR-14-3212

263. Cihoric N, Savic S, Schneider S, et al (2014) Prognostic role of FGFR1 amplification in early-stage non-small cell lung cancer. Br J Cancer 110:2914–2922 . doi: 10.1038/bjc.2014.229

264. Zhang L, Shay JW (2017) Multiple Roles of APC and its Therapeutic Implications in Colorectal Cancer. JNCI J Natl Cancer Inst 109: . doi: 10.1093/jnci/djw332

265. Aretz S (2005) Large submicroscopic genomic APC deletions are a common cause of typical familial adenomatous polyposis. J Med Genet 42:185–192 . doi: 10.1136/jmg.2004.022822

266. Werling RW, Yaziji H, Bacchi CE, Gown AM (2003) CDX2, a highly sensitive and specific marker of adenocarcinomas of intestinal origin: an immunohistochemical survey of 476 primary and metastatic carcinomas. Am J Surg Pathol 27:303–310

267. Tomasello G, Barni S, Turati L, et al (2018) Association of CDX2 Expression With Survival in Early Colorectal Cancer: A Systematic Review and Meta-analysis. Clin Colorectal Cancer 17:97–103 . doi: 10.1016/j.clcc.2018.02.001

268. Subtil C, Guérin E, Schneider A, et al (2007) Frequent rearrangements and amplification of the CDX2 homeobox gene in human sporadic colorectal cancers with chromosomal instability. Cancer Lett 247:197–203 . doi: 10.1016/j.canlet.2006.04.004

269. McGranahan N, Swanton C (2017) Clonal Heterogeneity and Tumor Evolution: Past, Present, and the Future. Cell 168:613–628 . doi: 10.1016/j.cell.2017.01.018

270. Parkin B, Ouillette P, Li Y, et al (2013) Clonal evolution and devolution after chemotherapy in adult acute myelogenous leukemia. Blood 121:369–377 . doi: 10.1182/blood-2012-04-427039

9 Acknowledgements

This work has been supported by the Research Fund (Progres Q39), by the National Sustainability Program I (NPU I) Nr. LO1503 provided by the Ministry of Education Youth and Sports of the Czech Republic and by the Fond of Mobility of the Czech Republic.

As my mentor Dr. Pavel Pitule has been available for many discussions regarding CTCs in CRC, revisions of papers and has guided me throughout the challenges of this thesis.

Dr. Pavel Ostašov has always been a vivid creator of ideas, equally interesting conversational partner while hunting project related solutions and also revised my manuscripts.

Special support at USC was provided by my second advisor, Dr. Peter Kuhn and also Dr. Jasmes Hicks, who offered all necessary equipment and consumeables for single-cell sequencing, but were also available for professional discussions and moral support. As well as Dr. Anna Sandstrom Gerdtsson who was my personal supervisor at USC for CRC and technique related questions, but also a friend and roommate.

Dr. Milena Králíčková has provided the major financial support by grant acquisition for this project and initiated the collaboration with the Kuhn-Hicks laboratory.

Dr. Petr Hošek has been my statistical support and provided me with immense insight on data analysis.

The surgeons and oncologists from the University Hospital in Pilsen have supported us by updating clinical data, coordinating blood sampling and supporting our collaboration.

Personal gratitude goes to all the members of the Kuhn-Hicks laboratory, who have been immensely helpful and supportive during scientific writing and experiments.

10 Publications

A summary of all composed publications regarding this thesis and projects executed during the time of this work are listed here and attached in the following order within chapter 10:

I. Circulating Tumor Cells: Fluid Surrogates of Solid Tumors; Review

Thiele J-A, Bethel K, Králíčková M, Kuhn P, 2017, Circulating Tumor Cells: Fluid Surrogates of Solid Tumors. Annu Rev Pathol Mech Dis 12:419–447. doi: 10.1146/annurev-pathol-052016-100256 **(IF_{2017} = 15.95)**

II. Multiplex protein detection on circulating tumor cells from liquid biopsies using imaging mass cytometry; Research Article

Gerdtsson E, Pore M, Thiele J-A, et al., 2018, Multiplex protein detection on circulating tumor cells from liquid biopsies using imaging mass cytometry. Converg Sci Phys Oncol 4:015002. doi: 10.1088/2057-1739/aaa013

(Journal has recently been selected for indexing in Clarivate Analytics Emerging Sources Citation Index (ESCI); listed in Web of Science as of next year).

III. Single-Cell Analysis of Circulating Tumor Cells; Book chapter

Thiele J-A, Pitule P, Hicks J and Kuhn P., Single-Cell Analysis of Circulating Tumor Cells. Methods Mol Biol., accepted in March 2018.

(Scopus cite $score_{2017}$ = 0.96)

IV. lncRNAs in healthy tissue have prognostic value in colorectal cancer; Research Article

Thiele J-A, Hosek P, Kralovcova E, Ostasov P, Liska V, Bruha J, Vycital O, Rosendorf J, Kralickova M, Pitule P, lncRNAs in healthy tissue have prognostic value in colorectal cancer, Submitted to BMC Cancer: June 2018 **(IF_{2017} = 3.28)**